

Thermodynamics and Universality in Anisotropic Higher Curvature Spacetimes

by

Wilson Brenna

A thesis
presented to the University of Waterloo
in fulfillment of the
thesis requirement for the degree of
Doctor of Philosophy
in
Physics

Waterloo, Ontario, Canada, 2016

© Wilson Brenna 2016

I hereby declare that I am the sole author of this thesis. This is a true copy of the thesis, including any required final revisions, as accepted by my examiners.

I understand that my thesis may be made electronically available to the public.

Abstract

In my thesis, I describe new results in the thermodynamics of black holes in two gravitational scenarios: spacetime anisotropy and higher curvature gravity. I focus on classifying the critical point of "Large Black Hole / Small Black Hole" phase transitions in higher curvature gravity in various dimensions, for both numerical and analytic black hole solutions. Special emphasis will be placed on five-dimensional cubic and quartic quasitopological gravity. I cover the motivation and document a number of higher curvature black hole solutions as well as the thermodynamic behaviour of these black holes when they are asymptotically Lifshitz symmetric (a form of anisotropy). I describe the methodology used to construct the set of thermodynamic potentials for black holes with general asymptotics from a collection of well-justified conjectures, followed by the development of procedures to numerically and analytically determine unknown quantities such as mass and thermodynamic volume from these conjectures. I will complete this thesis by extracting the critical exponents and thereby finding the universality class of the critical behaviour for a number of black hole solutions. This work has implications for the study of the gauge/gravity duality as well as for the dynamical behaviour of black holes.

Acknowledgements

Foremost, I would like to acknowledge the patience and support given to me by my parents, Dwayne and Beverley Brenna. They have always been supportive of my decisions and without them it would not have been this easy, and probably near impossible, for me to have reached this point in my career. Both talented educators, from a very young age they instilled upon me the importance of learning, and though neither are scientists they recognized my scientific curiosity and spent not just time and money, but vast mental effort to find mentors and opportunities that would allow me to pursue my ambitions.

The rest of my family - brothers, grandparents, and relatives - deserve mention because they have all had a hand in this work. Whether they offered the comfortable nostalgia of home, a needed distraction from work, or a place to stay when I have been travelling to a conference, I deeply appreciate their generosity and support.

My supervisor, Robert Mann, deserves recognition for every way he has helped this thesis come to fruition. His commitment to learning, both his own learning and that of his colleagues, graduate students, and undergraduate students, fosters a very healthy and productive atmosphere in his workgroup. His skill at organization and leadership means that there have always been opportunities available to travel, collaborate with others, and give academic presentations. His particular acuity for individualizing advice and tasks has really helped all of our group members flourish. And finally, his support and encouragement in publishing and giving talks has pushed all of us to succeed.

Many thanks go to my thesis committee: Niayesh Afshordi, Florian Girelli, Achim Kempf, Hari Kunduri, and Robert Myers; all contributed valuable and specific comments which improved the theoretical background, notation, and conceptual clarity of this thesis.

In addition, Eduardo Martín-Martínez has acted as a mentor, friend, and collaborator, with tireless dedication and a hands-on attitude. Because of his passion for relativistic quantum mechanics, I have been able to diversify my own work, which has been a very valuable personal development opportunity. Eduardo's excitement is contagious, and has made it easy to keep morale high when a calculation isn't converging or a publication has been in peer review for eight months.

Judy McDonnell, graduate coordinator for the department at University of Waterloo, has to be mentioned because of her ability to make things run smoothly. If you need a form signed or a question answered, she is somehow able to have already had this done by the time you ask, without any obstacle. Her impressive ability to keep the barriers that must surely exist hidden means that I can't even guess at the hours she must put in to keep the gears of the department turning.

I would like to acknowledge the friendship and assistance from my fellow colleagues with whom I have worked at the University of Waterloo: Aida Ahmadzadegan, Natacha Altamirano, Eric Brown, Melanie Chanona, Aidan Chatwin-Davies, Keith Copesey, Antonia Frassino, Daniel Grimmer, Sharmila Gunasekaran, Laura Henderson, Robie Hennigar, Danielle Leonard, Saoussen Mbarek, Paul McGrath, Michael Meiers, Keith Ng, Marius Oltean, Marvellous Onuma-Kalu, Miok Park, Razieh Pourhasan, Allison Sachs, Alexander Smith, Sean Stotyn, and Paulina Corona Ugalde. They have all made my time with this large and diverse workgroup a wonderful experience, and I look forward to the future as we all turn to the next chapters of our lives.

And, the friends, teachers, and mentors from my time at the University of Saskatchewan, TRIUMF, Heinrich-Heine Universität Düsseldorf, and Durham University, especially professors Rainer Dick, Kathryn McWilliams, and Isabel Trigger, all deserve recognition for the academic support they have offered, and particularly the many, many letters of reference.

Dedication

This thesis is dedicated to Canadian taxpayers - this work was funded almost entirely through public money, and its existence therefore depends on the willingness of the general Canadian population to support fundamental research.

Table of Contents

List of Tables	x
List of Figures	xi
1 Introduction	1
1.1 Anti-de Sitter Spacetimes	2
1.2 Gauge/gravity duality	5
1.3 Conventions	8
2 Higher Curvature Gravity Theories	10
2.1 Gauss-Bonnet and Lovelock Black Hole Thermodynamics	12
2.1.1 Temperature and Euclidean Periodicity	18
2.1.2 Entropy as a Noether Charge	21
2.1.3 Thermodynamics	23
2.2 Quasitopological Gravity	30
2.2.1 Entropy and Temperature	36
2.2.2 Thermodynamics	38
2.2.3 Quartic Quasitopological Gravity	42
2.3 Discussion	43

3	Lifshitz-symmetric Black Holes	46
3.1	Mass	49
3.1.1	Smarr Relation	50
3.1.2	Conditions on the Mass	50
3.1.3	An Expression for the Mass	53
3.1.4	Various Definitions of Mass	56
3.2	Exact Solutions	60
3.2.1	$z = 2, D = 4, k = -1$	60
3.2.2	$z = 4, D = 4, k = \pm 1, 0$	64
3.2.3	$z = 2, D = 5, k = 0$	66
3.2.4	$z = 3, D = 3, k = 0$	68
3.2.5	$z = D, k = 1, 0$	68
3.2.6	$z = 2(D - 2), k = 0$	70
3.2.7	Summary	72
3.3	A Specific Smarr Relation	73
3.4	The Reverse Isoperimetric Inequality	74
3.5	Numerical Solutions	75
3.5.1	Shooting Method	82
3.5.2	$z = 2$ 3 rd order quasitopological black hole	85
3.5.3	$z = 2$ 4 th order quasitopological black hole	86
3.6	Discussion	89
4	Universality Classes and Black Holes	92
4.1	The Universality Class	92
4.1.1	Critical Exponents and Universality	93
4.1.2	Application to the Van der Waals Model	94
4.1.3	AdS Reissner-Nordström Black Hole	96
4.1.4	Techniques for Numerical Black Holes	98

4.2	An Exact Quasitopological Black Hole	101
4.3	A Numerical Black Hole	107
4.4	Discussion	118
5	Conclusion	120
	References	125
	Appendices	138
A	Obtaining the Einstein Field Equations	139
B	Nonlinear Regression	143
C	Code	145
C.1	Maple Packages	145
C.2	Lifshitz Quasitopological Thermodynamics	152
C.3	Thermodynamic Mass and Volume	158

List of Tables

3.1	Values of the mass parameter \hat{m} for various methods of obtaining mass for the $z = 2$ solution (3.30).	64
3.2	Parameter values for the ansatz (3.44) for the $z = 4$ solution (3.39).	66
3.3	Comparison of alternative methods of obtaining the mass in section 3.1.4 with our thermodynamic methods of section 3.1.3 for the solutions considered here.	73
4.1	A table of critical exponents, computed for the Van der Waals gas.	96

List of Figures

2.1	The log-log plot of temperature versus entropy for asymptotically anti-de Sitter Lanczos-Gauss-Bonnet Black Holes in five dimensions for $k = -1, 0, 1$ (red, blue, black). Here the higher curvature coupling is given by $\lambda = 0.04$, while the cosmological constant is fixed at $\Lambda = -6(1 - \lambda)/L^2$ which does not ensure that the thermodynamics has the same asymptotic behaviour. The dashed solution is Einsteinian for comparison; $\lambda = 0$ in that case.	29
2.2	Cubic quasitopological black hole solutions for $k = 1$, $r_h = 2.0$, $\lambda = 0.04$, $\mu = 0.001$, where $Q = 0, 6, 12$ are in red, green, and blue, respectively. The cosmological constant is given here by $\Lambda = -6(1 - \lambda + \mu)/L^2$. The dotted solutions are quasitopological while the solid solutions are Einsteinian ($\mu = \lambda = 0$).	35
2.3	A plot of the parameter space for cubic quasitopological gravity's higher curvature couplings. The region interior to the red, blue, and green lines satisfies the cubic quasitopological energy flux positivity constraints (2.74).	37
2.4	The log-log plot of temperature versus entropy for asymptotically anti-de Sitter cubic quasitopological Reissner-Nordström Black Holes of $Q = 6$ (dotted), $Q = 3$ (dashed), $Q = 0.5$ (dash-dot), $Q = 0.1$ (long-dash), and $Q = 0$ (solid) for $k = -1, 0, 1$ (red, blue, green). Here the higher curvature couplings take the values $\lambda = 0.04, \mu = 0.001$, while the cosmological constant is fixed at $\Lambda = -6/L^2$ in order to ensure the same asymptotic behaviour of the thermodynamics.	39

2.5	The log-log plot of temperature versus entropy for asymptotically anti-de Sitter {cubic quasitopological - dotted, Gauss-Bonnet - solid, Einsteinian - dashed} uncharged black holes where $k = -1, 0, 1$ (teal, red, brown). Here the higher curvature couplings take the values $\lambda = 0.04, \mu = 0.001$ (when they exist), while the cosmological constant is fixed at $\Lambda = -6(1 - \lambda + \mu)/L^2$ in order to ensure that the metric functions have the same asymptotics, and so that all solutions see the same effective cosmological constant.	40
2.6	The log-log plot of temperature versus entropy for asymptotically anti-de Sitter quartic quasitopological black holes in five dimensions for $k = -1, 0, 1$ (red, blue, black). Here the higher curvature coupling is given by $\xi = 0.0006$ (solid) and $\xi = -0.0001$ (dashed), while the cosmological constant is fixed at $\Lambda = -6/L^2$ which ensures that the thermodynamics has the same asymptotic behaviour.	44
3.1	The log-log plot of temperature versus entropy for asymptotically anti-de Sitter cubic quasitopological uncharged numerical black holes where $k = -1, 0, 1$ (pink, blue, brown). Here the higher curvature couplings take the values $\lambda = 0.04, \mu = 0.001$, while the cosmological constant is fixed using (3.88) in order to ensure that the metric functions have the same asymptotics.	87
3.2	The log-log plot of temperature versus entropy for asymptotically anti-de Sitter cubic quasitopological uncharged numerical black holes where $k = -1, 0, 1$ (pink, black, brown). Here the higher curvature couplings take the values $\lambda = 0.04, \mu = 0.0003$, while the cosmological constant is fixed using (3.88) in order to ensure that the metric functions have the same asymptotics.	88
3.3	The log-log plot of temperature versus entropy for asymptotically anti-de Sitter five-dimensional quartic quasitopological uncharged numerical black holes where $k = -1, 0, 1$ (red/solid, green/dashed, blue/dotted, respectively). Here the higher curvature couplings take the values $\lambda = 0.04, \mu = 0.001, \xi = 0.0003$, while the cosmological constant is fixed using (3.104) in order to ensure that the metric functions have the same asymptotics.	90

4.1	A plot of the μ -dimensionless Gibbs free energy g versus μ -dimensionless temperature t where μ is negative. In this figure, we are in five dimensions, looking at a set of spherical uncharged black holes, with the parameter $\alpha = 4$. We see a characteristic “swallowtail” on the lower branch of the free energy, corresponding to a phase transition.	106
4.2	Three plots of $T_{RN-Pade}$ when $q = 0$ (solid blue) compared with the dataset generated from the exact temperature (4.16) (dashed green). The horizontal axis is the horizon radius r_h and the plots encompass values of $l = 3.66$, $l = 8.56$, and $l = 6.46$ respectively.	111
4.3	Three plots of the series expansion of $T_{RN-Pade}$ when $q = 1.0$ (solid red) compared with the $T_{RN-Pade}$ (solid blue) and the dataset generated from the exact temperature (4.16) (dashed green). The horizontal axis is the horizon radius r_h and the plots encompass values of $l = 3.66$, $l = 8.56$, and $l = 6.46$ respectively.	113
4.4	Two plots of the Gibbs free energy (obtained from numerical data) versus the series expansion of the temperature. On the top we have a larger range of cosmological constant considered, where the values of l are in the range $\{5.0, 5.5, 6.0, 6.5, 7.0\}$ ({Red, Blue, Green, Black, Orange}) while the figure on the bottom has l taking the range $\{6.01, 6.03, 6.05, 6.07, 6.09\}$, with the same colour profile.	115
4.5	The analytic (blue, solid) and series (red, dashed) inverse of $(\partial V/\partial P)_T$ is plotted versus l when $V = V_c$. We see a very good match near the critical point (when the inverse reaches zero).	116

Chapter 1

Introduction

In this thesis I will attempt to achieve two goals. The first will be to give a clear outline of the development of higher dimensional anisotropic black hole thermodynamics, in a way that is consistent and understandable. The second will be to summarize my contributions to this field in a way that is also consistent and with a high degree of detail, to make any future work on these topics as easy and straightforward as possible. Therefore, I have spent time unifying the notation of numerous papers, so you may notice some differences between the variables of this thesis and the sources referenced. Furthermore, in the interest of pedagogy I have provided a number of new illustrative examples that elucidate behaviour that either is relevant and important but uncommonly discussed (for example, the effect of choice of cosmological constant in higher curvature gravity (2.18)), is algebraically lengthy (like the details of the shooting method in section 3.5), or is conceptually interesting but to date has not yet yielded novel results (such as the content of section 4.3).

Contentwise, I will spend the second and third chapters on higher curvature and anisotropic theories of gravity respectively, particularly focusing on black holes and their thermodynamics, followed by a fourth chapter discussing the unification of these two ideas into “higher curvature anisotropic black holes”, the relationship of these black holes to thermodynamic universality, and a presentation of some related new results and methods. Much is currently understood about the solutions that completely obey various simple background symmetries, but this thesis will emphasize solutions that only asymptotically obey said symmetries in order to achieve more complicated behaviour (primarily thermodynamical behaviour). Sometimes algebraically sizeable exact solutions have been found, which I will present. Numerical methods are also used to probe scenarios for which we do not have exact solutions, and I will detail those as well.

The core of this thesis will be the work published over the course of my PhD which focuses on black hole thermodynamics. In particular, the thesis comprises the background and better part of my work on five-dimensional numerical Lifshitz symmetric quartic quasitopological black hole thermodynamics [1], criticality and the universality class of cubic quasitopological black holes in five dimensions [2], and the determination of mass and volume from a conjectured Smarr relation and a power series expansion of entropy and temperature [3]. These research papers build substantially on some of my previous work, namely the numerical Lifshitz symmetric cubic quasitopological black hole of [4] and the exact charged five-dimensional cubic quasitopological black hole solution found in [5]. Because this research has not yet been related to the studies of quantum detectors and temperature performed in [6, 7] (though this relationship may be examined in the foreseeable future, as an extension to background black hole metric functions is feasible and interesting), and to the topos quantum physics in [8], these other works will not be featured in this thesis, even though the papers [6, 7] were published over the course of my PhD.

Much of the work involved in writing this thesis consists of unifying the relatively different notation of the aforementioned articles, and of cataloguing the relevant knowledge in a way that is easy to read and understand. This thesis also features a pedagogical exercise in numerically obtaining the universality class of a black hole, in the hope that the ease of this approach is recognized and used towards a better understanding of thermodynamics and holography in scenarios where exact solutions to the Einstein Field Equations are not known (which is unfortunately a rather common scenario).

To complete this introduction I will discuss two of the fundamental ideas required to motivate and form a background for the work in this thesis: the anti-de Sitter spacetimes (and asymptotically anti-de Sitter spacetimes) and the gauge/gravity duality. The Lifshitz symmetric spacetimes will be introduced as spacetimes that break the symmetry of anti-de Sitter spacetime in a special way, while the study of higher curvature and Lifshitz symmetric solutions are both motivated here by the gauge/gravity duality.

1.1 Anti-de Sitter Spacetimes

An important aspect of the gauge/gravity duality, and a common asymptotic symmetry of many of the spacetimes described in this thesis, is the anti-de Sitter symmetry. In this section I will provide a brief outline of anti-de Sitter (AdS) spacetimes, primarily following more detailed illustrations such as [9].

Anti-de Sitter spacetimes begin with the embedding of a spatial hyperboloid surface,

which at constant time slices obeys

$$-Z^2 + X^2 + Y^2 + \dots = -\tilde{L}^2(T) \quad (1.1)$$

into a flat spacetime;

$$ds^2 = -dT^2 - dZ^2 + dX^2 + dY^2 + \dots \quad -T^2 - Z^2 + X^2 + Y^2 + \dots = -L^2 \quad (1.2)$$

is the metric and constraining equation where L is a lengthscale for the hyperbolic spacetime. I will relate it to the ‘‘AdS lengthscale’’ or ‘‘cosmological lengthscale’’ in this thesis.

In order to obtain the form of the metric that I will use in this thesis (2.63), I will need to perform a coordinate transform which combines three of the coordinates (here T, Z, X) into two new coordinates (t, r) by using the constraint on the squares of the coordinates from (1.2). The substitution

$$\begin{aligned} T &= \frac{r}{2L^2} \left(-t^2 + \frac{L^4}{r^2} + L^2 + y^2 + \dots \right) \\ X &= \frac{r}{2L^2} \left(-t^2 + \frac{L^4}{r^2} - L^2 + y^2 + \dots \right) \\ Z &= \frac{rt}{L} \\ Y &= \frac{ry}{L} \\ &\vdots \end{aligned} \quad (1.3)$$

is performed. This coordinate transform is smooth and invertible for positive radius r , i.e. it is a diffeomorphism, and will not alter the curvature (1.7).

This ultimately yields a line element

$$ds^2 = -\frac{r^2}{L^2} dt^2 + \frac{L^2 dr^2}{r^2} + \frac{r^2}{L^2} d\Omega_{D-2,0}^2 \quad (1.4)$$

which we can see takes the form of (2.63) for $f(r) \rightarrow 1$ and $g(r) \rightarrow 1$. This yields the $k = 0$ case of the constant curvature hypersurface, defined by

$$d\Omega_{D-2,k}^2 = d\theta_1^2 + k^{-1} \sin^2(\sqrt{k}\theta_1) \left(d\theta_2^2 + \sum_{i=3}^{D-2} \prod_{j=2}^{i-1} \sin^2 \theta_j d\theta_i^2 \right) \quad (1.5)$$

The essential property of this spacetime is its constant negative curvature. We can show this by computing the Ricci scalar; the only nonzero Christoffel symbols (see (2.6))

are

$$\begin{aligned}\Gamma_{tt}{}^r &= \frac{r^3}{L^4} & \Gamma_{tr}{}^t &= \frac{1}{r} & \Gamma_{rr}{}^r &= -\frac{1}{r} \\ \Gamma_{ri}{}^i &= \frac{1}{r} & \Gamma_{ii}{}^r &= -\frac{r^3}{L^2}\end{aligned}\tag{1.6}$$

where the indices i are the complete set of spacetime indices excluding $\{r, t\}$.

Then, the curvature scalar can be computed (the Ricci scalar is given by the equations (2.3)-(2.5)) as

$$R = -\frac{(D)(D-1)}{L^2}\tag{1.7}$$

where D is the total number of spacetime dimensions in (1.4). Thus, the AdS spacetime is said to have constant negative curvature, where the curvature is inversely proportional to L^2 .

Finally, since this is a constant curvature solution, the AdS spacetime is a solution to the vacuum Einstein field equations when a cosmological constant $\Lambda = -(D-1)(D-2)/2L^2$ is added to the action:

$$\mathcal{S} = \frac{1}{16\pi} \int d^D x \sqrt{-g} (R - 2\Lambda)\tag{1.8}$$

The AdS spacetime has a number of useful properties. Important here is that the nature of the negative curvature acts in a confining manner; light rays following null geodesics will reach the spatial boundary (located at $r \rightarrow \infty$) in finite coordinate time, and so boundary conditions need to be imposed in order to have a well-posed initial value problem.

Interpreting this type of confinement as a gravity theory with some external pressure will also give rise to the extended phase space thermodynamics that I discuss for various theories, starting in 2.1.3.

Finally, the notion of asymptotically anti-de Sitter spacetimes is relevant to this thesis. When I use the words asymptotically AdS, I mean a spacetime whose line element becomes equal to (1.4) as $r \rightarrow \infty$. The boundary is assumed to be $\mathbb{R} \times \mathcal{S}^{D-2}$, though few results in this thesis are dependent on this assumption. Studying spacetimes that are only asymptotically AdS allows for more complicated, thermodynamically interesting solutions than restricting ourselves to pure AdS, such as the AdS-Schwarzschild black hole in arbitrary dimension. The higher dimensional Schwarzschild black hole is commonly termed the Tangherlini black hole; in this thesis we will be mostly concerned with higher dimensional AdS-Schwarzschild black holes in addition to their extensions to theories with higher curvature, anisotropy, or Maxwell charges.

To obtain this solution we promote the metric (1.4) to a more general form with metric functions

$$ds^2 = -\frac{r^2}{L^2}f^2(r)dt^2 + \frac{L^2 dr^2}{r^2 f^2(r)} + \frac{r^2}{L^2}d\Omega_{D-2,k}^2 \quad (1.9)$$

where the constant curvature hypersurface is given by (1.5). The specific transformation used on pure AdS (1.2) to obtain these constant-curvature spatial slices is given by the transformations

$$\begin{aligned} T &= L\sqrt{1 + k\frac{r^2}{L^2}} \cos(\sqrt{k}t) \\ Z &= L\sqrt{1 + k\frac{r^2}{L^2}} \sin(\sqrt{k}t) \\ X &= r\frac{\cos(\sqrt{k}\theta_1)}{\sqrt{k}} \\ \Theta^{(i)} &= r\frac{\sin(\sqrt{k}\theta_1)}{\sqrt{k}} \cos(\theta_i) \prod_{j=2}^{i-1} \sin \theta_j \\ \Theta^{(D-1)} &= r\frac{\sin(\sqrt{k}\theta_1)}{\sqrt{k}} \prod_{j=2}^{D-2} \sin \theta_j \end{aligned} \quad (1.10)$$

where $Y = \Theta^{(2)}$, for example, and i ranges from 2 to $D - 2$, where as is convention in this thesis, D is the number of dimensions of the resultant metric (1.9).

This line element can describe an exact black hole solution; in this case the metric function $f^2(r)$ in (1.9) takes the form [10]

$$f^2(r) = k\frac{L^2}{r^2} - \frac{2\Lambda}{(D-1)(D-2)L^2} - \left(\frac{m}{r}\right)^{D-3} \quad (1.11)$$

where m is a term proportional to the black hole's mass.

In this solution, we now have the appearance of an event horizon with a temperature that we can compute. We will develop the procedure to do this, and to describe the thermodynamics of black holes like this, beginning in section 2.1.1.

1.2 Gauge/gravity duality

One of the motivations for a large portion of the work done in this thesis is the concept of a gauge/gravity duality, a general conjecture that a gravity theory (perhaps a string

theory, or maybe some theory that is classically approximated by Lovelock gravity) has non-perturbative relationships between the correlation functions of the local operators of a gauge theory (the “dual theory”) and the partition function of fields in the gravity theory.

This relationship has now been studied extensively, both in the original context of an $\mathcal{N} = 4$ super-Yang-Mills theory (a conformal field theory) and a five-dimensional gauged supergravity theory (which is asymptotically AdS_5) [11], and in a wide variety of spacetimes [12]. The most typical statement is that the asymptotically AdS_D gravity theory is dual to a conformal field theory on the boundary (in one fewer dimension), $\mathbb{R} \times \mathbb{S}^{D-2}$.

This is made more concrete through the GKP-Witten relation [9]

$$Z_{\text{CFT}_{D-1}} = Z_{\text{AdS}_D} \tag{1.12}$$

which states that the conformal field theory partition function is equivalent to that of the string theory in asymptotically AdS spacetime in one greater dimension [13, 14].

Commonly, solutions are known to a classical gravity theory, and in this case a limit of the string theory is taken which corresponds to a large number of colours in the gauge theory (N_c). The so-called “holographic dictionary” of relationships between parameters in the CFT and bulk classical gravity theory is constructed, and can be used to examine quantities in one theory that are difficult to compute in the other.

For example, the strongly coupled gauge theory’s partition function is challenging to evaluate due to a breakdown in perturbation theory, but if this corresponds to a classical gravitational theory, we can perform computations in the bulk which will correspond to quantities in the gauge theory. An example of this application is the computation of the shear viscosity in the $\mathcal{N} = 4$ Super-Yang-Mills plasma, using the AdS/CFT holographic dictionary [15].

In this thesis I will not go into detail on much of the specific and detailed work that has been done on the AdS/CFT correspondence, because it is voluminous and because the amount of required background would be burdensome. Instead, I am concerned with examining a broader concept, the idea that the relationship between gravitational theories and gauge theories can extend beyond conformal field theories and asymptotically anti-de Sitter gravity.

In addition to AdS/CFT, there has been plenty of interest in the extension to a dS/CFT correspondence, where the de Sitter spacetime (with a constant positive curvature) is hoped to show correspondence with a conformal field theory in one fewer dimension [16, 17, 18]. The move to de Sitter spacetimes adds challenges; for example, a black hole in asymptotically de Sitter spacetimes has a complicated thermodynamic relationship with the cosmological horizon; the expectation that both horizons have a temperature lead them to

form a system that is not necessarily in thermodynamic equilibrium, which makes studying the relationship between thermal conformal field theories and black holes challenging. Nonetheless, this research does provide evidence that a relationship between these theories is plausible.

Other proposed dualities abound in recent years, such as the relationship between near-horizon extremal Kerr black holes and CFTs [19], the relationship between asymptotically flat spacetimes and conformal field theories [20], and various extensions of AdS/CFT to physical systems such as superconductors [21] and ideal fluids [22].

Grouping these studies together comprises the conjectured gauge/gravity duality. Essentially, when it comes to gravity theories, the search is on for their corresponding dual, and for insights from exotic spacetimes or condensed matter physics that can be applied to give a deeper understanding of the precise mathematical relationship between such disparate theories.

This thesis is concerned with what could be viewed as a coarse-graining of the gauge/gravity duality. Instead of finding a gauge theory which exactly corresponds to the partition functions of whichever gravity theory, I instead discuss and develop techniques to relate these theories only in certain locations of thermodynamic parameter space.

The tool I use to do this is universality, a feature exhibited by systems at Thermodynamic criticality, and so I focus on the classification of criticality of gravitational systems, and on developing tools to simplify identifying criticality and obtaining the corresponding universality classes. Critical points are properties of many thermodynamic systems with phase transitions. The phenomenon is associated with the indistinguishability of phases; a critical point will end a line of phase transitions. A number of curious features emerge near criticality, such as correlations being formed over diverging lengthscales [23]. As criticality is approached the theory therefore becomes spatially non-local. Other properties of the system will also diverge, and the nature of these divergences is what will allow us to classify the systems into universality classes. Near criticality the macroscopic thermodynamic phenomena are the same for theories of the same universality class.

Knowing the universality class is an important step to understanding the gauge/gravity duality. If a black hole solution has a universality class that isn't shared with any known condensed matter systems, then there exists a very interesting question to pose: has holography broken down? Can it be salvaged? Or could this be a path towards uncovering interesting new models in condensed matter physics?

This approach is relatively young, but in this thesis I will outline some of the preliminary work that has been done on the topic of understanding universality in the context of the gauge/gravity duality.

1.3 Conventions

Briefly, it is important that I make a short note about the various conventions used in this thesis. Numerical quantities will be in standard equation-face, e.g. a . Operators and other quantities which may not commute (such as matrices) will be written using a boldface, e.g. \mathbf{a} . Blackboard bold face typesetting will be used as in standard mathematics to represent mathematical entities like such as the set of complex numbers \mathbb{C} or the set of real numbers \mathbb{R} . In a small divergence from standard notation, the curly typeface \mathcal{S} is used to represent the sphere, since S will be used for the entropy and \mathcal{S} will be used for the action.

For D -dimensional manifolds, I will use Greek indices which range over every dimension D , while Latin indices will be used for quantities on lower-dimensional submanifolds. For example, working in a 5-dimensional spacetime, Greek indices α will run from 0 to 4, while on a 4-dimensional hypersphere embedded in the spacetime, Latin indices i will be used, and will run from 0 to 3.

The metric sign convention will be the usual one used in general relativity: $(-, +, +, \dots, +)$. The standard conventions for partial and covariant derivatives will be used:

$$\frac{\partial}{\partial x^\mu} T_\nu \equiv \partial_\mu T_\nu \equiv T_{\nu,\mu}$$

where partial derivatives can be represented by tensor indices following a comma (and covariant derivatives following a semicolon).

I will generally refer to horizons in this thesis, keeping in mind that there are many different notions of a “horizon” in general relativity. Unless otherwise indicated, when I use the term horizon, it will denote the event horizon of the black hole - the bifurcate Killing horizon formed by the $D - 2$ dimensional surface on which the timelike Killing field’s norm is zero; i.e. the Killing field becomes null [24].

The horizon radius will be denoted by r_h . In most of the content, the general notation for a lengthscale will be l , while the lengthscale generated by the cosmological constant will be L . However, to agree with conventions in the literature, in much of chapter 3, the opposite notation will be used; l for the cosmological lengthscale and L for a general dimension of “length”.

I shall attempt to consistently keep Planckian natural units. Thus, $c = \hbar = G = k_B = k_e \equiv 1$ for the majority of numerical quantities in this thesis.

The area of a unit hypersurface will be denoted $\omega_{D,k}$ where D is the dimension of the hypersurface and k is the topology. Here $k \in \{-1, 0, 1\}$, where -1 is a hyperbolic surface, 0

is planar, and 1 is spherical. Since the context of this work does not require regularization of these surface areas, I will occasionally explicitly evaluate $\omega_{D,1}$ but I will leave this area symbolic when $k = -1, 0$. In the spherical case, this evaluates to

$$\omega_{D,1} = \frac{2\pi^{(D+2)/2}}{\Gamma(\frac{D}{2} + 1)} \tag{1.13}$$

$$\Gamma\left(\frac{D}{2} + 1\right) \equiv \int_0^\infty dx \cdot x^{\frac{D}{2}} e^{-x}$$

This variable will also be used to represent the hypervolume of the unit sphere in D dimensions, which is given by $\omega_{D+1,1}/2\pi$.

The hypersurface area will often arise in this thesis as the result of the integral

$$\omega_{D,k} = \int_{\Sigma_k} \sqrt{\sigma_k} \tag{1.14}$$

where $\sqrt{\sigma_k}$ is the square root of the determinant of the metric tensor of the hypersurface and Σ_k is the hypersurface.

Finally, computational algebra software was used for a number of high-level computations in this thesis. For compatibility and algorithm documentation, the versions used were Maxima 5.34.1 [25], Maple 13 [26], and Mathematica 10.4 [27].

Chapter 2

Higher Curvature Gravity Theories

In this chapter I will elaborate on the reasons for studying various classes of higher curvature black hole solutions, and I will encapsulate my work on black hole thermodynamics in higher curvature gravity.

To attain higher curvature solutions, we begin with a modification of the Einstein-Hilbert action, which consists of the Ricci scalar $\mathcal{L}_1 \equiv R$ coupled to the square root of the determinant of the metric tensor, by adding terms which are higher (and lower, in the case of a cosmological constant) in powers of the tensorial expressions of curvature for the manifold:

$$\mathcal{S} = \frac{1}{16\pi} \int d^D x \sqrt{-g} (-2\Lambda + \mathcal{L}_1 + \mathcal{F}(R, R_{\mu\nu}, R_{\mu\nu\alpha\beta})) \quad (2.1)$$

$$= \frac{1}{16\pi} \int d^D x \sqrt{-g} \left(-2\Lambda + \sum_i \mu_i \mathcal{L}_i \right) \quad (2.2)$$

where D is the number of spacetime dimensions, Λ is the cosmological constant, \mathcal{L}_1 is the Ricci scalar, g is the determinant of the metric tensor $g_{\mu\nu}$, and the function $\mathcal{F}(R, R_{\mu\nu}, R_{\mu\nu\alpha\beta})$ is some scalar combination of the Ricci scalar, Ricci tensor, and Riemann tensor. We can group this function into combinations of terms that are linear in curvature (e.g. the Ricci scalar), quadratic in curvature (e.g. the square of the Ricci scalar) and so on, with a coupling constant μ_i for the terms that are of i^{th} order in curvature. These curvature tensors are built from the theory's metric tensor as

$$R_{\mu\nu\rho}{}^\sigma = \partial_\nu \Gamma_{\mu\rho}^\sigma - \partial_\mu \Gamma_{\nu\rho}^\sigma + \Gamma_{\lambda\nu}^\sigma \Gamma_{\mu\rho}^\lambda - \Gamma_{\lambda\mu}^\sigma \Gamma_{\nu\rho}^\lambda \quad (2.3)$$

$$R_{\mu\nu} = R_{\mu\lambda\nu}{}^\lambda \quad (2.4)$$

$$R = g^{\mu\nu} R_{\mu\nu} \quad (2.5)$$

and the Christoffel symbols are given by [28]

$$\Gamma_{\nu\alpha}^{\mu} = \frac{1}{2}g^{\mu\lambda} \left(\frac{\partial g_{\alpha\lambda}}{\partial x^{\nu}} + \frac{\partial g_{\lambda\nu}}{\partial x^{\alpha}} - \frac{\partial g_{\nu\alpha}}{\partial x^{\lambda}} \right) \quad (2.6)$$

where $g_{\mu\nu}$ is the metric tensor.

In the case when no higher curvature terms are added to the action, and only the Ricci scalar, cosmological constant, and matter terms are used, I denote these as the Einsteinian solutions. In this thesis I will focus on the development of solutions to the Einstein field equations when higher curvature terms are present.

First, I'll motivate these types of solutions. The addition of higher curvature terms in this form may be pathological, since if time derivatives higher than second order appear in the field equations, the theory will likely suffer from an Ostrogradski instability [29]. This completely classical instability is particularly toxic to canonical quantization, yielding negative energy modes that can cause the theory to suffer from uncontrollable particle production [30]. At the level of the Hamiltonian, the instability arises because of the appearance of terms linear in canonical momenta, which makes the Hamiltonian unbounded from below. There are some caveats and this stability can be 'cured'; we are free to explore functions \mathcal{F} which avoid this instability, or specific solutions that may result in a bounded Hamiltonian.

This basis for studying modifications to general relativity has had broad success for a wide variety of functions \mathcal{F} . One popular example is when $\mathcal{F} = f(R)$, a function of only powers of the Ricci scalar. This is popularly termed $f(R)$ gravity, and has been employed in inquiries into inflation and dark energy [31]. It is able to avoid instabilities through a degeneracy which appears when only powers of the Ricci scalar (and not Riemann or Ricci tensor, for example) are considered. There is also a wealth of work in modifying the gravitational action in other ways; a few examples include dRGT massive gravity [32], and generalized Brans-Dicke theory [31]. However, none of these models will be explicitly considered in this thesis. Instead we will look at higher curvature terms that eliminate third order and higher derivatives from the field equations.

Another justification for the introduction of higher curvature modifications is the hypothesis that we know about the low-energy sector of gravity, and so Einsteinian gravity forms a good low-energy limit but especially in higher dimensions, it seems natural to continue adding the Euler invariants to the theory, as we appear to observe both possible invariants in our four-dimensional theory of gravity [33, 34]. This line of reasoning shares overlap with pursuits of the quantum gravity community, and there have been indications that paths towards theories of quantum gravity can yield higher curvature terms, for example [35, 36], or even semiclassical arguments from one-loop contributions of matter fields

to the effective action [37]. I shall discuss some of these concepts in more depth later on in this thesis as I examine solutions in higher curvature theories of gravity.

Finally, in the context of gauge/gravity duality, it is expected that these higher curvature modifications in the bulk have substantive impact on the dual theory, such as the dual theory having a finite number of charges, or the expansion of the parameter space and therefore an expansion of the potential dual theories that can be studied [38, 39, 40, 41, 42].

I shall work on the quasitopological theories, which are similar to the Lovelock theories that will be described below. Both of these theories work by adding specially chosen terms to the action which, in the right combinations, remove any higher order derivatives in the field equations. This ensures that the theory's behaviour arises from at most a set of coupled second order nonlinear partial differential equations, avoiding Ostrogradski's instability.

My motivation for considering these theories in particular is because in addition to being conceptually simple in their avoidance of instabilities, they show similarity with terms from string theory, namely the quadratic Gauss-Bonnet term. These terms are therefore somewhat natural in their extension of Einsteinian gravity to high-curvature (potentially quantum gravity) scenarios.

2.1 Gauss-Bonnet and Lovelock Black Hole Thermodynamics

To motivate my work and for some historical background, a potential avenue around the problems introduced by generic higher curvature terms is the specific combination of terms that will maintain field equations which are always at most second-order in the metric tensor. These terms are built from lower-dimensional Euler characteristics, and are denoted *Lovelock terms*.

The Lagrangian densities for these characteristics have a relatively elegant expression,

$$\mathcal{L}_i = \frac{1}{2^i} \delta_{\beta_1 \beta_2 \dots \beta_{2i-1} \beta_{2i}}^{\alpha_1 \alpha_2 \dots \alpha_{2i-1} \alpha_{2i}} R_{\alpha_1 \alpha_2}^{\beta_1 \beta_2} \dots R_{\alpha_{2i-1} \alpha_{2i}}^{\beta_{2i-1} \beta_{2i}} \quad (2.7)$$

$$\delta_{\beta_1 \beta_2 \dots \beta_{2i-1} \beta_{2i}}^{\alpha_1 \alpha_2 \dots \alpha_{2i-1} \alpha_{2i}} \equiv \det \begin{vmatrix} \delta_{\beta_1}^{\alpha_1} & \dots & \delta_{\beta_{2i}}^{\alpha_1} \\ \vdots & & \vdots \\ \delta_{\beta_1}^{\alpha_{2i}} & \dots & \delta_{\beta_{2i}}^{\alpha_{2i}} \end{vmatrix} \quad (2.8)$$

where δ_{β}^{α} is the Kronecker delta function [43, 44].

Counterterms were proposed in [44] and are applied in, for example, [45]. Here I ignore these terms, though they will later reappear in my discussion of black hole mass.

Each term has a dimension below which it is a topological invariant, contributing only to the action as a total derivative. The i^{th} term will contribute to the equations of motion in spacetime dimensions $D > 2i$. This implies that in 3+1 dimensions, the only contributing Lovelock term is $\mathcal{L}_1 = R$. Further, in 4+1 dimensions, the second Lovelock term contributes; this term is known as the Gauss-Bonnet term: $\mathcal{L}_2 = R^2 + R^{\mu\nu\alpha\beta} R_{\mu\nu\alpha\beta} - 4R^{\mu\nu} R_{\mu\nu}$.

In this subsection I will examine the Gauss-Bonnet term in a pedagogical way. Most of what is said will generally apply to higher curvature theories, and extending the concepts here to higher curvature will become more clear when I discuss quasitopological gravity. The action for this theory with a cosmological constant and Gauss-Bonnet term can be written

$$\mathcal{S} = \frac{1}{16\pi} \int d^D x \sqrt{-g} \left(-2\Lambda + R + \mu_2 (R^2 + R^{\mu\nu\alpha\beta} R_{\mu\nu\alpha\beta} - 4R^{\mu\nu} R_{\mu\nu}) \right) \quad (2.9)$$

This gravitational action formed from the two Lagrangian densities $\mathcal{L}_1, \mathcal{L}_2$ is also sometimes known as the Lanczos, Gauss-Bonnet, or Lanczos-Gauss-Bonnet action, due to its initial publication by Lanczos in the 1930s [46]. It became a hot topic when it was implicated as the appropriate ghost-free low-energy limit of heterotic $E_8 \times E_8$ superstring theory [47]. There, it was also suggested that higher order Lovelock terms have a place in this low-energy limit.

The context of this thesis is on the implications of higher curvature terms on gauge/gravity dualities. It is currently expected that this type of duality should also hold for higher dimensional, higher curvature theories, but the exact details of the gauge theory that would correspond to a five-dimensional Lanczos-Gauss-Bonnet gravity theory are not yet well understood [48].

To this end, one direction we can take from the gravity side is to push the boundaries of what is known, and work towards extending the thermodynamic picture of the theory. Black holes in Lanczos-Gauss-Bonnet gravity have been known since at least the late 1980s to exhibit interesting behaviour, including the effect whereby Lovelock terms allow black holes with zero temperature at finite mass [34]. The entropy of these black holes also no longer obeys the standard relationship (where it is directly proportional to the event horizon area), and it is instead corrected by a term proportional to the coupling constant for the Gauss-Bonnet term that appears in the action.

Hyperbolicity of the theory has been directly studied in recent years [49] and while the theory does not always possess a well-posed initial value problem, the black holes we consider in AdS will be protected from the breakdown of hyperbolicity by the conditions on

positivity of energy flux in the dual CFT. It is highly likely that the quasitopological black holes introduced in section 2.2 will have similar behaviour since they share field equations with the Lovelock theories. For the higher curvature anisotropic black holes considered in this thesis, hyperbolicity remains an open question.

The relative simplicity of the black hole thermodynamics allows us to characterize the thermodynamic phase space of exact and numerical solutions in the theory, and this inches us closer to understanding the nature of the gauge/gravity duality in this context. Phase transitions and criticality in five-dimensional Lanczos-Gauss-Bonnet gravity can give insight into whatever thermodynamic behaviour the 4 dimensional gauge dual will exhibit, possibly even predicting new behaviour in a strongly coupled dual theory.

We therefore want to find the thermodynamic potentials, such as the Gibbs free energy, and examine thermodynamic stability, phase transitions, and critical points. In the interest of providing a reference that can be used to learn about holography, it is important to clearly document the variety of scenarios that we encounter: positive and negative cosmological constant, different branches of solution of the metric functions, asymptotic behaviour, *et cetera*.

We will examine the thermodynamics of higher curvature asymptotically AdS theories by interpreting the mass of the black hole as an enthalpy as per [50]. Here the cosmological constant will generate a thermodynamic pressure term $P = -\Lambda/8\pi$. The justification for this specific form of the pressure will be detailed in 2.1.3.

The holographic dual to the Lanczos-Gauss-Bonnet gravity theory was published in 2009 [51], establishing a dictionary and constraints on the theory. The major constraint is the positivity of the energy flux in the dual CFT, which ultimately results in a constraint on the values of the coupling μ_2 :

$$-\frac{(3D-1)(D-3)}{4(D+1)^2} \leq \frac{(D-3)(D-4)\mu_2}{L^2} \leq \frac{(D-3)(D-4)(D^2-3D+8)}{4(D^2-5D+10)^2} \quad (2.10)$$

where D is the total number of dimensions of the theory. In this thesis, I will be careful to remain within positivity bounds for higher curvature coupling constants, as I will always want a well conditioned dual theory.

Black holes may be found in these theories with a static and spherically symmetric metric ansatz,

$$ds^2 = -f^2(r)dt^2 + \frac{dr^2}{g^2(r)} + r^2 d\Omega_{D-2,k}^2 \quad (2.11)$$

where $d\Omega_{D-2,k}^2$ is the line element of a $D-2$ dimensional hypersurface of constant-curvature (spherical, hyperbolic, planar) topology when k is $(1,-1,0)$:

$$d\Omega_{D-2,k}^2 = d\theta_1^2 + k^{-1} \sin^2(\sqrt{k}\theta_1) \left(d\theta_2^2 + \sum_{i=3}^{D-2} \prod_{j=2}^{i-1} \sin^2 \theta_j d\theta_i^2 \right) \quad (2.12)$$

Exact solutions can be found for Gauss-Bonnet, third-order, and fourth-order Lovelock theories; in Gauss-Bonnet gravity with the action (2.9), one exact solution takes the form [52, 53]

$$f^2(r) = g^2(r) = k + \frac{r^2}{2(D-3)(D-4)\mu_2} \left(1 - \sqrt{1 + \frac{128\pi^2(D-3)(D-4)\mu_2 M}{(D-2)\omega_{D-1,k} r^{D-1}} + \frac{8(D-3)(D-4)\mu_2 \Lambda}{(D-1)(D-2)}} \right) \quad (2.13)$$

where M is a constant of integration that equals the mass (discussed later in 3.1.4). Generalization of the exact solutions to higher order Lovelock gravity can be performed, but the metric functions will arise as solutions of a higher-degree polynomial, and no closed radical solution can be given for theories that are higher than quartic in higher curvature couplings. Furthermore, each new term places a lower bound on the dimension of the theory; fifth order Lovelock gravity would require $D \geq 11$. Partly because of this, and partly because of a lack of convincing motivation to study these solutions at the moment, most work remains at quartic order or below.

Commonly, a redefinition of $\lambda \equiv \mu_2(D-3)(D-4)/L^2$ is performed, which simplifies the resulting expressions for metric functions as well as thermodynamic quantities. The solution (2.13) asymptotically (at large r) becomes

$$f^2(r) \rightarrow \frac{r^2}{2L^2\lambda} \left(1 - \sqrt{1 + \frac{8\lambda\Lambda L^2}{(D-1)(D-2)}} \right) \quad (2.14)$$

We can simplify this upon substitution of a specific value of the cosmological constant; for asymptotically AdS this choice typically takes one of two values; the first is the standard for asymptotically AdS Einsteinian gravity, $\Lambda = -(D-1)(D-2)/2L^2$. This is chosen because it allows one to compare the higher curvature theories directly with Einsteinian gravity a little more easily; the action for the theories is the same aside from the higher curvature terms [5]. One potential pitfall of this convention is that the asymptotics of the metric

function can behave unexpectedly, asymptotically depending on the value of the higher curvature coupling. For example, in this case the metric function is asymptotically

$$f_\infty(r) \rightarrow \frac{r^2}{2L^2\lambda} \left[1 - \sqrt{1 - 4\lambda} \right] \quad (2.15)$$

which implies that our metric has an effective cosmological constant

$$\Lambda^{\text{eff}} = -\frac{1 - \sqrt{1 + 4\lambda}}{2L^2\lambda} \quad (2.16)$$

In order to easily compare solutions with the same asymptotics, which becomes more important when they vary such as in Lifshitz symmetric spacetimes, another convention is to fix the cosmological constant to guarantee that

$$\lim_{r \rightarrow \infty} f(r) = r^2/L^2 \quad (2.17)$$

The cosmological constant will then take the form [1]

$$\Lambda = -\frac{(D^2 - 3D + 2)}{2L^2} (1 - \lambda) \quad (2.18)$$

We can most easily derive this from the characteristic polynomial of the Lovelock solutions. This polynomial, arising as a solution of the field equations, gives all branches of this family of exact Lovelock solutions [48, 45]. For Lanczos-Gauss-Bonnet, it is

$$-2\Lambda + \frac{(k - f^2(r))}{r^2} + \lambda \frac{(k - f^2(r))^2 L^2}{r^4} = \frac{\tilde{M}}{r^{D-1}} \quad (2.19)$$

Asymptotically, the solution for $f^2(r) \rightarrow r^2/L^2$ is

$$\Lambda = -\frac{1}{2L^2} (1 - \lambda) \quad (2.20)$$

In order to fix our effective cosmological constant to $(D-1)(D-2)/2L^2$ we only need to add this dimension dependent prefactor to this solution for Λ .

While this type of approach is useful for comparing the metric functions for different values of the higher curvature terms, it is important to take into consideration the effect that a cosmological constant that is dependent on higher curvature couplings has on the thermodynamics. The solutions for different values of the parameter λ , for example,

will have different temperatures and so for examining the thermodynamic behaviour between different values of the higher curvature parameters, it is often best to use a fixed cosmological constant for all solutions.

Before turning to the thermodynamics of this solution, we need to discuss the possible branches. A more comprehensive examination of the Lovelock solutions [48] is needed to completely understand the relevant asymptotics. The characteristic polynomial (2.19) clearly has two solutions, only one of which we examined. This is a general feature of the Lovelock characteristic polynomial; i^{th} order Lovelock will have i branches of solution for the metric functions, and in each case one of these branches will not generally reduce to the set of solutions in $(i - 1)^{\text{th}}$ order Lovelock gravity as the coupling constant $\mu_i \rightarrow 0$.

In this case I discussed the branch that does reduce to the $\mu_2 = 0$ solution, but in this thesis I will typically allow for any possible solutions that have the correct asymptotics. The other branch (with a plus sign in front of the square root) will diverge like $r^2/\mu_2 L^2$ with small μ_2 .

There are a few important points to mention: first, the thermodynamics of the solutions can be computed from the level of the characteristic polynomial and so our thermodynamic description will encompass all of the branches. This means that at the level of this thesis, aside from when we specify exact solutions, we are looking at the stability of any of the branches. If there is a horizon radius that only one branch can reach, the thermodynamics at that horizon radius will then reflect the thermodynamics of only that branch.

A careful analysis [48] is able to distinguish between branches, which is important when considering stability with respect to the vacua for example, or extended phase space thermodynamics where the branches are deviating from one another considerably, but from a numerical context we are unable to study individual branches and so I instead work in a regime where continuity is paramount. Here the horizon radius is varied smoothly as long as the temperature function is smooth, and if it becomes discontinuous, the numerical procedure halts. This helps to ensure that we remain on a single branch.

The second point is that the thermodynamics' agnosticism to the branches of solutions is a mixed blessing; as can be seen from (2.16), the higher curvature terms produce an effective cosmological constant, and this "constant" differs depending on the branch that is considered. While we can group all of the branches under the same thermodynamics, we need to ensure that our solutions have the asymptotics that we expect (and that we may require). Accidentally making conclusions in an AdS scenario when the asymptotics are in fact de Sitter creates a large pitfall as thermal effects from the de Sitter cosmological horizon would then need to be considered in a proper thermodynamic analysis.

This is another benefit for the "unifying" cosmological constant approach - if we use a

cosmological constant like (2.18), we can manifestly guarantee that our solutions always have the correct asymptotics. When this becomes relevant I will discuss it later in this thesis. In the following subsection on thermodynamics as well as the section on quasitopological gravity, I will show plots of both conventions of cosmological constant to show the different effects on the thermodynamic behaviour.

First, before I explore the thermodynamics, I will describe the methodology used to obtain a temperature and an entropy for these black holes.

2.1.1 Temperature and Euclidean Periodicity

To facilitate the determination of the temperature of these black holes, we can employ the relationship between the statistical partition function and the path integral for gravity. This relationship agrees with other methods of determining temperature, for example, the Hawking temperature defined by the surface gravity κ

$$T_H = \frac{\kappa}{2\pi} \tag{2.21}$$

and therefore this method is widely used [54].

The Matsubara finite-temperature field theory partition function is the same as the path-integral quantum field theory partition function if the QFT imaginary time coordinate has periodicity equal to the inverse temperature of the thermal field theory. Extending this to static relativistic theories, the inverse temperature can be associated with the periodicity of the Euclidean time coordinate multiplied by the square root of the g_{tt} component of the metric tensor. The condition of regularity in the Euclidean metric is used to obtain this temperature.

An important comment is that this component varies with position, and so naturally (due to redshift) the temperature of black holes is dependent on the position of the space-time observer. The convention for framing black hole thermodynamics in asymptotically flat spacetimes is to evaluate g_{tt} at infinity. In the case where we have non-asymptotically flat solutions, the radius at which we define temperature is the Tolman radius [55, 56]. It is outside of the scope of this thesis but the notion of an observer for the spacetime thermodynamics fixes a coordinate system in which we can evaluate a temperature and a volume; these are the quantities that appear in the first law. This notion remains compelling but is not fully understood, especially for stationary (rather than static) spacetimes. I introduce this concept here to point out that we must be careful regarding observer-dependent quantities in black hole thermodynamics.

Begin by considering an asymptotically flat, static, Euclideanized black hole spacetime [54, 57], where the time coordinate of (2.11) has been Wick-rotated under the operation $t \rightarrow \tau = it$:

$$ds_E^2 = f^2(r)d\tau^2 + \frac{dr^2}{g^2(r)} + r^2 d\Omega_{D-2,k}^2 \quad (2.22)$$

Since this is an asymptotically flat spacetime as $r \rightarrow \infty$, the metric (2.22) becomes

$$ds_E^2|_{r \rightarrow \infty} \sim d\tau^2 + dr^2 + r^2 d\Omega_{D-2,1}^2 \quad (2.23)$$

which has an $\mathbb{R}^2 \times \mathcal{S}^{D-2}$ topology, but when the Wick rotation requires periodicity of τ , the topology is $\mathbb{R} \times \mathcal{S}^{D-2} \times \mathcal{S}^1$. Near-horizon, assuming the periodicity of τ to be α , the metric (2.22) takes the form

$$ds_E^2|_{r \rightarrow r_h} \sim \left(\frac{\alpha}{2\pi}\right)^2 R^2 d\theta^2 + dR^2 + r_h^2 d\Omega_{D-2,k}^2 \quad (2.24)$$

after redefining the radial coordinate by

$$R = \int \frac{dr}{r\sqrt{g^2(r)}} \quad (2.25)$$

and the time coordinate by $\theta = 2\pi\tau/\alpha$, and after applying the regularity conditions (given in equation (12.5.8) in [54]). This derivation is performed in detail for an anisotropic spacetime below, and it directly applies to this case as well, so I will not go into detail yet.

The metric (2.24) is the metric of a cone [58] but if $\alpha = 2\pi$ we obtain a $\mathbb{R} \times \mathcal{S}^{D-2} \times \mathcal{S}^1$ space. In order to avoid a conical singularity and to be able to compare theories in this spacetime with the thermal field theory partition function, we set $\alpha = 2\pi$ which will let us compute the temperature. In this case the periodicity of the Euclidean time coordinate means we have a cylinder, both near the horizon and asymptotically, which is the type of spacetime desired; it is the one under which the spacetime partition function can be interpreted as that of a thermal field theory.

For the case in which we are interested, with AdS-like asymptotics, we can build on this approach. The Euclideanized metric looks like

$$ds_E^2 = \left(\frac{r}{L}\right)^{2z} f^2(r)d\tau^2 + \frac{L^2 dr^2}{r^2 g^2(r)} + r^2 d\Omega_{D-2,k}^2 \quad (2.26)$$

for some constant exponent z (required later, for the anisotropy we introduce in section 3), and we can expand near-horizon by transforming the radial coordinate $r \rightarrow R =$

$\int Ldr/r\sqrt{g^2(r)}$, because we are interested in computing the temperature at a horizon, when $f^2(r_h) = 0$. To first order in $(r - r_h)$, $f^2(r) \simeq (r - r_h)\tilde{f}^2(r_h)$, $g^2(r) \simeq (r - r_h)\tilde{g}^2(r_h)$, and

$$R \simeq \frac{2L^2\sqrt{(r - r_h)}}{\sqrt{r^2\tilde{g}^2(r_h)}} \quad (2.27)$$

Then, (2.26) becomes

$$ds_E^2 \simeq R^2 \left(\frac{r_h^{2(z+1)}}{4L^{2(z+1)}} \tilde{g}^2(r_h)\tilde{f}^2(r_h) \right) d\tau^2 + dR^2 + (r(R))^2 d\Omega_{D-2,k}^2 \quad (2.28)$$

which, after a final change of variable

$$\tau \rightarrow \theta = \left(\frac{r_h^{z+1}}{2L^{z+1}} \tilde{g}(r_h)\tilde{f}(r_h) \right) \tau$$

becomes

$$ds_E^2 \simeq R^2 d\theta + dR^2 + (r(R))^2 d\Omega_{D-2,k}^2 \quad (2.29)$$

which means θ must have periodicity 2π for regularity.

The periodicity of τ corresponds to the inverse temperature, so the inverse temperature of this spacetime is therefore

$$T^{-1} = \frac{4\pi L^{z+1}}{r_h^{z+1}\tilde{g}(r_h)\tilde{f}(r_h)} \quad (2.30)$$

and so the temperature is given by

$$T = \frac{1}{4\pi} \left(\frac{r_h}{L} \right)^{z+1} \sqrt{(f^2(r_h)'g^2(r_h)')} \quad (2.31)$$

where the prime denotes the derivative of the function with respect to r . This last relationship holds since

$$f^2(r) \simeq (r - r_h)\tilde{f}^2(r_h) + \mathcal{O}((r - r_h)^2)$$

and so

$$\left. \frac{df^2(r)}{dr} \right|_{r=r_h} = \tilde{f}^2(r_h) + \mathcal{O}(r - r_h)_{r=r_h} = \tilde{f}^2(r_h) \quad (2.32)$$

This expression is quite general and will be used throughout this thesis; in this section we apply it to the Gauss-Bonnet metric functions (2.13), where $z = 1$ and $f(r) = g(r)$.

For this solution, the temperature evaluates to

$$T = \frac{2r_h^3 + L^2kr_h - 2\lambda r_h^3}{2L^2\pi(r_h^2 + 2L^2k\lambda)} \quad (2.33)$$

when $\Lambda = -6(1 - \lambda)/L^2$, and

$$T = \frac{2r_h^3 + L^2kr_h}{2L^2\pi(r_h^2 + 2L^2k\lambda)} \quad (2.34)$$

when $\Lambda = -6/L^2$.

2.1.2 Entropy as a Noether Charge

The entropy of black holes has also featured strongly in the development of black holes as useful thermodynamic objects in relativity. For non-extremal black holes, the entropy is not typically a controversial issue as semiclassical approaches usually agree with Noether charge methods [48] though there are occasional discrepancies [59].

A semiclassical approach derives entropy from the partition function, which arises from the Euclidean action of the black hole. The thermodynamic formula for the entropy is given by [60]

$$S = -\left(\beta \frac{\partial}{\partial \beta} - 1\right) \log(Z) \quad (2.35)$$

where β is the inverse temperature T^{-1} , the partial derivatives are taken at fixed pressure, volume, charge, etc. [61], \tilde{S} is the Euclidean action, and Z is the partition function

$$Z = \int \mathcal{D}\Psi e^{-\tilde{S}} \approx e^{-\tilde{S}} \quad (2.36)$$

$$\tilde{S} = \beta H - \frac{1}{4} \mathcal{A} \quad (2.37)$$

In addition, H is the Hamiltonian of the theory and \mathcal{A} is the area of the black hole's event horizon. The method of steepest descent is used to approximate the integral (with measure $\mathcal{D}\Psi$ over all Euclidean configurations with periodic imaginary time, as in 2.1.1).

A number of other approaches in the Euclidean action regime have been compared with the Wald method, such as pair creation and boundary term methods, in [61].

In this thesis I will employ the Wald entropy formalism [62], which is defined by a Noether charge arising from the diffeomorphism invariance of the Lagrangian. In particular,

the simplest derivation is to take the Riemann tensor as some independent field in the Lagrangian, and the field equation from the variation of the Lagrangian with respect to the Riemann tensor is first obtained:

$$\mathcal{Y}^{\mu\nu\alpha\beta} \equiv \frac{\delta\mathcal{L}}{\delta R_{\mu\nu\alpha\beta}} \quad (2.38)$$

I do not have a good interpretation for the geometric significance of the variation of with respect to the Riemann tensor other than the fact that this approach yields a compact expression for the conserved current arising from diffeomorphism invariance.

The expression (2.38) is used to construct a covariant quantity called the symplectic potential form [24], which is utilized to build a current that is conserved under diffeomorphisms. From this current, the Iyer/Wald entropy can be defined by the integral over a closed surface as

$$S = -2\pi \oint d^{D-2}x \sqrt{\tilde{g}} \mathcal{Y}^{\mu\nu\alpha\beta} \hat{\epsilon}_{\mu\nu} \hat{\epsilon}_{\alpha\beta} \quad (2.39)$$

where \tilde{g} is the induced metric on the horizon and $\hat{\epsilon}_{\alpha\beta}$ is the binormal to the horizon, defined when ξ_μ is a Killing field normal to the horizon and n_μ is the unit normal to the horizon: $\hat{\epsilon}_{\alpha\beta} = \xi_{[\alpha} n_{\beta]}$ [62]. This entropy has been shown to obey the first law of thermodynamics (which I will elaborate upon later in this thesis).

In practise the Wald entropy turns out to be an easily calculable quantity for a variety of solutions that arise from the same action because for the higher curvature spacetimes considered here, it is proportional to the area of the horizon, with ‘‘correction’’ terms that appear due to the higher curvature couplings.

In Gauss-Bonnet gravity, the general Wald integral simplifies to [53]

$$S = \frac{1}{4} \int_{\Sigma_h} d^{D-2}x \sqrt{\tilde{g}} (1 + 2\mu_2 \tilde{R}) \quad (2.40)$$

where \tilde{R} is the Ricci scalar of the $D - 2$ dimensional horizon metric. Similar approaches have extended this to Lovelock couplings [63].

For the constant curvature horizon topologies considered here, when $\Lambda = -(D - 1)(D - 2)/2L^2$, this simplifies even further to yield

$$S = \frac{\mathcal{A}}{4} \left(1 + \frac{2\mu_2 k (D - 2) (D - 3)}{r_h^2} \right) \quad (2.41)$$

$$= \frac{r_h^{D-2} \omega_{D-2,k}}{4} \left(1 + \frac{2\lambda k L^2 (D - 2)}{(D - 4) r_h^2} \right) \quad (2.42)$$

which is the expression for the entropy of the black holes of horizon radius r_h with a Gauss-Bonnet term.

Briefly, I should comment on the negativity of entropy. Commonly, negative entropy is ignored, such as in [2]. This need not be done, as discussed in [53]. Redefining the entropy to give a lower bound of zero is possible, and it ends up with a scenario where black holes with finite horizon area have a non-zero entropy, since in this case the negative Gauss-Bonnet parameter also yields a finite size black hole with zero mass. In this thesis, the critical points that we need occur at horizon radii where the entropy is always positive, and so we do not need to concern ourselves with the appearance of negative entropy; typically we use the standard definition (2.41) and do not plot black holes with negative entropy.

2.1.3 Thermodynamics

Continuing to build the structure that I will use later in this thesis, the next step is to completely describe the thermodynamics of the Gauss-Bonnet black hole. Ultimately we will want expressions for the thermodynamic potentials, but for those we will need the mass, described in section 3.1. So, for this chapter, we will be satisfied with the quantities that are easily calculable from the temperature, entropy, and pressure. As a sanity check, we can ensure that the first law of thermodynamics is satisfied (it must be, since the Wald entropy is constructed to explicitly obey this relationship):

$$dM = TdS + \Phi dQ \tag{2.43}$$

This first law is a product of the revelation that various black hole parameters obey simple relationships analogous to the laws of thermodynamics; here M is the mass of the black hole (which can be a troublesome concept, as we shall later see), Q is the Maxwell charge of the black hole, and Φ is the electric potential of the Maxwell charge, taken to be at the horizon [3]. In general, ΦdQ can be extended to any “work terms” that will appear by adding, e.g. magnetic fields, to the thermodynamic system.

Historically, this relationship with the first law of thermodynamics was identified in the early 1970s. The Euler integral of the first law expression (2.43) was discovered for Kerr black holes [64] (this Euler integral is therefore referred to in this thesis as the Smarr relation), followed by the discovery of the relationship between the differentials of black hole quantities and the thermodynamic potentials [65].

However, we can immediately spot a parameter that is conspicuously missing from the relationship (2.43) - the cosmological constant. Its absence isn’t coincidental; if the

cosmological constant were to appear as an additional term in the first law, the differential nature of the relationship means that if we don't consider a variable cosmological constant, we will never uncover the additional term.

There are good reasons to expand our thermodynamic considerations to include a variable cosmological constant. It is wise to be wary of this scenario, because a time-varying cosmological constant has wide implications in the observable cosmology [66, 67, 68]. Especially important for this thesis is the observation that a time-varying cosmological constant would spoil our notions of temperature, entropy, and mass, making it more challenging to understand the system's thermodynamics. Fortunately, extending the thermodynamics to allow for a cosmological constant term does not require the cosmological constant to vary within the gravity theory. I will consider an ensemble of spacetimes, and so I can formulate a complete thermodynamic description, including the traversal through this ensemble, which is not performed in coordinate time. This not only lets us build the thermodynamic potentials in a way that is consistent with dimensional scaling of (2.44), but it also yields a framework for those who may wish to (carefully) explore theories with a time-varying cosmological constant.

The current understanding of mass as a thermodynamic quantity in black hole spacetimes with a cosmological constant is that it is not the internal energy of the spacetime, but instead it is the enthalpy [50]. Treating the cosmological constant as a thermodynamic variable [69] can be done in a way that yields a thermodynamic volume which agrees, in the simplest static cases, with the volume of the black hole as observed by a freefalling observer with zero velocity at the Tolman radius [56]. Questions still remain about how general this statement is; for rotating black holes, the spacetime is no longer static but it is stationary, and the relevant observer that yields this volume is an open question [70].

Overall, understanding the thermodynamics of spacetimes with a cosmological constant, where the cosmological constant acts as a pressure, has blossomed into a very active area of research in recent years [71, 72, 73, 74, 75, 70, 76, 76, 77, 78, 79, 80, 81, 82, 83, 45, 84] and it is hoped to yield insight into thermodynamics in general relativity with non-Minkowski asymptotics, which is relevant to understanding both the gauge/gravity duality as well as the thermodynamics of our own universe.

An intuitive argument for why the first law without a pressure is insufficient arises from the lengthscale generated by having a cosmological constant [50]. We can regard the first law as a relationship between the mass, entropy, and (perhaps) pressure. Eulerian scaling means that if a function obeys the scaling relationship $f(\alpha^p x, \alpha^q y) = \alpha^r f(x, y)$ on

its dependent variables, we must have

$$rf(x, y) = p \frac{\partial f}{\partial x} x + q \frac{\partial f}{\partial y} y \tag{2.44}$$

by taking partial derivatives with respect to the “lengthscale” α , and then setting $\alpha = 1$.

This argument can be applied to the thermodynamics of more typical systems, but because normally the entropy is extensive and additive, it obeys the relationship $S(\lambda U, \lambda V, \lambda N) = \lambda S(U, V, N)$, and the Eulerian scaling in (2.44) just yields $p = q = r = 1$. For black holes, entropy is related to the area rather than the volume, and so the scaling in the Smarr relation is unusual. This makes it an interesting relationship to study.

We have a good idea what the scaling of mass, entropy, and pressure should be. The area-law interpretation of entropy in section 2.1.2 indicates that $[S] \sim [l]^{D-2}$, where l is some dimensionful unit of length. We saw that additional higher curvature terms did not spoil this relationship; the cosmological lengthscale or the lengthscale of the coupling constant combines with that of the horizon radius to yield the same overall scaling as the area term. If the pressure is proportional to the cosmological constant, it should scale like $[P] \sim [l]^{-2}$, because it adds to the Ricci scalar in the action, which has spatial second derivatives of the (dimensionless in length) metric tensor. Finally, an argument for the scaling of mass is the dimensionality of the gravitational constant G which appears in front of the action (though we normalize it to 1 here). Keeping $c = 1$, $G \sim [l]/[M]$ and the integral in the action should have dimensionality $[l]^D/[l]^2$ so for a dimensionless action $[M] \sim [l]^{D-3}$.

In this case, $\alpha = l$ for the Eulerian scaling relationship and we find, using $f = M(S, P)$, that

$$(D - 3)M = (D - 2) \left(\frac{\partial M}{\partial S} \right)_P S - 2 \left(\frac{\partial M}{\partial P} \right)_S P \tag{2.45}$$

where pressure is defined by [50]

$$P = -\frac{\Lambda}{8\pi} \tag{2.46}$$

The constant factor used here is the one which gives agreement between the expected thermodynamic volume of the $D = 4$ Schwarzschild black hole (a spatial sphere of size equal to the horizon radius) when the temperature uses the horizon temperature in the coordinate system of an infalling observer with zero velocity at infinity (the rain observer). Remember that the volume is not a covariant notion and will differ depending on the coordinates of chosen observer.

Varying the cosmological constant needs to yield an extended first law; in the form that is compatible with this Smarr relation it suggests that the mass is related to the enthalpy of the black hole;

$$dM = TdS + VdP \tag{2.47}$$

Then,

$$\left(\frac{\partial M}{\partial S}\right)_P = T, \quad \left(\frac{\partial M}{\partial P}\right)_S = V \tag{2.48}$$

so the extended Smarr relation for uncharged black holes with a cosmological constant takes the form

$$(D - 3)M = (D - 2)TS - 2PV \tag{2.49}$$

If we were to add a Maxwell charge, for example, the Smarr relation and first law would respectively be

$$dM = TdS + VdP + \Phi dQ \tag{2.50}$$

$$(D - 3)M = (D - 2)TS - 2PV + (D - 3)\Phi Q \tag{2.51}$$

Here I need to give some additional background about the origin of this relationship, and some alternative methods of obtaining a thermodynamic construction like this. I choose to use a relatively general scaling argument, relying on the knowledge of the dimensionality of the thermodynamic properties I define. This is not the only way - the work in [50], for example, uses a geometrical derivation of the Smarr relation, relying on a Komar integral as well as the known fall-offs of metric functions in asymptotically anti-de Sitter space [85].

This geometric approach should be applicable here; however, the reason that I primarily rely on a scaling argument is discussed in the section on Lifshitz black holes 3. The fall-off behaviour is more complicated while the dimensional scaling of the thermodynamic quantities is not, so the scaling approach should apply without modification to spacetimes with more complicated fall-off behaviour.

While my approach in this thesis does ascribe significance to the first law, I merely apply these thermodynamic concepts to build a method for studying black hole thermodynamics in a way that easily handles a variety of asymptotic behaviour. At this point I do not assert that this technique is any more fundamental than the geometric nature of general relativity, since much of the interpretation here will rely on a good understanding of the Einstein Field Equations. There does exist independent work examining whether general relativity can emerge from thermodynamic principles, c.f. [86].

I will focus on the known phase transition in higher dimensional spherical AdS black hole spacetimes. This is similar to the Hawking-Page transition [87]. There exist two black

holes with the same temperature, but they have different horizon radius (and different mass), and the larger can be thermodynamically preferred. The question of whether it is thermodynamically preferred to the thermal vacuum has been addressed by examining the free energy of both solutions [48]. It can be seen that the larger AdS spherical black hole is thermodynamically preferred for Lovelock theories of gravity. In this situation if a black hole is to exist, the smaller black hole will phase transit to the larger via tunneling or some other physical process.

With the quantities we have already computed, the quickest way to observe this behaviour is by computing the specific heat. Recall from the second law of thermodynamics

$$S(T) = \int_{T_0}^T dt \cdot \frac{\delta Q}{t} = \int_{T_0}^T C(t) \frac{dt}{t} \quad (2.52)$$

where T_0 is some reference temperature (defining our point of reference for the entropy). Then,

$$\frac{dS}{d(\log(T))} = C(T) \quad (2.53)$$

so we can determine the sign of the specific heat (and therefore the stability) knowing only the temperature and the entropy.

Note that when I say stability here, I mean local stability. We have not completely calculated what the black hole becomes - it may be thermodynamically favourable to phase transit to a larger black hole or it may radiate away, or it could radiate to a smaller black hole that is stable. The precise scenario we are interested in is the phase transition to another black hole, so I will generally ignore the possibilities of a non-black hole background in this thesis. We do know from previous work, however, that in the simple spherical Lovelock context, the large black hole is thermodynamically preferred to the vacuum and to the small black hole [48]. I will work through the tools we need to compute the thermodynamic potentials in section 4.2, and that is when we can ultimately compute the free energy and determine stable solutions.

For the black holes with a Gauss-Bonnet coupling, we therefore plot entropy and temperature of these black holes on a log-log scale (for readability) and observe that when the slope of the curve is negative, the specific heat is also negative. This means that a decrease in entropy will correspond to an increase in temperature, and in similar fashion to the four-dimensional Schwarzschild black hole, these black holes will be unstable.

The log of the temperature is plotted versus the log of the entropy for the five-dimensional asymptotically AdS Gauss-Bonnet black hole of (2.19) in figure 2.1 for topologies $k = -1, 0, 1$. Here a specific value of the Gauss-Bonnet coupling is used, $\lambda = 0.04$. We

observe that there is a region of stable and unstable black hole solutions for the spherical topology for the dashed solution (when $\lambda = 0$, i.e. the Einsteinian case), while hyperbolic and planar topologies all have positive specific heat. This is indicative that in the $k = 1$ case, there is a phase transition between the small and large black holes for five-dimensional Einsteinian AdS black holes.

Here, $\lambda = 0.04$ is large enough to remove the instability and create spherical black holes which are stable for all radii. Smaller values of λ , for example, $\lambda = 0.01$ are sufficient to still observe a region of instability.

Furthermore, one can note that the asymptotic behaviour is different for different solutions by examining the right-hand side of the figure 2.1. This is because here, the cosmological constant was $\Lambda = -6(1 - \lambda)/L^2$ with $L = 1$ (for future reference, numerical plots will be in units of L , with the entropy also being written in units of the unit hypersurface (1.13), since in this thesis I do not attempt to define a regularization scheme for $k = -1$, for example). Had we used $\Lambda = -6/L^2$, all of the lines would converge to the same value for large black holes. This is indicative of the effect of the higher curvature Gauss-Bonnet term: it contributes primarily in the strong gravity regime (small black hole horizons will have higher surface gravity).

There exist constraints on the value of this coupling [88, 89, 41] due to holographic considerations. In five dimensions, these constraints (2.10) become [90]

$$-\frac{7}{36} \leq \lambda \leq \frac{9}{100} \quad (2.54)$$

which are important to consider when adding the higher curvature terms. In addition, we also consider only the black hole solutions that have positive entropy, and finally, we ensure that the horizon radius is real and positive (no naked singularities) and that the asymptotics are as desired (AdS in this case).

Because we have an exact solution (2.19), we can examine the thermodynamic effect of the Gauss-Bonnet term analytically [5]. Taking $D = 5$, $k = 1$, and $\Lambda = -6/L^2$, the specific heat takes the form

$$C_P = \frac{r \left(3r_h^2 + \frac{3}{2}L^2k \right) \left(r_h^2 + 2\lambda k L^2 \right)^2}{4k^2 L^4 \lambda + 24r_h^2 k \lambda - 2k L^2 r_h^2 + 4r_h^4} \quad (2.55)$$

which exhibits discontinuities due to roots in its denominator for certain values of λ and r_h .

In this case, the easiest way to obtain the specific heat exactly is from the interpretation of the mass as enthalpy; then

$$C_P = \left(\frac{\partial M}{\partial T} \right)_P \quad (2.56)$$

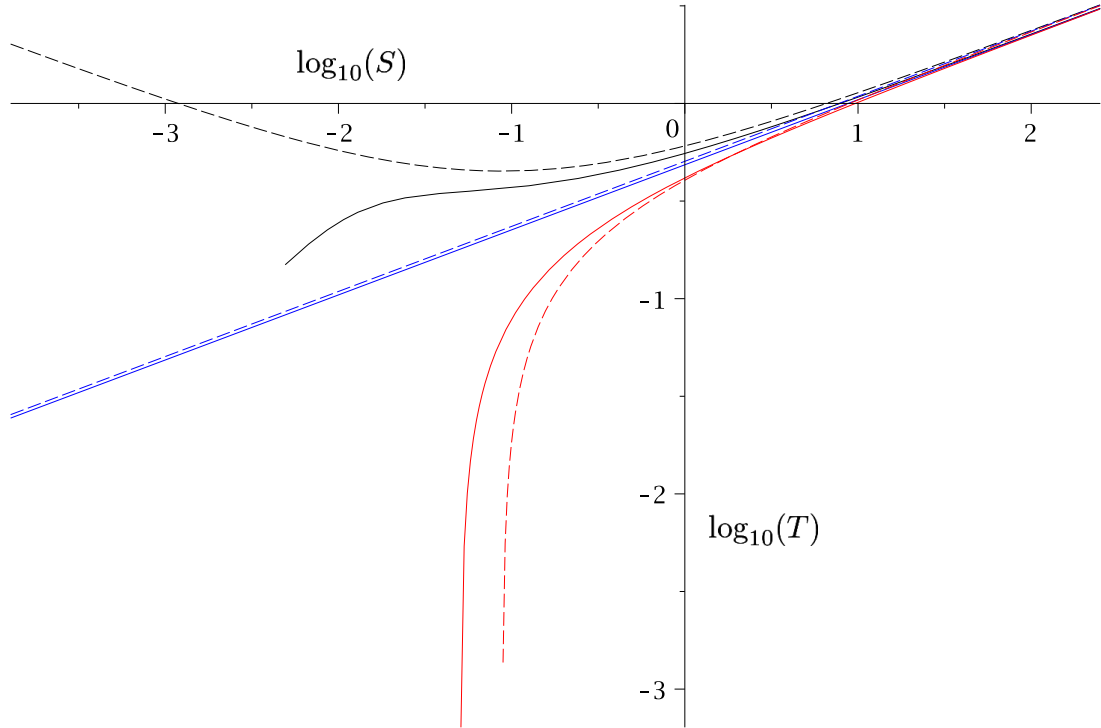


Figure 2.1: The log-log plot of temperature versus entropy for asymptotically anti-de Sitter Lanczos-Gauss-Bonnet Black Holes in five dimensions for $k = -1, 0, 1$ (red, blue, black). Here the higher curvature coupling is given by $\lambda = 0.04$, while the cosmological constant is fixed at $\Lambda = -6(1 - \lambda)/L^2$ which does not ensure that the thermodynamics has the same asymptotic behaviour. The dashed solution is Einsteinian for comparison; $\lambda = 0$ in that case.

so

$$C_P = \left(\frac{\partial M}{\partial r_h} \right)_l \left(\frac{\partial T}{\partial r_h} \right)_l^{-1} \quad (2.57)$$

In fact our mass \tilde{M} is not exactly equal to the mass of this black hole, merely proportional; this approach still works to identify the divergences of the specific heat. Applying this method here yields

$$C_P \sim \frac{16\pi L^2 r \left(3r_h^2 + \frac{3}{2} L^2 k \right) \left(r_h^2 + 2\lambda k L^2 \right)^2}{4k^2 L^4 \lambda + 24r_h^2 k \lambda - 2k L^2 r_h^2 + 4r_h^4} \quad (2.58)$$

This also tells us the relationship between the mass M and our mass parameter \tilde{M} . Being comfortable using mass parameters instead of the mass, and even more importantly using only other quantities like entropy and temperature, is crucial for when we will move to numerical black holes. In these cases we only have control over horizon radius and cosmological lengthscale so obtaining a mass parameter is challenging, let alone knowing the exact mass.

From observing the specific heat (2.55), we can see that it has zeroes for the $k = -1$ black holes, which turn out to be where the temperature would change sign to a negative temperature (which we do not consider here).

The singularities in the specific heat should correspond to a phase transition in the thermodynamic system, and so we can identify roots of the denominator;

$$r_h = \frac{L}{2} \sqrt{1 - 12\lambda + \sqrt{144\lambda^2 - 40\lambda + 1}} \quad (2.59)$$

is an example of one of the roots. For the Lanczos-Gauss-Bonnet black hole we can conceivably have two real roots. These locations are important to identify, since I shall be concerned with finding critical points in section 4.1 and I will do this making use of the knowledge of where the specific heat is singular, as we expect that one of these singular points (on the edge of where singularity occurs) will correspond to place where the thermodynamic potentials will have a finite first derivative, though in a numerical context this behaviour will have to be extracted from numerical data.

2.2 Quasitopological Gravity

The quasitopological gravity theories were first introduced in 2010 [91], followed shortly by an independent discovery featuring a presentation of the couplings and their holographic implications [90, 42].

The appeal of the quasitopological terms in this context is that they maintain field equations that are second order in terms of derivatives of the metric functions. We do not get something for nothing - this holds only in the case of spherical symmetry and if we break this symmetry we will have a theory with third order field equations. However, an added benefit is that these terms, unlike the Lovelock terms, are no longer topological invariants. That is, they impart nontrivial effects in dimensions lower than the Lovelock terms. In particular, the third and fourth order quasitopological terms have an effect in $D = 5$, while the only nontrivial Lovelock term in this dimension is the second order Gauss-Bonnet term. This nature will be exploited later on, because of the way holography is so intimately related to dimension.

The characteristic polynomial given from the equations of motion is the same up to conventions as that of Lovelock gravity of the same order, so in the context of the metric functions and the thermodynamics, the interesting avenue of research in quasitopological gravity is in dimensions in which the Lovelock terms are topological invariants, which amounts to studying the Lovelock solutions when their coupling parameter is appropriately redefined to absorb the dimensionally-dependent terms that go to zero in the Lovelock action [4].

In this thesis I will use the quasitopological terms primarily in five dimensions, to give additional complexity (and interesting behaviour!) to the (thermodynamic) parameter space of general relativity. Spherical symmetry will always be imposed. Much of the analysis of Lanczos-Gauss-Bonnet and Lovelock black holes will apply to the solutions that we discuss here.

Let us consider a general dimensional action with the third and fourth order quasitopological terms as an extension of the Lanczos-Gauss-Bonnet action (so $D \geq 5$): (2.9)

$$\mathcal{S} = \frac{1}{16\pi} \int d^D x \sqrt{-g} \left(-2\Lambda + \mathcal{L}_1 + \mu_2 \mathcal{L}_2 + \mu_3 \mathcal{X}_3 + \mu_4 \mathcal{X}_4 - \frac{1}{4} F_{\mu\nu} F^{\mu\nu} \right) \quad (2.60)$$

where $F_{\mu\nu}$ is the electric field strength for a Maxwell field which we have added in order to obtain charged black hole solutions.

The cubic quasitopological term takes the form

$$\begin{aligned} \mathcal{X}_3 = & R_{\mu}^{\nu} R_{\alpha}^{\beta} R_{\nu}^{\tau} R_{\beta}^{\sigma} R_{\tau}^{\mu} R_{\sigma}^{\alpha} + \frac{1}{(2D-3)(D-4)} \left(\frac{3(3D-8)}{8} R_{\mu\alpha\nu\beta} R^{\mu\alpha\nu\beta} R \right. \\ & - 3(D-2) R_{\mu\alpha\nu\beta} R^{\mu\alpha\nu}{}_{\tau} R^{\beta\tau} + 3D R_{\mu\alpha\nu\beta} R^{\mu\nu} R^{\alpha\beta} \\ & \left. + 6(D-2) R_{\mu}^{\alpha} R_{\alpha}^{\nu} R_{\nu}^{\mu} - \frac{3(3D-4)}{2} R_{\mu}^{\alpha} R_{\alpha}^{\mu} R + \frac{3D}{8} R^3 \right) \end{aligned} \quad (2.61)$$

while in the quartic term the constant coefficients are [92]

$$\begin{aligned}
c_1 &= -4(D-4)(2D^6 - 32D^5 + 195D^4 - 581D^3 + 876D^2 - 596D + 118) \\
c_2 &= 8(D-2)(D^7 - 11D^6 + 30D^5 + 102D^4 - 810D^3 + 1959D^2 - 2113D + 860) \\
c_3 &= -(D-2)(D^7 - 9D^6 + 5D^5 + 245D^4 - 1234D^3 + 2644D^2 - 2724D + 1108) \\
c_4 &= 16(D-2)^2(2D^4 - 34D^3 + 183D^2 - 389D + 274) \\
c_5 &= 64(D-3)(D-2)^2(4D^3 - 30D^2 + 75D - 58) \\
c_6 &= -96(D-2)(D-3)(2D^4 - 15D^3 + 37D^2 - 31D + 4) \\
c_7 &= -64(D-2)(3D^2 - 14D + 14)(D^2 - 5D + 7) \\
c_8 &= -32(D-2)^2(D-4)^2(3D^2 - 14D + 14) \\
c_9 &= 16(D-1)(D-2)(D-3)(D-4)(3D^2 - 14D + 14) \\
c_{10} &= D^5 - 36D^4 + 302D^3 - 1060D^2 + 1683D - 980 \\
c_{11} &= 56D^5 - 656D^4 + 3032D^3 - 6848D^2 + 7448D - 3104 \\
c_{12} &= 160D^5 - 1776D^4 + 7808D^3 - 17008D^2 + 18336D - 7808 \\
c_{13} &= 12D^6 - 206D^5 + 1512D^4 - 5712D^3 + 11816D^2 - 12738D + 5568 \\
c_{14} &= -D^8 + 14D^7 - 82D^6 + 276D^5 - 684D^4 + 1527D^3 - 2741D^2 + 2929D - 1292
\end{aligned}$$

and the quartic term takes the form

$$\begin{aligned}
\mathcal{X}_4 &= c_1 R_{\mu\nu\alpha\beta} R^{\alpha\beta\gamma\delta} R^{\lambda\kappa}_{\gamma\delta} R_{\lambda\kappa}{}^{\mu\nu} + c_2 R_{\mu\nu\alpha\beta} R^{\mu\nu\alpha\beta} R_{\gamma\delta} R^{\gamma\delta} + c_3 R R_{\mu\nu} R^{\mu\alpha} R_{\alpha}{}^{\nu} + c_4 (R_{\mu\nu\alpha\beta} R^{\mu\nu\alpha\beta})^2 \\
&+ c_5 R_{\mu\nu} R^{\mu\alpha} R_{\alpha\beta} R^{\beta\nu} + c_6 R R_{\mu\nu\alpha\beta} R^{\mu\alpha} R^{\beta\nu} + c_7 R_{\mu\nu\alpha\beta} R^{\mu\alpha} R^{\nu\gamma} R^{\beta}_{\gamma} + c_8 R_{\mu\nu\alpha\beta} R^{\mu\alpha\gamma\delta} R^{\nu}_{\gamma} R^{\beta}_{\delta} \\
&+ c_9 R_{\mu\nu\alpha\beta} R^{\mu\alpha} R_{\gamma\delta} R^{\nu\gamma\beta\delta} + c_{10} R^4 + c_{11} R^2 R_{\mu\nu\alpha\beta} R^{\mu\nu\alpha\beta} + c_{12} R^2 R_{\mu\nu} R^{\mu\nu} \\
&+ c_{13} R_{\mu\nu\alpha\beta} R^{\mu\nu\gamma\delta} R_{\gamma\delta}{}^{\alpha}_{\kappa} R^{\beta\kappa} + c_{14} R_{\mu\nu\alpha\beta} R^{\mu\gamma\beta\delta} R_{\kappa\gamma\lambda\delta} R^{\kappa\nu\lambda\beta}
\end{aligned} \tag{2.62}$$

Here, because the results will be directly extended to Lifshitz asymptotics as well, the static, spherically symmetric metric ansatz has the scaling behaviour brought outside of the metric functions, taking the form

$$ds^2 = -\frac{r^2}{L^2} f^2(r) dt^2 + \frac{L^2 dr^2}{r^2 g^2(r)} + \frac{r^2}{L^2} d\Omega_{D-2,k}^2 \tag{2.63}$$

where for AdS asymptotics the metric functions $f(r), g(r) \rightarrow 1$ as $r \rightarrow \infty$ and the hypersurface line element is again given by equation (2.12).

Numerical solutions up to the quartic case were described in [1]. In this section I only consider exact solutions, and the numerical work will be presented in the more general context of asymptotically Lifshitz spacetimes, in section 3.5.

We found an exact black hole solution in the case where $D = 5$; this is a cubic quasitopological black hole with a Maxwell charge, known as the Reissner-Nordström Cubic Quasitopological black hole [5]. In this work we extracted some dimensional- and lengthscale-dependent coefficients from the higher curvature couplings for simplicity in some computation. The new coupling parameters are

$$\frac{\lambda L^2}{(D-3)(D-4)} = \mu_2 \quad \frac{(16D-24)\mu L^4}{(3D^4-42D^3+205D^2-414D+288)} = \mu_3 \quad (2.64)$$

where in $D = 5$ the constant prefactors simplify to $1/2$ and $-7/4$, respectively. Commonly, $\mu \rightarrow -\mu$ is used, for example in [42] and [5] but here I will attempt to keep to the convention in (2.64).

The field equations, after substituting the ansätze $f^2(r) = N^2(r)g^2(r)$ and $A_t = q\frac{r}{L}h(r)$, and performing a functional variation of the action with respect to $g(r), N(r), h(r)$ (c.f. Appendix A), become

$$(-1 + 2\lambda\kappa - 3\mu\kappa^2)N' = 0 \quad (2.65)$$

$$\left(3r^4 \left[-\frac{\Lambda}{6}L^2 - \kappa + \lambda\kappa^2 - \mu\kappa^3\right]\right)' = \frac{q^2 r^3}{2} \left[\left(\frac{(rh)'}{N}\right)^2 \right] \quad (2.66)$$

$$\left(\frac{r^3}{N}(rh)'\right)' = 0 \quad (2.67)$$

where $\kappa = (g^2(r) - \frac{L^2}{r^2}k)$. It can be checked with some algebra that these equations have a solution

$$g^2(r) = \frac{kL^2}{r^2} + \frac{-\lambda}{3\mu} + \frac{1}{12\mu} \left[\left(\sqrt{\Gamma + J^2(r)} + J(r)\right)^{\frac{1}{3}} - \left(\sqrt{\Gamma + J^2(r)} - J(r)\right)^{\frac{1}{3}} \right] \quad (2.68)$$

$$J(r) = 36 \left(-4\mu^2 \Lambda L^2 - 8 \frac{M\mu^2}{r^4} + 2 \frac{Q^2}{r^6} - 8\mu\lambda + \frac{16}{9}\lambda^3 \right) \quad (2.69)$$

$$\Gamma = -(16(3\mu + \lambda^2))^3 \quad (2.70)$$

$$A = Q \frac{dt}{2\sqrt{2}Lr^2} \quad (2.71)$$

$$N = 1 \quad (2.72)$$

where M and Q are dimensionful constants from integration that are related to the mass and charge of the black hole, respectively, and Q is proportional to q , from the previous

ansatz for the vector potential. This is only a specific branch of the general solution; the complete set of solutions is made up of three branches, as roots of the cubic equation

$$-\frac{\Lambda}{6}L^2 - \kappa + \lambda\kappa^2 - \mu\kappa^3 = \frac{M}{3r^4} - \frac{Q^2}{24r^6} \quad (2.73)$$

Discussing the various branches of the characteristic polynomial is important at this stage. In particular, it is necessary to note that the principal solution and the real solution are no longer synonymous for the metric function solutions to cubic and higher polynomials. Above we have chosen the typically real valued solution of the cubic where no complex values appear in the solution. Of course, for various values of the parameters this solution is not guaranteed to remain real, but more importantly here, the solution may not be one of the two [one] which reduce(s) to the quadratic (Lanczos-Gauss-Bonnet) [linear (Einsteinian)] solution(s). In fact the solution we have selected does not reduce to either of the Lanczos-Gauss-Bonnet solutions as $\mu \rightarrow 0$.

When not fixing the asymptotic behaviour of $f(r)$, care must be taken that the solution has the expected asymptotics; in this case different branches of the solution can have non-AdS asymptotics, and the convenient Table 1 in [90] can be used to determine the valid black hole solutions; the solution presented in this section is guaranteed to avoid ghostly AdS vacua and has black hole solutions for $\mu, \lambda > 0$ (i.e. vacua where the kinetic term for the graviton has the incorrect sign).

The metric function $g^2(r)$ is plotted for this solution in figure 2.2 [5], for a horizon radius $r_h = 2.0$ and charge parameters of $Q = 0$, $Q = 6$, and $Q = 12$. Note that the asymptotic value of the metric function is unity due to our choice of the cosmological constant. Further, note that these charged black holes have metric functions which cross zero twice; it will be important when we develop a numerical procedure for finding similar black holes that we are careful to compute quantities at the outer horizon.

In the case of quasitopological gravity, as in that of higher dimensional Lovelock gravity, the constraints on the parameter space become richer. In cubic quasitopological gravity, holographic considerations of positivity of energy fluxes in the dual CFT yield a constraint similar to (2.10) [42]:

$$\begin{aligned} 1 - 10f_\infty\lambda - 189f_\infty^2\mu &\geq 0 \\ 1 + 2f_\infty\lambda + 855f_\infty^2\mu &\geq 0 \\ 1 + 6f_\infty\lambda - 1317f_\infty^2\mu &\geq 0 \end{aligned} \quad (2.74)$$

where $f_\infty = f_\infty(\lambda, \mu)$ is a function of the higher curvature couplings λ and μ - this derivation was performed in the situation where the cosmological constant is fixed at $-6/L^2$. This

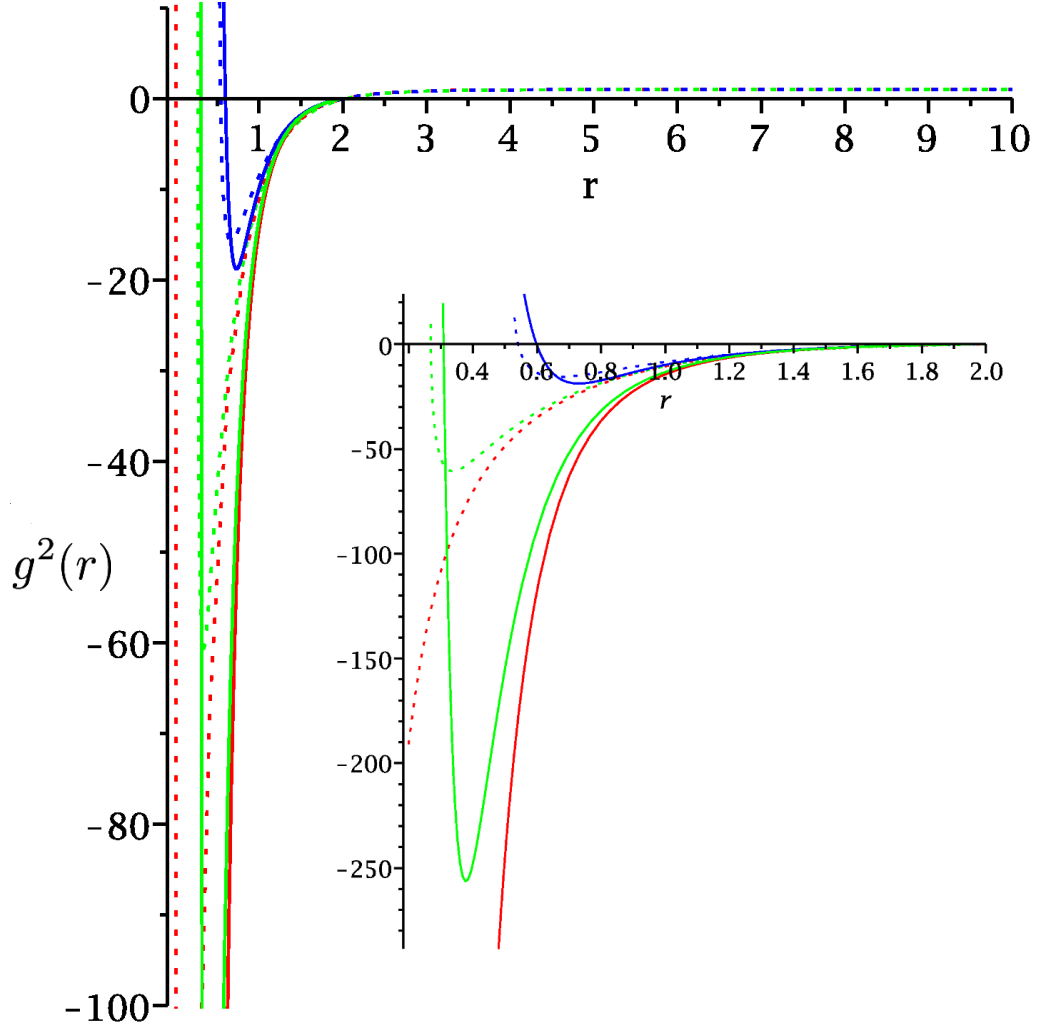


Figure 2.2: Cubic quasitopological black hole solutions for $k = 1$, $r_h = 2.0$, $\lambda = 0.04$, $\mu = 0.001$, where $Q = 0, 6, 12$ are in red, green, and blue, respectively. The cosmological constant is given here by $\Lambda = -6(1 - \lambda + \mu)/L^2$. The dotted solutions are quasitopological while the solid solutions are Einsteinian ($\mu = \lambda = 0$).

contrasts with the general formalism where the cosmological constant is allowed to vary (and therefore here becomes a function of λ, μ) while the asymptotic behaviour of the metric functions is fixed. Nonetheless both approaches are equivalent and will result in the same constraints on μ, λ : $1 - f_\infty + \lambda f_\infty^2 - \mu f_\infty^3 = 0$ and since the constraints limit μ, λ to small values, f_∞ will remain close to one and its principal value can be found, allowing us to graphically view the constraints. This is shown in figure 2.3.

We discuss the thermodynamic behaviour of the solution (2.73) at length in [5], and we also present a general solution for higher order (K^{th} order) quasitopological curvature terms, which takes the form

$$\left(r^{D-1} \sum_{k=0}^K \mu_k \kappa^k \right)' = \frac{r^{D-2}}{2} \left[\left(\frac{Q}{r^{D-2}} \right)^2 \right] \quad (2.75)$$

from the field equations

$$(-1 + 2\lambda\kappa - 3\mu\kappa^2)N' = 0 \quad (2.76)$$

$$\left((D-2)r^{D-1} \left[-\frac{\Lambda}{(D-1)(D-2)} 2L^2 - \kappa + \lambda\kappa^2 - \mu\kappa^3 \right] \right)' = \frac{q^2 r^{D-2}}{2} \left[\left(\frac{(rh)'}{N} \right)^2 \right] \quad (2.77)$$

$$\left(\frac{r^{D-2}}{N} (rh)' \right)' = 0 \quad (2.78)$$

and typically the cosmological constant is taken to be $\Lambda = -(D-1)(D-2)/2L^2$.

2.2.1 Entropy and Temperature

The entropy of the quasitopological black hole is obtained in a very similar way to the Lanczos-Gauss-Bonnet and Lovelock black holes. Following a similar Wald/Iyer entropy approach to section 2.1.2, the entropy is given by [90]

$$S = \frac{A}{4} \left(1 + 2 \frac{(D-2)\lambda k L^2}{(D-4)r_h^2} + \frac{3(D-2)\mu k^2 L^4}{(D-6)r_h^4} \right) \quad (2.79)$$

The temperature of these black holes is found in a manner completely analogous to section 2.1.1, by using the metric function in the expression (2.31). It is

$$T = \frac{1}{4\pi (r_h^4 + 2k\lambda L^2 r_h^2 + 3k^2 \mu L^4)} \left[\frac{(D-1)r_h^5}{L^2} + (D-3)k r_h^3 + (D-5)k^2 \lambda L^2 r_h + \frac{(D-7)k^3 \mu L^4}{r_h} - \frac{(D-3)Q^2}{r_h^{2D-9}} \right] \quad (2.80)$$

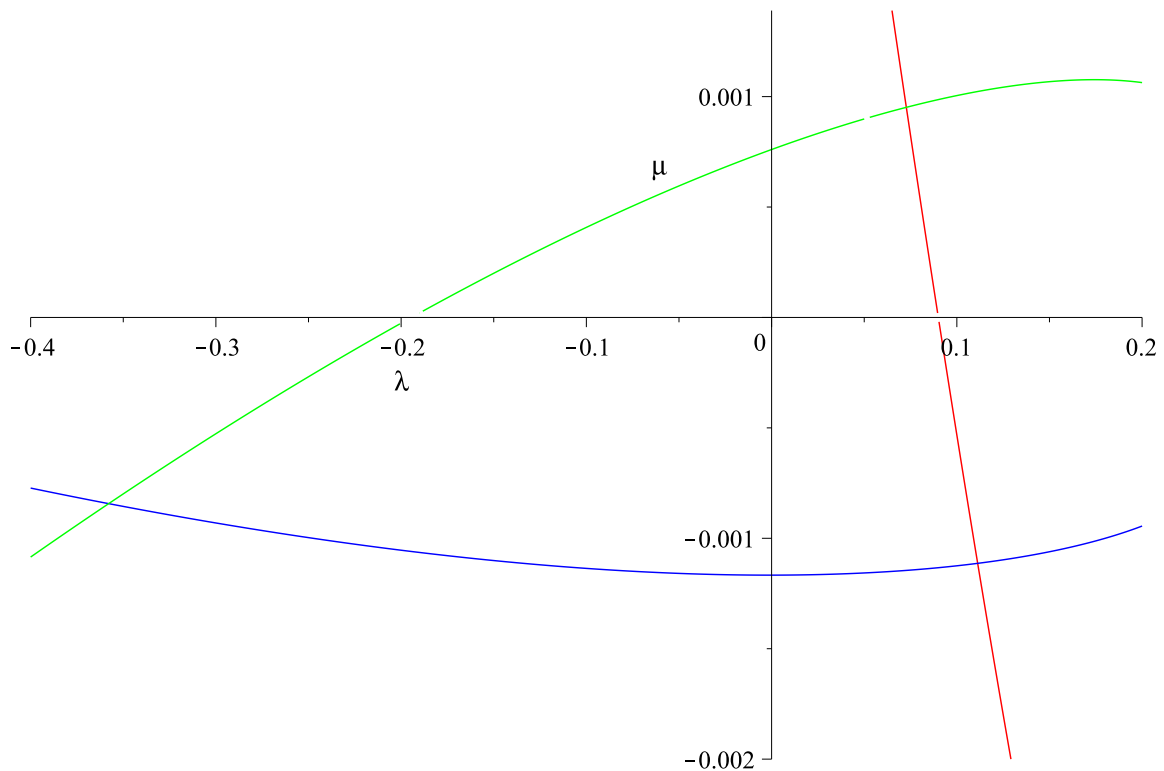


Figure 2.3: A plot of the parameter space for cubic quasitopological gravity's higher curvature couplings. The region interior to the red, blue, and green lines satisfies the cubic quasitopological energy flux positivity constraints (2.74).

2.2.2 Thermodynamics

In this section we use the convention for the cosmological constant, as discussed in section 2.1.3 to ensure that our solutions are always asymptotically AdS. In this specific five-dimensional case this amounts to

$$\Lambda = -\frac{6(1 - \lambda + \mu)}{L^2} \quad (2.81)$$

We can investigate the phase behaviour of these black holes by plotting the temperature and entropy on a log-log plot, as done in the Gauss-Bonnet section 2.1. In this case we see that certain values of the coupling parameters will yield the removal of the unstable small spherical black hole - all black holes will be stable. For the parameters $\lambda = 0.04$, $\mu = 0.001$, we can see this stability in figure 2.4 [5] for multiple values of charge. Larger positive values of μ along with larger positive values of λ will remove the instability that is seen in the Einsteinian case.

We can also perform a comparison to the Einsteinian and Lanczos-Gauss-Bonnet theories. This plot, in figure 2.5, was generated using the numerical procedure later detailed in section 3.5.2, but comprehensively checked for consistency with the exact solutions presented in this section. We can see again how the cubic quasitopological term directly has an effect similar to λ in removing the phase transition. This is sufficient to identify the magnitude of terms and their general effect, which we will need to examine universality, but to go further we can look at the specific heat.

The specific heat can again be examined analytically, as we have the exact solution (2.73). In the $k = 0$ case, the specific heat has one real root at

$$r_h = \frac{Q^{1/3}}{48^{1/6}} \quad (2.82)$$

when $\Lambda = -6/L^2$ (where here I have gone back to the regime where asymptotics vary based on λ, μ). This is not unexpected; the thermodynamics of the planar $k = 0$ case are the same as those of the non-higher curvature solutions, since the higher curvature contributions to the entropy vanish when $k = 0$.

However, it is important to note that this root of the specific heat corresponds to the case where the Kretschmann scalar $R^{\alpha\beta\gamma\delta}R_{\alpha\beta\gamma\delta}$ diverges at the black hole horizon; this condition suggests that a curvature singularity is about to appear at the horizon, i.e. the black hole is extremal.

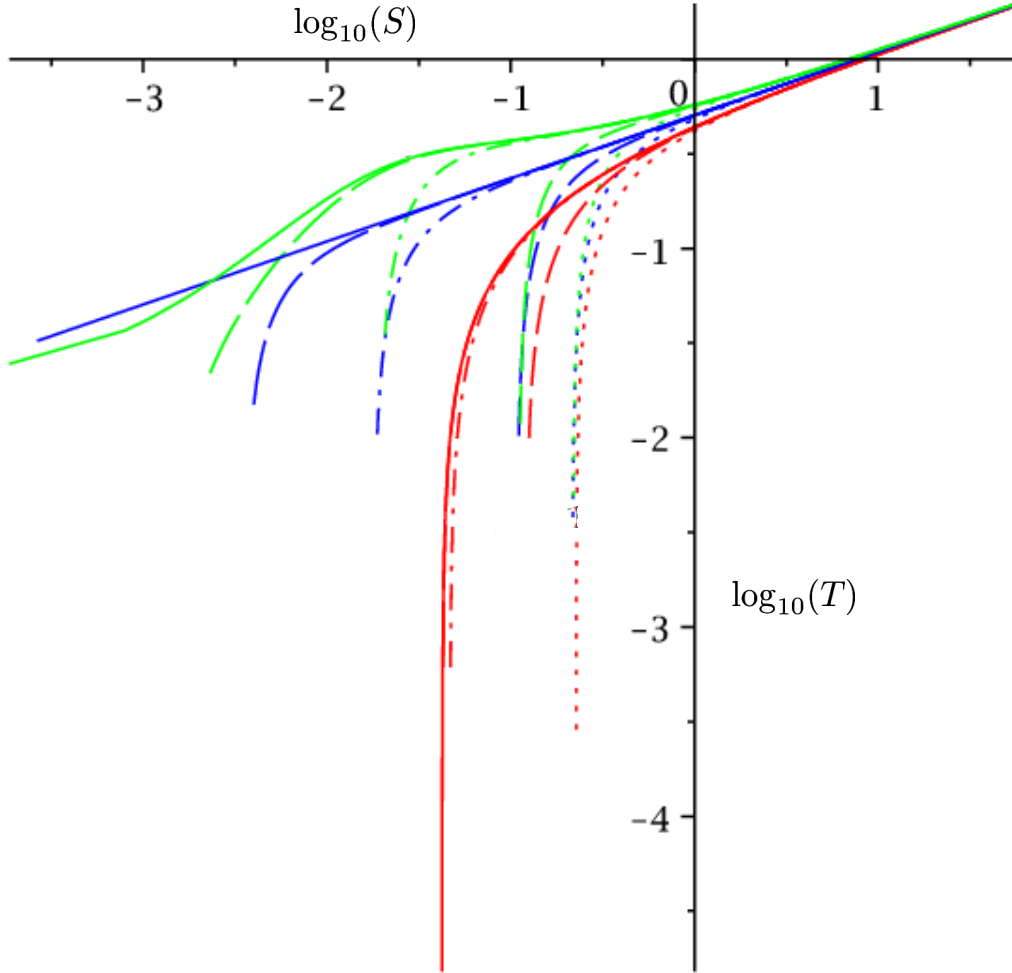


Figure 2.4: The log-log plot of temperature versus entropy for asymptotically anti-de Sitter cubic quasitopological Reissner-Nordström Black Holes of $Q = 6$ (dotted), $Q = 3$ (dashed), $Q = 0.5$ (dash-dot), $Q = 0.1$ (long-dash), and $Q = 0$ (solid) for $k = -1, 0, 1$ (red, blue, green). Here the higher curvature couplings take the values $\lambda = 0.04, \mu = 0.001$, while the cosmological constant is fixed at $\Lambda = -6/L^2$ in order to ensure the same asymptotic behaviour of the thermodynamics.

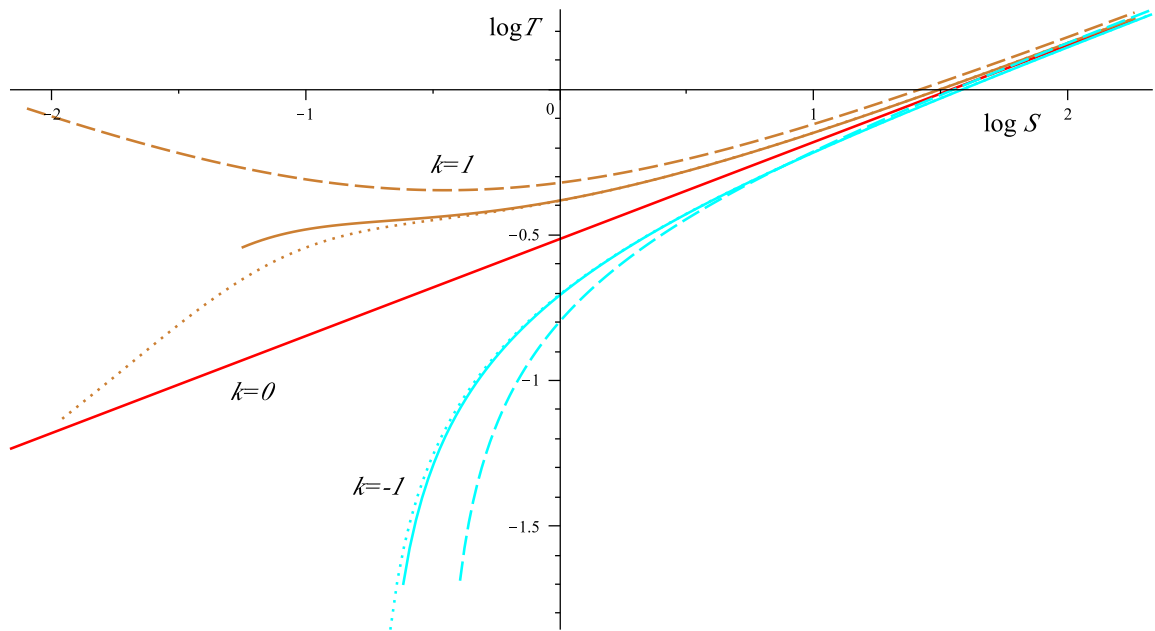


Figure 2.5: The log-log plot of temperature versus entropy for asymptotically anti-de Sitter {cubic quasitopological - dotted, Gauss-Bonnet - solid, Einsteinian - dashed} uncharged black holes where $k = -1, 0, 1$ (teal, red, brown). Here the higher curvature couplings take the values $\lambda = 0.04, \mu = 0.001$ (when they exist), while the cosmological constant is fixed at $\Lambda = -6(1 - \lambda + \mu)/L^2$ in order to ensure that the metric functions have the same asymptotics, and so that all solutions see the same effective cosmological constant.

Since I am interested in non-extremal black holes, the conditions I use to probe the extremal values are not a guarantee of extremality but instead are devised to avoid extremal behaviour out of an abundance of caution. That said, examining the solutions graphically leads us to the conclusion that the behaviour we are excluding is indeed a naked singularity produced from moving past extremality. This ultimately amounts to examining the characteristic polynomial (2.73) and using the condition that the maximum value of $M/3r^4 - Q^2/24r^6$ is equal to the characteristic polynomial evaluated at $g(r) = 0$. Doing this can be related to the divergence of the Kretschmann scalar and qualitatively, it corresponds to the turning point of the function g which occurs when $g(r) = 0$. This is because

$$\partial_r \kappa = \frac{d}{dr} W[\kappa] \left[\frac{\partial W[\kappa]}{\partial \kappa} \right]^{-1} \quad (2.83)$$

where $W[\kappa]$ is the characteristic polynomial, equal to the right hand side of (2.73).

The resultant extremality condition amounts to

$$Q^2 = \frac{16}{3} r_{h-Ex}^2 M \quad (2.84)$$

where for the planar black hole,

$$M = 3r_h^4 \left(1 + \frac{Q^2}{24r_h^6} \right) \quad (2.85)$$

so

$$r_{h-Ex}^6 = \frac{Q^2}{3} \left(\frac{3}{16} - \frac{3}{24} \right) = \frac{Q^2}{48} \quad (2.86)$$

and we see that the singularity in the planar case actually cannot exist as the transition in the specific heat occurs at extremality.

In the $k = 1$ case, the specific heat given by (2.57) is

$$C_P \sim \frac{12\pi (-48r^6 - 24r^4L^2 + 24\mu L^6 + Q^2) (-r^4 - 2\lambda r^2L^2 - 3\mu L^4)^2}{r(\mathcal{J} - 48r^6\lambda L^4 - 336r^4\mu L^6 - 3Q^2\mu L^4 - 48r^{10} + 24r^8L^2 + 72\mu^2L^{10} - 5Q^2r^4)} \quad (2.87)$$

$$\mathcal{J} \equiv -288r^8\lambda L^2 - 720r^6\mu L^4 - 144\mu\lambda r^2L^6 - 8Q^2\lambda r^2L^2$$

up to a constant of proportionality, since here M is a mass parameter rather than the exact mass.

The form of the specific heat reveals that the cubic quasitopological term appears to have an interesting impact on the zeroes of the specific heat, however, this is a red herring as the zeroes of the specific heat occur where temperature becomes negative.

The structure of roots of the specific heat creates a fifth order polynomial in r_h^2 , meaning we have potentially a very rich phase diagram for these black holes. Specific values of charge which yield a divergence in the specific heat, i.e. a phase transition, were found in [5].

2.2.3 Quartic Quasitopological Gravity

Finally, a quartic quasitopological term can be added to the action which yields a solution very similar to (2.68) [1]. The quartic quasitopological term yields the characteristic equation, in the uncharged case (the only one which was studied),

$$-\frac{\Lambda}{6}L^2 - \kappa + \lambda\kappa^2 - \mu\kappa^3 + \xi\kappa^4 = \frac{M}{3r^{D-1}} \quad (2.88)$$

with two solutions being

$$f^2(r) = k + \frac{r^2}{l^2} \left(-\frac{\mu}{4\xi} + \frac{1}{2}R \pm \frac{1}{2}E \right) \quad (2.89)$$

where

$$R = \left(\frac{\mu^2}{4\xi^2} - \frac{2\lambda}{3\xi} + \left(\frac{D}{2} + \sqrt{\Delta} \right)^{1/3} + \left(\frac{D}{2} - \sqrt{\Delta} \right)^{1/3} \right)^{1/2}, \quad (2.90)$$

$$E = \left(\frac{3\mu^2}{4\xi^2} - \frac{2\lambda}{\xi} - R^2 - \frac{1}{4R} \left[\frac{-4\lambda\mu}{\xi^2} - \frac{8}{\xi} + \frac{\mu^3}{\xi^3} \right] \right)^{1/2} \quad (2.91)$$

and

$$\begin{aligned} \Delta &= \frac{C^3}{27} + \frac{D^2}{4} \\ C &= \frac{-3\mu - \lambda^2}{3\xi^2} - \frac{4\gamma}{\xi} \\ D &= \frac{2}{27} \frac{\lambda^3}{\xi^3} - \frac{1}{3} \left(-\frac{\mu}{\xi^2} + 8 \frac{\gamma}{\xi} \right) \frac{\lambda}{\xi} + \frac{\mu^2\gamma}{\xi^3} + \frac{1}{\xi^2} \\ \gamma &= -\frac{\Lambda}{6}L^2 - \frac{M}{3r^4} \end{aligned} \quad (2.92)$$

In a manner much the same as for cubic black holes, the temperature and entropy can be computed; for $\Lambda = -6/L^2$ in five dimensions,

$$T = \frac{2r_h^8 - 2L^8k^4\xi - L^6k^3\mu r_h^2 + L^2kr_h^6}{2L^2\pi \left(r_h^7 + 2L^2k\lambda r_h^5 + 3L^4k^2\mu r_h^3 + 4L^6k^3\xi r_h \right)} \quad (2.93)$$

while the higher curvature entropy is

$$S = \frac{\mathcal{A}}{4} \left(1 + 2 \frac{(D-2)\lambda k L^2}{(D-4)r_h^2} + \frac{3(D-2)\mu k^2 L^4}{(D-6)r_h^4} + \frac{4(D-2)k\xi L^6}{(D-8)r_h^6} \right) \quad (2.94)$$

As before, one has control over the stability of the black hole by adjusting the quartic coupling parameter. We can see this in figure 2.6, where a sufficiently positive parameter ensures that the instability disappears. Therefore, the quartic quasitopological coupling can be used to obtain and remove first order phase transitions in these black holes, and it acts as yet another five dimensional thermodynamic parameter. These results indicate that future work in extended phase space, where the higher curvature parameters vary as thermodynamic quantities, may also yield critical behaviour.

2.3 Discussion

The focus in this chapter was on presenting a background for studies in higher curvature gravity. I began by introducing higher curvature terms to the Einstein-Hilbert action, first by discussing general terms and then by motivating the special set of terms that allow the field equations to remain second-order in derivatives of the metric tensor.

I showed how solutions in these scenarios could be obtained, first with a discussion of holographic constraints on higher curvature couplings, followed by a short analysis of Lovelock black holes, with specific focus on black holes in spacetimes with the second-order Lanczos-Gauss-Bonnet term.

I described a number of methods for obtaining temperature and entropy, and detailed the methods that are used in this thesis. Importantly, the section on Gauss-Bonnet black holes features a strong introduction to the use of the cosmological constant as a thermodynamic pressure term - I show the history of this usage and the restrictions on defining a pressure in black hole thermodynamics, namely the construction of a Smarr relation and first law, and how Eulerian scaling (one among a number of reasons) is used to formulate the “extended phase space thermodynamics”. I also briefly discuss how thermodynamic volume will act as a conjugate quantity to the pressure, how it fixes the constant factors in the pressure, and how its non-covariance means that care must be taken to specify the observer when formulating the thermodynamics of a black hole.

In the section on quasitopological gravity, we saw how curvature terms could be added which are not the Lovelock topological invariants but still allow for second-order field

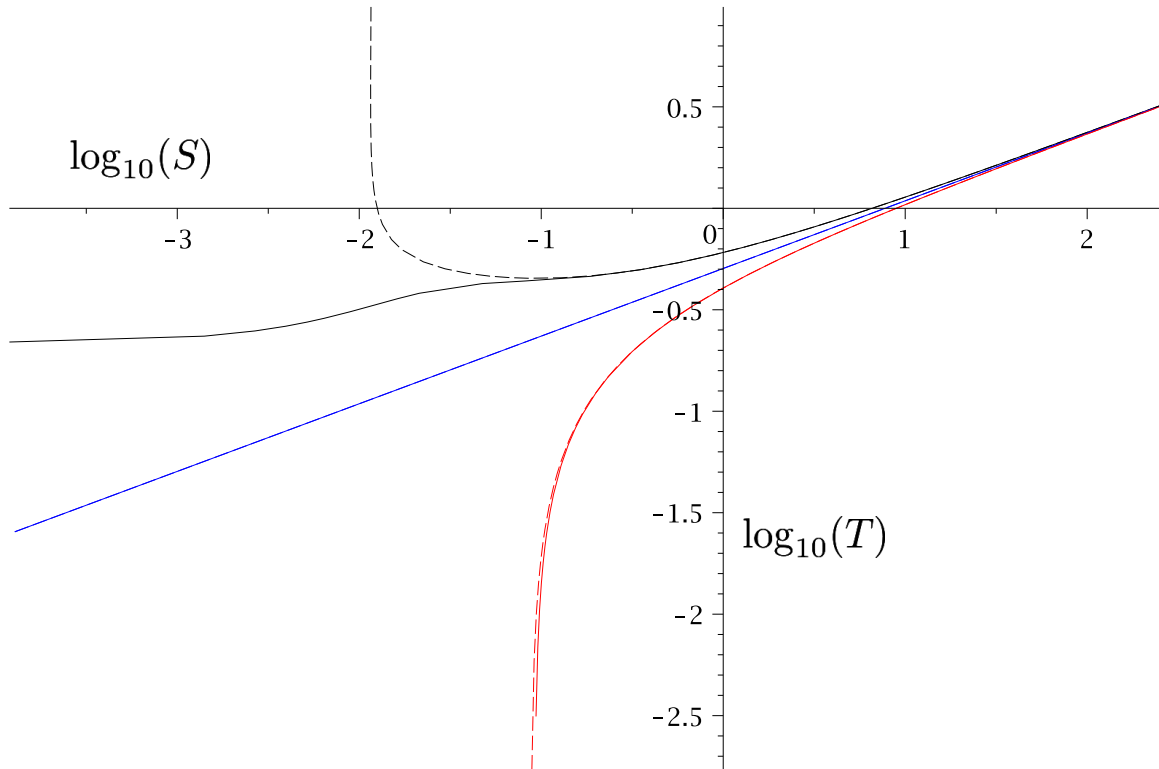


Figure 2.6: The log-log plot of temperature versus entropy for asymptotically anti-de Sitter quartic quasitopological black holes in five dimensions for $k = -1, 0, 1$ (red, blue, black). Here the higher curvature coupling is given by $\xi = 0.0006$ (solid) and $\xi = -0.0001$ (dashed), while the cosmological constant is fixed at $\Lambda = -6/L^2$ which ensures that the thermodynamics has the same asymptotic behaviour.

equations in certain scenarios. Namely, the quasitopological terms give this desired feature for spherically symmetric solutions. Essentially, these terms allow us access to the extra parameter space of cubic and higher Lovelock gravity while remaining in five dimensions, a prudent scenario for exploring gauge/gravity holography with physical, four-dimensional gauge theories.

I showed the effects of these quasitopological terms on black holes and presented exact solutions for cubic and quartic quasitopological gravity, with an explanation of the characteristic polynomial and the various branches of solution.

The research into Lovelock and quasitopological gravity will be further justified later in this thesis, where we use the expanded parameter space to examine interesting thermodynamic behaviour in five dimensions, including a critical point that does not require a Maxwell charge to exist.

Chapter 3

Lifshitz-symmetric Black Holes

As terminology in modified gravity, *Lifshitz scaling* is an anisotropy in the time coordinate. In particular, it is usually defined as the scaling [93]

$$t \rightarrow \lambda^z t, \quad r \rightarrow \lambda^{-1} r, \quad x \rightarrow \lambda x \quad (3.1)$$

The parameter z controls the degree of the anisotropy, where $z = 1$ corresponds to the usual anti-de Sitter scaling. Typically values of $z = 2$, $z = 3$, or $z = D$ are considered.

Work featuring this metric symmetry can be justified on group theoretic grounds. For example, when $z = 2$ the metric features symmetries from the Lifshitz or Schrödinger group [94]. The Schrödinger group is the most symmetric, obtained [95] by combining the Galilean algebra (spatial translations P^i , rotations M^{ij} , Galilean boosts K^i , and temporal translation H)

$$\begin{aligned} [M^{ab}, M^{cd}] &= i(\delta^{ac} M^{bd} + \delta^{bd} M^{ac} - \delta^{ad} M^{bc} - \delta^{bc} M^{ad}) \\ [M^{ab}, P^c] &= i(\delta^{ac} P^b - \delta^{bc} P^a) \\ [M^{ab}, K^c] &= i(\delta^{ac} K^b - \delta^{bc} K^a) \\ [K^a, H] &= iP^a \end{aligned} \quad (3.2)$$

with the additional anisotropic structure which corresponds to a central charge (“non-relativistic mass”) m along with a dilatation D which generates the scaling (3.1) and a special conformal transformation C ; these extra symmetries manifest in an $SL(2, \mathbb{R})$

algebra

$$\begin{aligned}
[D, P^a] &= -iP^a \\
[D, K^a] &= iK^a \\
[P^a, K^b] &= -i\delta^{ab}m \\
[D, H] &= -2iH \\
[D, C] &= 2iC \\
[H, C] &= iD
\end{aligned}
\tag{3.3}$$

Through the relationship between $SL(2, \mathbb{R})$ and $SL(2, \mathbb{C})$ (the universal cover of the Möbius group), one might notice that by motivating the Schrödinger group in this manner we are constructing the non-relativistic form of the conformal group, in a similar fashion to how the conformal group is often built from the symmetries corresponding to scale invariant theories with Poincaré symmetry (see, for example, [96, 97]).

In my research I consider only the Lifshitz symmetry which possesses the $SL(2, \mathbb{R})$ component (3.3) (the anisotropy) and not the Galilean boost symmetries.

These types of spacetimes are interesting for a number of reasons. One paper of substantial impact to the quantum gravity community was due to Hořava [98]. He showed that a specific example of these spacetimes, now known as Hořava-Lifshitz gravity, was power-counting renormalizable. Appearing to have potential viability for a unified theory, this flavour of modified gravity has been well studied.

In this thesis, I shall focus on another motivation: the holographic correspondence with anisotropic gauge theories. It is expected that the varying anisotropy will manifest dynamic critical behaviour, evidenced by the quantity of research on models for dynamic universality. For example, work on the $z \sim 3$ dynamical universality class of the critical point in QCD [99] or the $z = 2$ directed percolation models [100] provide models where dynamic universality classes may be investigated. Experimental evidence of non-equilibrium phenomena is challenging to obtain; however, suggestive behaviour has been observed, for example, for directed percolation [101]. We expect that an anisotropic gravitational theory will feature some effect from the anisotropy, and the hope is that this can be related to known behaviour of anisotropic condensed matter systems.

So, the idea behind breaking this scaling symmetry in the temporal direction is to examine a dynamical scaling in relativity. In condensed matter physics this anisotropy is theoretically better understood, and it is usually mentioned with regards to *critical slowing down* or *dynamic critical phenomena* [23]. The scaling parameter z relates to the equilibration of the system over some timescale; near criticality the amount of time needed

to reach equilibrium is typically divergent (as it is related to the correlation length which diverges), and this equilibration time can be characterized by a dynamical critical exponent which turns out to be z ; $\omega^{-1} \sim \xi^z$ where ω is the characteristic frequency of the model [23].

The holographic interest therefore originally motivated work in constructing gravitational (bulk) metrics which manifest this type of symmetry, as an approach towards holographically studying gauge theories with these symmetry groups. Most importantly, the Schrödinger group received attention, where the approach was to take the 3-dimensional Schrödinger group corresponding to a gas of fermions at unitarity (a specific condition on the scattering cross-section), and through a series of embeddings, relate it to a relativistic toy gravity theory with this symmetry [95]. In addition, it was shown [102, 103] that the Lifshitz symmetry alone is enough to obtain a Schrödinger symmetry on the boundary of the theory, which means we can remain hopeful that our Lifshitz symmetric bulk can be used to model Schrödinger symmetric gauge theories.

In this thesis and in my research, I have worked on the development of tools to examine whether the dynamical critical exponent z acts in the same way with respect to black hole criticality.

For my work on this topic, I primarily consider the case where the Lifshitz symmetry is supported by a Proca field (a massive spin-1 field), though there are a number of ways to recognize the asymptotically Lifshitz spacetimes. In the former case, the general higher curvature action will then be

$$\mathcal{S} = \frac{1}{16\pi} \int d^D x \sqrt{-g} \left(-2\Lambda + \mathcal{L}_1 + \mu_2 \mathcal{L}_2 + \mu_3 \mathcal{X}_3 + \mu_4 \mathcal{X}_4 - \frac{1}{4} F_{\mu\nu} F^{\mu\nu} - \frac{1}{2} m^2 A_\mu A^\mu - \frac{1}{4} \mathcal{F}_{\mu\nu} \mathcal{F}^{\mu\nu} \right) \quad (3.4)$$

where $\mathcal{F}_{\mu\nu}$ is the electric field strength for a Maxwell charge, while $F_{\mu\nu}$ is the field strength (with corresponding vector potential A_μ) of the Proca field.

Here, because the results will be directly extended to Lifshitz asymptotics as well as pure Lifshitz spacetimes, the static, spherically symmetric metric ansatz has the scaling behaviour (3.1). The ansatz is then

$$ds^2 = - \left(\frac{r}{L} \right)^{2z} f^2(r) dt^2 + \frac{L^2 dr^2}{r^2 g^2(r)} + r^2 d\Omega_{D-2,k}^2 \quad (3.5)$$

where as before, $d\Omega_{D-2,k}$ is given by (2.12), and the limiting behaviour is $f(r)|_{r \rightarrow \infty} = 1$ and $g(r)|_{r \rightarrow \infty} = 1$. The fall-off behaviour of these metric functions is important in understanding

traditional derivations of mass for these black holes, for example. In this thesis I am mostly concerned with application to numerical solutions, and no assumptions on falloff behaviour are made beyond the condition that at very large r (on the order of $r = 10^8$), the metric functions are equal to unity within ten digits of precision. The fall-off can be examined exactly from order-by-order solutions to the equations of motion from a large- r series expansion; I will discuss this in section 3.5. Because sub-leading terms can become next-to-leading order terms when z is varied, the discussion of fall-off is relatively complicated.

Note that for the remaining sections, excluding the numerical solutions in section 3.5, I will denote the cosmological lengthscale as l rather than L - the capital L will be used to refer to a general dimension of length, in keeping with the published work on this topic [3].

3.1 Mass

The most immediate obstacle in describing the asymptotically Lifshitz black holes thermodynamically is the lack of an agreed-upon mass for the numerical solutions. Numerous attempts have been made to identify inconsistencies in the various techniques that are used to obtain a mass, focusing on the results for exact solutions. Unfortunately, these exact asymptotically Lifshitz black holes are often unusual beasts, with strong restrictions on parameters that are usually independent, such as the cosmological constant and the horizon radius. For example, work has been done [104, 105] to understand Hamilton-Jacobi variations in these theories, reaching the conclusion that the traditional quasilocal techniques are not acceptable in all cases because the asymptotics can fix values of fields in the theory, and the loss of independence of these fields has to be handled carefully.

With our asymptotically Lifshitz black holes and the thermodynamic work of sections 2.1.1 - 2.1.3, we are in a position where the entropy, temperature, and pressure are computable via holographic or scaling arguments, but it initially appears that without a well defined mass (and therefore enthalpy) the thermodynamics cannot be fully specified.

However, we found in a previous paper that the Smarr relation is robust enough to be trustworthy insofar as describing black hole thermodynamics. In [3] we observed that the D -dimensional Smarr relation remains the same when higher curvature terms are added to the action, even when they modify the asymptotics to be anisotropic. In this context we found that given a convergent power series expansion of the temperature, entropy, and pressure, the Smarr relation can be used, along with the first law of thermodynamics and the set of independent lengthscales, to fix all remaining thermodynamic quantities.

Therefore, the “thermodynamic” mass and volume can be found algebraically from the temperature, pressure, entropy, and its derivatives.

In this section I will present our thermodynamic approach towards finding a mass and volume, and then in section 3.2, I will analyze its results in comparison to the various previous attempts at obtaining a mass in exact asymptotically Lifshitz black hole solutions.

3.1.1 Smarr Relation

The first step in understanding the thermodynamics of asymptotically Lifshitz black holes is to examine the algebraic relationship between the functions appearing in the first law (2.50), known as the Smarr relation [64]. Because the Proca charge ends up fixed by the asymptotics in both the exact and numerical solutions, we conjecture [3] that the only quantities which appear in the Lifshitz Smarr relation will be related to the number of independent lengthscales at the level of the action. Therefore, a Maxwell field will generate a lengthscale, as well as the coupling constant for higher curvature terms. Since we do not consider the thermodynamics of varying μ_2 or μ_3 in this thesis, we will ignore the latter set of terms, and our Smarr relation will be the same as justified earlier in (2.51).

The form of the Smarr relation is not entirely trivial; there exists an alternative Smarr relation for Lifshitz black holes which depends on the critical parameter z [106, 107, 108, 109, 110, 111, 112]

$$(D + z - 2)M = (D - 2)TS \tag{3.6}$$

and initially it appears that this is in disagreement with equation (2.51). Primarily, the mass appears to have a lengthscale that is dependent on the critical parameter, and there is an absence of any pressure or volume terms. We will later show in section 3.3 that (3.6) is a specific case of the Smarr relation (2.49) when $k = 0$ and the temperature takes a simple form.

We then ask whether, given the Smarr relation (2.51) and the first law of thermodynamics (2.50), we can constrain the mass and volume if the temperature, entropy, and pressure are known.

3.1.2 Conditions on the Mass

There are a number of small details which must be dealt with before the Smarr relation and first law can yield a “thermodynamically consistent” mass and volume.

First, a difficulty appears when fundamental lengthscales become dependent in the black hole solution. For example, if $r_h = r_h(l)$, the conjectured scaling of the mass means that $[M] = l^{(D-3)}$, so the first law (2.50) yields only one equation,

$$\left(\frac{\partial M}{\partial l}\right) = T \left(\frac{\partial S}{\partial l}\right) + V \left(\frac{\partial P}{\partial l}\right) \quad (3.7)$$

which can be simplified to (neglecting Q for now)

$$(D-3)\frac{M}{l} = (D-2)\frac{TS}{l} - 2\frac{VP}{l} \quad (3.8)$$

which we can see does not yield an independent equation from the $Q = 0$ Smarr relation (2.49).

The only constraint that the algebraic Smarr relation provides is that there exists a one-parameter family of solutions, $M(l), V(l)$, or equivalently $M(V)$. In [3], we proposed a number of approaches that can be used to define a mass; currently no consensus exists on the correct methodology in all cases, however, future numerical and analytical work may be able to build on our inquiry and elucidate the masses for these asymptotically Lifshitz black holes with dependent lengthscales.

1. The first approach suggested is to introduce a fictitious mass parameter. This dimensionless parameter \tilde{m} will appear in the metric function to artificially separate the lengthscales l and r_h until the mass is determined, after which the limit $\tilde{m} \rightarrow 0$ can be taken. The choice of the exact form of the term

$$\tilde{m} \left(\frac{l}{r}\right)^p$$

by selecting a value of p will specify which solution along the one-parameter family we will take. We can then compare p with some expected values; for example $p = (D-1)$ corresponds to the common scaling of the mass term in the metric function, while $p = (D+z-2)$ is a plausible ansatz based on some exact Lifshitz symmetric solutions. We can determine the mass for a number of guesses for p , and compare with other methods to try to understand how this term should behave. Furthermore, this approach could be used to match an exact solution with some limit of a numerical solution, and while this will not be done in this thesis it remains an interesting avenue for future work.

2. The other approaches involve making a more strict assumption about the thermodynamic ambiguity. The second approach involves taking r_h and l as independent quantities until the thermodynamics are specified. That is, we apply a modified first law

$$\begin{aligned} M(r_h, l) &= \int dr_h \frac{\partial M(r_h, l)}{\partial r_h} \\ &= \int dr_h T(r_h, l) \frac{\partial S(r_h)}{\partial r_h} \end{aligned} \quad (3.9)$$

to obtain M , holding l fixed. We then vary M with respect to l to obtain an equation which can be solved for the volume,

$$\frac{\partial M(r_h, l)}{\partial l} = V(r_h, l) \frac{\partial P(l)}{\partial l} \quad (3.10)$$

This amounts to supposing that $S = S(r_h)$ and $P = P(l)$ until the solution for M, V is obtained, as in this case the first law (2.50) becomes

$$\frac{\partial M}{\partial r_h} = T \frac{\partial S}{\partial r_h} \quad \frac{\partial M}{\partial l} = V \frac{\partial P}{\partial l}$$

and the part of the first integral which only depends on l , $M_l(l)$, is assumed to be zero since as $r_h \rightarrow 0$, we want $M \rightarrow 0$.

3. Thirdly, we can assume a fixed value for a thermodynamic parameter. This comes from the interpretation that terms added to the action contribute towards new length-scales in the thermodynamics, and therefore towards a new parameter in the Smarr relation.

This is related to why, for example, we do not introduce a charge and potential for the Proca field in Lifshitz spacetimes into the Smarr relation and first law. The charge of the Proca field is fixed by the Lifshitz asymptotics and so it is not productive to add a new term to the Smarr relation which is completely dependent on the entropy and pressure. This term would only make a conceptual distinction between the Proca charge and the mass or volume, for example, since the dependence means that a ‘‘Proca potential’’ could be grouped into another term. If we find that it greatly simplifies interpretation, then it is probably a good idea to separate the concepts, but until that situation occurs it is much simpler to consider only independent lengthscales.

In this context, if the Ricci scalar corresponds to the lengthscale r_h , and the cosmological constant corresponds to l , then when $r_h = r_h(l)$, the most compelling decision will be to eliminate S , M , or V from the Smarr relation and first law. Since we have an independent and trusted expression for S in these cases, we will typically experiment with enforcing $M = 0$ or $V = 0$ and examining the outcome by looking at the remainder of the thermodynamics.

There is a more general approach, which is to consider the single lengthscale (say, r_h) as contributing towards both M and V in some way; this turns out to be conceptually equivalent to the first approach mentioned, where the choice of p is a decision that splits up the temperature-entropy term's contributions among M and V .

Ultimately, these approaches are all very ad-hoc; the hope is that through using these guesses, some pattern can be gleaned from the thermodynamics that indicates the correct course of action for dealing with these highly constrained black holes. It may be that their thermodynamics is simply ill-posed, since in this case we have an entropy that is dependent on volume, but we will do our best to study how the thermodynamics may appear in the case that it may agree with some independent results.

3.1.3 An Expression for the Mass

Here I present the main result of [3], the expression for the thermodynamic mass from the power series expansion of the temperature, pressure, and entropy of black holes with Lifshitz or AdS asymptotics.

The insight here is to use a power expansion of the thermodynamic quantities M , V , T , Φ , and S , in each of the lengthscales. The reason for doing this is that in general the equations given by the first law and Smarr relation are nonlinear, and a series expansion turns out to yield an exact solution. The mass and volume for the black hole solutions we consider below will feature expressions for these quantities which are conducive to a series form.

The convention we use for the expansion in the charge parameter(s) q_u is given by the

following set of expressions:

$$M(r_h, l, q_u) = M_0 + \sum_{u=1}^U \sum_{i=1}^{N_u} M_{iu}(r_h, l) q_u^{\mathbf{a}_i}, \quad M_{iu} = \sum_{j,k} M_{ijk} r_h^{\gamma_{jku}} l^{\delta_{jku}}, \quad (3.11)$$

$$T(r_h, l, q_u) = T_0 + \sum_{u=1}^U \sum_{i=1}^{N_u} T_{iu}(r_h, l) q_u^{\mathbf{a}_i}, \quad T_{iu} S = \sum_{j,k} T_{iju} S_{0k} r_h^{\gamma_{jku}} l^{\delta_{jku}} \quad (3.12)$$

$$V(r_h, l, q_u) = V_0 + \sum_{u=1}^U \sum_{i=1}^{N_u} V_{iu}(r_h, l) q_u^{\mathbf{a}_i}, \quad V_{iu} P = \sum_{j,k} V_{iju} P_{0k} r_h^{\gamma_{jku}} l^{\delta_{jku}} \quad (3.13)$$

$$\Phi = \sum_{u=1}^U \sum_{i=1}^{N_u} \Phi_{iu}(r_h, l) q_u^{\mathbf{a}_i - 1}, \quad \Phi_{iu} = \sum_{j,k} \Phi_{ijk} r_h^{\gamma_{jku}} l^{\delta_{jku}} \quad (3.14)$$

where M_0 , V_0 and T_0 satisfy the uncharged Smarr relation. The exponents \mathbf{a}_i are the power of q_u in this series expansion, N is the number of terms in this expansion, U is the number of charge parameters in the metric function (in the case where we might add two Maxwell fields to the action, for example), and the exponents $\gamma_{jku}, \delta_{jku}$ correspond to the powers of r_h and l in the corresponding series expansion in these variables. More explicitly,

$$T_{iu} S = \sum_j T_{iju} r_h^{\alpha_{ju}} l^{\beta_{ju}} \sum_k S_{0k} r_h^{\tilde{\alpha}_k} l^{\tilde{\beta}_k} \quad (3.15)$$

where $\alpha_{ju} + \tilde{\alpha}_k = \gamma_{jku}$ and $\beta_{ju} + \tilde{\beta}_k = \delta_{jku}$.

Because of the way the solution is structured, it is easiest to perform the series expansion in both r_h and l together - the reason that these variables are grouped together is because we want to allow $S = S(r_h, l)$, whereas in this framework we do not allow q_u to appear in any of the dynamical first-law quantities S , P , or $Q_{u' \neq u}$.

This is tantamount to the expression

$$\frac{\partial M_u}{\partial Q_u} dQ_u = \Phi_u dQ_u \quad (3.16)$$

arising from the first law; we do not in general assume that a similar expression holds for T, S, r_h and V, P, l .

Finally, the terms $M_{ijk}, T_{iju}, V_{iju}, P_{0k}, S_{0k}$, and Φ_{ijk} are constant coefficients - they do not depend on the dynamical variables r_h, l , or q_u . Since $[q_u^{\mathbf{a}_i}] = \mathbf{a}_i(D-3)$, $\gamma_{jku} + \delta_{jku} = -(\mathbf{a}_i - 1)(D-3)$.

With this series expansion, the Smarr relation and 1st-law will break into

$$(D-3)M_{iu} = (D-2)T_{iu}S - 2V_{iu}P + (D-3)\frac{\Phi_{iu}Q_{iu}}{q_u} \quad (3.17)$$

$$\frac{\mathbf{a}_{iu}M_{iu}}{Q_{iu}} = \frac{\Phi_{iu}}{q_u} \quad (3.18)$$

$$(D-3)M_0 = (D-2)T_0S - 2V_0P \quad (3.19)$$

$$dM_0 = T_0dS + V_0dP \quad (3.20)$$

where the first pair of equations holds for $i \neq 0$.

We initially solve the $i = 0$ case, and then show that the $i \neq 0$ case is solved in exactly the same way. First, create the series expansions of M_0, T_0, V_0 in (3.13), such that for example

$$M_{00} = \sum_{j,k} M_{0jk0} r_h^{\gamma_{jk0}} l^{\delta_{jk0}}$$

Notice that for the correct scaling on M_{00} , $\gamma_{jk} + \delta_{jk} = (D-3)$. Taking partial derivatives of the uncharged first law (3.20) yields the set of two equations

$$\frac{\partial M_0}{\partial r_h} = T_0 \frac{\partial S}{\partial r_h} \quad \frac{\partial M_0}{\partial l} = T_0 \frac{\partial S}{\partial l} + V_0 \frac{\partial P}{\partial l} \quad (3.21)$$

At this point we assume that the series expansion for P only contains one term, so the index k is unnecessary in the $V_{iu}P$ expansion. In keeping with the ‘‘cosmological constant as pressure’’ paradigm, $[P] \sim 1/l^2$.

Then, through some algebra and the series expansion, the partial derivatives can be evaluated and the powers of r_h, l can be eliminated to produce a set of linear equations with the solutions

$$M_{0jk0} = \frac{T_{0j0}S_k \tilde{\alpha}_k}{\gamma_{jk0}} \quad (3.22)$$

$$V_{0jk0} = \frac{T_{0j0}S_k}{2P_0\gamma_{jk0}} ((D-2)\gamma_{jk0} - (D-3)\tilde{\alpha}_k) \quad (3.23)$$

where $\tilde{\alpha}_k$ is the power of r_h appearing in the entropy term S_j in its series expansion (3.15).

One point of note is that this solution does not hold when $\gamma_{jk0} = 0$. In this case, the scenario appears to be rather pathological as the mass will not tend to zero as $r_h \rightarrow 0$. For these terms, it is possible to make progress with assumptions about their form; for the

exact solutions considered below we need not worry. Some examples where consideration of these terms may be necessary are in soliton solutions or in a series expansion about numerical Lifshitz solutions [113, 114, 115].

This result is very interesting - for uncharged black holes with a cosmological constant, some plausible assumptions about the form of the Smarr relation are enough to tightly constrain the thermodynamics, even when the cosmological constant is interpreted as pressure (without a pressure term, the Smarr relation $(D - 3)M = (D - 2)TS$ trivially yields mass from temperature and entropy).

The next step is to find a solution that applies to the charged case as well. Conveniently, substituting (3.18) into the first Smarr relation (3.17), we obtain a Smarr relation very similar to (3.19);

$$(D - 3)(1 - \alpha_{iu})M_{iu} = (D - 2)T_{iu}S - 2V_{iu}P$$

where we have successfully eliminated Φ_h, Q_h . This expression is also subject to two first-law equations similar to (3.21).

Therefore, essentially the same set of equations results, and solutions can again be obtained in the fashion of (3.22) and (3.23), but where the relationship between the powers γ and δ now features α_{iu} . This generalizes the power series method to a larger thermodynamic context with an arbitrary set of independent work terms.

The Maxima code to solve for thermodynamic mass and volume, given a simple series expression for the metric function and the entropy and cosmological constant, is shown in Appendix C.3.

3.1.4 Various Definitions of Mass

Here I will outline a few of the alternative formulations of mass in Lifshitz symmetric spacetimes which I will compare with the thermodynamic mass of section 3.1.3.

The difficulty of defining a mass in general relativity has led us to a veritable zoo of masses, obtained by exploiting symmetries of the spacetime, Hamiltonian foliations and counterterm methods, and gauge invariance. I will therefore only list a few of the potential contending approaches to a ‘‘Lifshitz mass’’, in order to compare them to results that we obtain by constraining solutions thermodynamically. Note that this list is by no means exhaustive, and future study might indicate that a suitable mass exists which was not considered here.

Komar Mass

The Komar mass [116, 117, 28, 118] is generated by the timelike Killing vector of a spacetime; it takes the form

$$\mathcal{M}_K = -\frac{1}{8\pi} \int_{\mathcal{S}_\infty} dS_{\alpha\beta} \nabla^\alpha \xi_t^\beta \quad dS_{\alpha\beta} = -2n_{[\alpha} r_{\beta]} \sqrt{\sigma} d^2\theta \quad (3.24)$$

where θ make up the angular coordinates on the boundary sphere (taken to spatial infinity) \mathcal{S}_∞ , σ is the determinant of the metric on this surface, ξ is the timelike Killing vector for the spacetime, n is the timelike normal to the hypersurface \mathcal{S}_∞ , and r is the spacelike normal.

This mass requires an asymptotically timelike Killing vector, so it applies to stationary spacetimes. We only consider these spacetimes in this thesis but mention this because it is potentially restrictive, and because our thermodynamically inspired mass could be applicable to nonstationary spacetimes if thermodynamic equilibrium can be maintained.

Arnowitt-Deser-Misner Mass

The Arnowitt-Deser-Misner (ADM) mass [119, 28, 120, 118] is computed in (3+1) dimensional asymptotically flat spacetimes via an integral of extrinsic curvature over a spherical two-surface at infinity:

$$\mathcal{M}_{ADM} = -\frac{1}{8\pi} \int_{\mathcal{S}_\infty} d^2\theta \sqrt{\sigma} (K - K_0) \quad K \equiv \sigma^{AB} K_{AB} \quad (3.25)$$

where K is the extrinsic curvature of the two-sphere \mathcal{S}_∞ as embedded in flat spacetime, and the coordinates A, B take two values as they correspond to the coordinates of the induced metric on \mathcal{S}_∞ (which has determinant σ), $d\theta^A$.

K_0 is used to subtract the infinite contribution from flat spacetimes; this is the extrinsic curvature of \mathcal{S}_∞ , $K_{AB} \equiv n_{\alpha;\beta} e_A^\alpha e_B^\beta$ where n_α is the spacelike unit normal to the two-sphere, as for the Komar mass, and e_A^α are the tangent vectors on \mathcal{S}_∞ .

Because we deal with non asymptotically-flat spacetimes in this thesis, the ADM formalism does not directly apply, but I will refer to an approach towards finding the exact mass as ‘‘ADM-like’’ when it uses a similar formula, evaluating the extrinsic curvature of a hypersurface at infinity in time and one spatial coordinate. If the selection of the background spacetime yielding K_0 is nonstandard the particular background used should be specified.

Brown-York Mass

The Brown-York (BY) mass [121, 56, 105] provides a quasilocal formalism for the mass of these black holes. It requires the computation of the Brown-York boundary stress tensor [122],

$$T_{(BY)}^{\alpha\beta} = T^{\alpha\beta} + \frac{1}{4\pi\sqrt{-\gamma}} \frac{\delta\mathcal{S}_{ct}}{\delta\gamma_{\alpha\beta}} \quad (3.26)$$

where the stress-energy-momentum tensor is defined by [62]

$$T_{\mu\nu} = \frac{-2}{\sqrt{-g}} \frac{\delta\mathcal{S}_{\text{matter}}}{\delta g^{\mu\nu}} \quad (3.27)$$

and where the last term in (3.26) contains a functional derivative of the action counterterms (see the note below on counterterms) with respect to the metric after ADM decomposition, $ds^2 = -N^2 dr^2 + \gamma_{\mu\nu} (dx^\mu + N^\mu dr) (dx^\nu + N^\nu dr)$. The first term arises from the canonically conjugate momentum to $\gamma_{\mu\nu}$, and the mass is integrated from the proper energy density

$$\mathcal{M}_{BY} = \int_{\Sigma} d^2\theta \sqrt{\sigma} N n^\mu n^\nu T_{\mu\nu}^{(BY)} \quad (3.28)$$

where Σ is the boundary two-surface (which we may generalize to higher dimensions) and n is again the timelike normal of this surface.

Note that the canonical momentum part will integrate to a form similar to (3.25),

$$\mathcal{M}_{BYCM} = -\frac{1}{8\pi} \int_{\Sigma} d^2\theta \sqrt{\sigma} (K - K_0) \quad K \equiv \sigma^{AB} K_{AB} \quad (3.29)$$

which becomes the ADM mass when we evaluate on the surface at spatial infinity; $\Sigma \rightarrow \mathcal{S}_\infty$.

In this thesis, I will be interested in these quasilocal masses when evaluated at spatial infinity, so be aware that when I attach a number to the ‘‘Brown-York Mass’’ I am referring to a mass obtained using the Brown-York formalism evaluated on a surface at spatial infinity.

Hollands-Ishibashi-Marolf Mass

The Hollands-Ishibashi-Marolf (HIM) mass [123] is another quasilocal formalism that uses Hamiltonian methods. It was reached through a deeper look at the counter-term subtraction that makes the Brown-York approach tick. It was seen [124] that if non-metric fields

are nonzero at the spatial boundary, a generalization of counter-term subtraction should be used. This yields a quasilocal mass similar to, but not the same as, the Brown-York mass. This method of obtaining this mass is rather involved, and its machinery is not directly relevant to this thesis, so I will exclude a complete derivation.

The essential difference from the Brown-York mass is that the functional variation is taken with respect to a set of asymptotic frame fields which handle the nonzero values of, say, a Proca field, when we consider Lifshitz symmetric spacetimes. This ultimately causes $T_{(BY)}^{\mu\nu} = T_{(HIM)}^{\mu\nu}$ except for the case where $\mu = \nu = t$. The application of this approach in asymptotically Lifshitz spacetimes was studied in [105].

Wald Formula

The Wald formula can be used to find a 1st-law mass [62, 24, 125, 126, 106] by examining the Lagrangian under diffeomorphisms exactly as in section 2.1.2. Here a quantity $\delta\mathcal{H}$ (which is quite involved and out of context to elaborate upon in this thesis) is defined by using $\delta\mathcal{L}$, the variation of the Lagrangian under a diffeomorphism, such that $\delta\mathcal{H}_{r_h}$ (the aforementioned quantity evaluated on the horizon) yields $T\delta S$ and $\delta\mathcal{H}_{r\rightarrow\infty}$ is interpreted as the mass. This approach yields a first law which is then integrated to give a mass. For further details on this method see section 2.1.2.

Counterterms

This suffices as a brief summary of the methods mentioned in this thesis, but a number of other techniques are used (sometimes partially) to specify a mass. My list is by no means exhaustive and additional methods, especially Hamiltonian methods, have been applied to the AdS background context [123].

I should also comment that as typically implemented, Wald and the other Hamiltonian methods mentioned above require counterterms for a well-defined action. These counterterms are not unique and must be decided upon. See, for example, the work in [127, 128, 129]. The decision for the Lifshitz symmetric spacetimes that we shall consider is not universally agreed upon, and for this reason often authors will use the validity of the first law of thermodynamics to fix the counterterms and obtain a mass, as performed in [130] for example.

The way in which the thermodynamic framework which we propose goes beyond these methods is that it utilizes a consistent Smarr relation to obtain the mass. However, we would not expect to disagree with those approaches which fix the counterterms except in

cases where the lengthscales are not independent. This is for the same reason that we would not expect to disagree with any work that proposes a mass which agrees with the first law - our thermodynamic description finds the only mass that satisfies that relation, while the “unknown counterterm” approaches fix the counterterm(s) to agree with the first law.

3.2 Exact Solutions

The problem of finding exact solutions to the Einstein Field Equations is challenging, and it remains difficult even when constraining the problem to feature asymptotically Lifshitz symmetry. Nonetheless, a number of exact solutions have been found, some of which feature horizons and are termed Lifshitz-symmetric black holes. Typically the solutions are obtained through a massive simplification by imposing strong symmetries (spherical, static, and the like) as well as by fixing the Lifshitz critical exponent z to take a specific value (commonly $z = 2$, $z = 3$, or $z = D$), and finally through intense and skilful mathematical scrutiny of the resultant field equations.

In this thesis, I use the exact solutions that are known in order to learn about the thermodynamics of Lifshitz-symmetric black holes. The ideal testbed would be a Lifshitz-symmetric exact solution with a mass parameter m , a Maxwell field of charge parameter q , and an entirely unconstrained Lifshitz critical exponent z . Unfortunately, no such solution is yet known.

In this section I will collect and describe the set of solutions that have been found exactly, and I will make comments on their thermodynamics. Later, I will discuss an interesting relationship that we have found these black holes break, called the reverse isoperimetric inequality [70].

Below, I will classify these solutions based on z , D , and k . I will use the method of section 3.1.3 to find the thermodynamic mass and volume, which I will compare with the results of other methods.

3.2.1 $z = 2$, $D = 4$, $k = -1$

The first exact Lifshitz black hole I will discuss is that which was discovered in 2009 [131], a “topological” Lifshitz black hole. It has a constant negative curvature horizon topology,

and the metric functions of (3.5) are

$$f^2(r) = g^2(r) = 1 - \frac{l^2}{2r^2} \quad (3.30)$$

where for this black hole, $z = 2$, $D = 4$. It follows from the action

$$\mathcal{S} = \frac{1}{16\pi} \int d^4x \sqrt{-g} \left(R - 2\Lambda - \frac{1}{4} F_{\mu\nu} F^{\mu\nu} - \frac{1}{12} H_{\mu\nu\tau} H^{\mu\nu\tau} - \frac{C}{\sqrt{-g}} \epsilon^{\mu\nu\alpha\beta} B_{\mu\nu} F_{\alpha\beta} \right) \quad (3.31)$$

which we can see has no higher curvature components but does have two fields added; a fairly unusual field configuration is used to obtain this exact solution with the $z = 2$ Lifshitz asymptotics, known as the Background Field model, where a two-form gauge field is “topologically coupled” to a so-called axion potential. These fields have historically been of interest as they are the basis for a topological quantum field theory [132], but in this thesis they are of interest only insofar as they are able to produce the required Lifshitz asymptotics, as noted in [93].

This black hole constrains parameters in the action to be dependent, therefore, some of the simplifying assumptions made above cannot be used to determine the mass. As is usual for the Lifshitz symmetric black holes, the cosmological constant and the coupling constant C are fixed as

$$\Lambda = -\frac{z^2 + z + 4}{2l^2}, \quad 2z = (Cl)^2. \quad (3.32)$$

while the gauge fields are

$$F_{tr} = 2\frac{r}{l^2}, \quad H_{r\theta\phi} = 2r \sinh \theta. \quad (3.33)$$

The cosmological constant in this specific dimensionality with $z = 2$ is $\Lambda = -5/l^2$. From the metric (3.33) and the cosmological constant (3.32), the thermodynamic variables are calculated as

$$T = \frac{1}{4\pi l}, \quad S = \frac{r_h^2}{4} \omega_{2,-1} = \frac{l^2}{8} \omega_{2,-1}, \quad P = \frac{5}{8\pi l^2} \quad (3.34)$$

where $r_h = \frac{l}{\sqrt{2}}$ is found from the equation $f(r_h) = 0$.

Attempts at studying the thermodynamics of this black hole have been made [131]. Because the exact black hole has only a single free parameter (l), it is challenging to make a meaningful analysis. However, a numerical solution was found [131] from which plots of entropy versus temperature can be generated and stability can be investigated.

Mass was not computed in the original work, though it was suggested that the mass may be zero, due to similarities that this black hole shares with the topological AdS black

hole [133, 134]. In that research, the mass of the topological black holes was computed via the ADM-like method (3.25).

Later, for this $z = 2$ solution, the Brown-York and Hollands-Ishibashi-Marolf masses were computed in [105]. This work uses conventions, including a coordinate system chosen for constant r foliation, which are different than those used here. This makes their masses slightly tricky to compare with ours, but we can convert their solutions by redefining their free parameter \hat{l} in order to make their horizon radius agree with ours;

$$r_h = \frac{\hat{l}}{\sqrt{8}} = \frac{l}{\sqrt{2}}$$

such that $\hat{l} = 2l$. Their masses are, for $v^2 \equiv 8\pi$,

$$\mathcal{M}_{BY} = \frac{\hat{l}\omega_{2,-1}}{8v^2} = \frac{l\omega_{2,-1}}{32\pi}$$

while for minimal surface terms in the action (where coefficients have been fixed by imposing a set of conditions such as finiteness of the on-shell action and conserved charges)

$$\mathcal{M}_{HIM} = \frac{3\hat{l}\omega_{2,-1}}{32v^2} = \frac{3l\omega_{2,-1}}{128\pi}$$

and using an extended action (where additional surface terms were added to allow independent variations of the asymptotic behaviour of the metric function and the gauge field),

$$\mathcal{M}_{HIM}^{(E)} = \frac{l\omega_{2,-1}}{128\pi}.$$

The premise of [105] was that in the minimal action context, asymptotically Lifshitz spacetimes have problems with the Brown-York approach because the Proca field is fixed by the Lifshitz asymptotics and its contribution to the energy cannot be considered independently from those of the metric. Ultimately this problem with Hamilton-Jacobi analysis of asymptotically Lifshitz spacetimes needs to be understood to be confident in the mass of this class of black hole [104].

A final comparative approach involves taking the limit of $m = 0, D = 4$ of the dilaton solution in section 3.2.5 to guess at the mass for the solution (3.30). The dilaton solution would have $\mathcal{M}_K = 0$ in this case. Of course, this is at best a guess since this solution requires the dilaton to exist for $z = 2$ (it is specified for $z = 4$). For this dilaton solution, we can see that $M = 0$ and $V = l^3\omega_{2,-1}/48$, and were we able to substitute of $D = 4$ and

$z = 2$ and redefine l such that the metric function (3.57) agrees with equation (3.30). This is only suggestive, since the dilaton theory requires $z = D = 4$, but it is plausible that mass could behave in a similar fashion.

We now apply our thermodynamic technique to constrain the mass. We note that the lack of independent lengthscales means that we consider one of the options in section 3.1.2. Dimensionally, the expression for the mass must take the form

$$M = \frac{\hat{m}l\omega_{2,-1}}{32\pi} \quad (3.35)$$

where \hat{m} is a dimensionless constant. The Smarr relation then becomes

$$\frac{\hat{m}l\omega_{2,-1}}{32\pi} = (D-2)TS - 2PV = 2\left(\frac{l\omega_{2,-1}}{32\pi}\right) - 2\frac{5}{8\pi l^2}V$$

yielding

$$V = (2 - \hat{m})\frac{l^3}{40}\omega_{2,-1} \quad (3.36)$$

for the thermodynamic volume.

For comparative purposes, the Brown-York mass ($\hat{m} = 1$), the Hollands-Ishibashi-Marolf (HIM) mass ($\hat{m} = 3/4$), its value from the extended action ($\hat{m} = 1/4$), and zero mass ($\hat{m} = 0$) constitute previously known values for the mass. The volume for any of these approaches can be determined from (3.36).

Applying the first of our approaches to handle dependent lengthscales, we add a fictitious term to the metric function to yield

$$f^2(r) = 1 - \frac{l^2}{2r^2} + \tilde{m}\frac{l^p}{r^p} \quad (3.37)$$

where p will be selected based on guesses for the falloff. The power $p = D-1 = 3$ has the same falloff as the AdS-Schwarzschild case, yielding $\hat{m} = 1/4$, while a power of $p = D + z - 2 = 4$ agrees with the form of the mass term in the dilatonic solution [135], and yields $\hat{m} = 0$.

We can assume independence at the action level, following the second of our dependent lengthscale techniques. The entropy will be given by $S = \frac{r_h^2}{4}\omega_{2,-1}$ and we find that $\hat{m} = 1$.

A final possibility is to fix $V = 0$, yielding $\hat{m} = 2$, or $M = 0$, yielding $\hat{m} = 0$. In order for the thermodynamic volume and mass to remain positive, we find the condition $0 \leq \hat{m} \leq 2$ must be true.

More suggestive is the agreement with the extended action Hollands-Ishibashi-Marolf approach. The suggested $(D-1)$ scaling for the mass is in agreement with this result,

method	\hat{m}
Brown-York	1
HIM	3/4
HIM-extended	1/4
$p = (D - 1)$	1/4
$p = (D + z - 2)$	0
$M = 0$	0
$V = 0$	2
r_h, l independent	1

Table 3.1: Values of the mass parameter \hat{m} for various methods of obtaining mass for the $z = 2$ solution (3.30).

indicating that an action that allows for the independent variation of the Proca field and metric tensor may be the most compatible with the correct $(D - 1)$ scaling of mass. Interestingly, the Brown-York mass, which ignored any problems with independent variation, returned a result in agreement with our method of assuming that r_h and l are independent until the thermodynamics were computed.

In order to confirm our supposition, comparison with the HIM mass for additional Lifshitz black holes remains for future work. The results from this subsection are tabulated in table 3.1.

3.2.2 $z = 4, D = 4, k = \pm 1, 0$

Next, we consider an asymptotically Lifshitz black hole with a Maxwell charge. The action, auxiliary fields, and metric function take the form [107, 136]

$$\mathcal{S} = \frac{1}{16\pi} \int d^4x \sqrt{-g} \left(R - 2\Lambda - \frac{1}{4}H^2 - \frac{m^2}{2}B^2 - \frac{1}{4}F^2 \right) \quad (3.38)$$

$$f^2(r) = g^2(r) = 1 + a \frac{kl^2}{r^2} - b \frac{k^2l^4}{r^4} - \frac{q^2l^2}{2r^4} \quad (3.39)$$

$$B_t = \sqrt{\frac{3}{2}} \frac{r^4}{l^4} f(r), \quad A_t = \frac{r^2}{l^3} q \quad (3.40)$$

where $\Lambda = -12/l^2$. The coefficients are fixed by $a = 1/10, b = 3/400$. Note that as in the previous example, the cosmological lengthscale and horizon radius are not independent.

The case where $k = 0$ and $q = 0$ is a valid solution, but there is no horizon; it is pure Lifshitz, so while we detail its thermodynamics, we remain interested in $k = \pm 1$, where k

indexes the topology of the horizon as in 1.3. When charge is considered $k = 0$ will also become important.

This black hole has the temperature, charge, entropy, and pressure of

$$T = \frac{1}{2\pi l} \left(-ak \frac{r_h^2}{l^2} + 2bk^2 + \frac{q^2}{l^2} \right), \quad Q = \frac{1}{4\pi} \int *F = \frac{q}{2\pi} \omega_{2,k} \quad (3.41)$$

$$S = \frac{r_h^2}{4} \omega_{2,k}, \quad P = \frac{3}{2\pi l^2} \quad (3.42)$$

and the horizon is located at

$$r_h = \sqrt{l \left(-\frac{akl}{2} + \sqrt{\frac{1}{4}a^2k^2l^2 + bk^2l^2 + \frac{q^2}{2}} \right)}. \quad (3.43)$$

Here we were unable to find any previous derivations for the mass of this black hole. We therefore present a number of plausible scenarios for the mass which result from our thermodynamic method, without any comparative study.

The ansatz for mass in section 3.2.1 becomes more complicated in theories with a Maxwell charge, and we now need to use two parameters \hat{m} and \hat{w} , where these parameters are still dimensionless but can be composed of powers of q/l and r_h/l . We find that the expressions for thermodynamic mass and volume are then

$$M = \frac{\hat{m}l\omega_{2,k}}{800\pi} + \frac{\hat{w}r_h^2q^2\omega_{2,k}}{4l^3\pi} \quad (3.44)$$

$$V = \left(3k^2 \frac{r_h^2}{l^2} - 20k \frac{r_h^4}{l^4} - \hat{m} \right) \frac{l^3\omega_{2,k}}{2400} + (\hat{w} + 1) \frac{q^2r_h^2\omega_{2,k}}{12l} \quad (3.45)$$

Since we have used an integration approach to obtain the charge (by integrating the Maxwell field strength), we can exactly obtain the electric potential in terms of the charge parameter q and the other lengthscales,

$$\Phi = \frac{\partial M}{\partial Q} = \hat{w} \frac{r_h^2}{l^3} q \quad (3.46)$$

There are a number of ways in which we can plausibly examine the parameters \hat{w} and \hat{m} . The first is to use a fictitious scaling $p = (D + z - 2)$, but we also examined the case where b in the metric function $f^2(r)$ is no longer a fixed parameter but instead a variable,

because this term in the metric function shares the same falloff as the M term in the $D = 4$ Reissner-Nordström black hole, and so it may be reasonable to check whether it can behave similarly here. Finally, we also consider r_h, l, q independent at the level of the action, and treat these quantities independently in the entropy and temperature through the first law, until we finally substitute their dependence into the results.

For the purposes of reference, we reproduce the table of these results in table 3.2. We find that in the uncharged case, the power scaling $p = (D + z - 2)$ case yields a mass of zero, which is plausible since at least from the level of background subtraction this black hole has no free parameters and the correct Lifshitz background to subtract may simply be the solution itself.

We also find that treating b as a free parameter yields a finite mass, and most interestingly, this approach yields zero electric potential at the horizon. If this is later shown to be a reasonable claim for this type of black hole, then the scaling of a fictitious mass in the metric function of power scaling $p = 4 = D$ (equivalent to treating b as a free parameter) may be justified.

method	Q	k	\hat{m}	\hat{w}
$p = (D + z - 2)$	0	1, -1	0	0
	q	1, -1, 0	$50 \frac{q^2 r_h^2}{l^4}$	$-\frac{1}{4}$
$b = b(r_h, l, q, a)$	0	1	$\frac{1}{48}$	0
	0	-1	$\frac{9}{80}$	0
	q	1, -1	$5 \left(k \frac{r_h^4}{l^4} + \frac{40}{3} \frac{r_h^6}{l^6} \right)$	0
r_h, l, q independent	q	0	0	$\frac{1}{2}$

Table 3.2: Parameter values for the ansatz (3.44) for the $z = 4$ solution (3.39).

3.2.3 $z = 2, D = 5, k = 0$

For more diversity we can move to asymptotically Lifshitz black holes with actions that have higher curvature terms. In fact, there is a specific combination of higher curvature terms that can be used to satisfy the Lifshitz asymptotics without the need for a Proca field [137], and the next two black holes will use this type of action.

In five dimensions, a $k = 0$ black hole can be found using the action [138]

$$\mathcal{S} = \frac{1}{16\pi} \int d^D x \sqrt{-g} \left([R - 2\Lambda] + aR^2 + bR^{\mu\nu} R_{\mu\nu} \right. \\ \left. + c [R_{\mu\nu\rho\sigma} R^{\mu\nu\rho\sigma} - 4R_{\mu\nu} R^{\mu\nu} + R^2] \right) \quad (3.47)$$

$$f^2(r) = g^2(r) = \left(1 - \frac{ml^{5/2}}{r^{5/2}} \right) \quad (3.48)$$

where the specific couplings are ‘tuned’ to take the values $a = -16l^2/725$, $b = 1584l^2/13775$, $c = 2211l^2/11020$.

For this solution, the entropy, temperature, and pressure can be computed as

$$S = \frac{396r_h^3 \pi \omega_{3,0}}{551} \quad (3.49)$$

$$T = \frac{5r_h^2}{8\pi l^3}, \quad P = \frac{2197}{4408\pi l^2} \quad (3.50)$$

Note that this solution is the first asymptotically Lifshitz black hole that we will consider that has two independent lengthscales, l and r_h . The thermodynamic approach we have proposed therefore yields a single mass and volume which agree with the Smarr relation and first law; this yields

$$M = \frac{1782}{2197} \frac{r_h^5 \pi \omega_{3,0}}{l} \cdot \left(\frac{2197l \omega_{3,0}}{3 \times 2204 \pi l^2} \right) = \frac{297}{1102} \cdot \frac{r_h^5 \omega_{3,0}}{l^3} \quad (3.51)$$

$$V = \left(\frac{5r_h^2}{8\pi l^3} \frac{1188\pi r_h^2 \omega_{3,0}}{551} \right) r_h (-3) \left(\frac{5}{\pi l^2} \frac{-2197}{2204} \right)^{-1} \\ = \frac{1782}{2197} \cdot \frac{r_h^5 \pi \omega_{3,0}}{l} \quad (3.52)$$

A Brown-York method has been applied to compute the mass of this black hole, but as discussed in section 3.1.4, counterterms were required to finish this computation, and they are not uniquely known. In [130], the counterterms were fixed by a first-law method, so it is expected that the mass determined in [138] through this approach will agree with (3.51) (and indeed, it agrees!). Nevertheless, we have obtained the same mass independent of any of the quasilocal formalism used in [138], and our approach is very easy and straightforward to implement. What is more, we have obtained the thermodynamic volume, which will later be useful in any examination of the universality class of these types of black holes.

3.2.4 $z = 3, D = 3, k = 0$

In three dimensions, a planar black hole exists similar to the one presented in section 3.2.3, with the action (3.47) but the metric function and cosmological constant [139, 138]

$$f^2(r) = g^2(r) = \left(1 - m \frac{l^2}{r^2}\right) \quad (3.53)$$

$$\Lambda = -13/2l^2$$

and the coefficients $a = -3l^2/4$, $b = 2l^2$, and $c = 0$.

The temperature and entropy can be computed for this solution as

$$S = 2\pi r_h \quad P = 13/16\pi l^2 \quad T = r_h^3/2\pi l^4 \quad (3.54)$$

This solution has two independent lengthscales, and so we compute the thermodynamic mass and volume in a similar fashion to section 3.2.3, yielding

$$M = \frac{r_h^4}{4l^4}, \quad V = \frac{8\pi r_h^4}{13l^2} \quad (3.55)$$

Similar to section 3.2.3, the mass was computed up to counterterms which were fixed via a first-law [138], and this computation agrees with our expression (3.55).

So far we have seen two asymptotically Lifshitz black holes which have independent horizon radius and cosmological length, and our thermodynamic method has successfully obtained a mass that agrees with alternate derivations.

3.2.5 $z = D, k = 1, 0$

This exact solution was found in Einstein-Dilaton-Maxwell gravity, where the action has a dilaton added as well as a set of N Maxwell fields which couple to the dilaton [135]. The

particular action and solution found is

$$\mathcal{S} = \frac{1}{16\pi} \int d^D x \sqrt{-g} \left[R - 2\Lambda - \frac{1}{2} (\partial\phi)^2 - \frac{1}{4} \sum_{i=1}^N e^{\lambda_i \phi} F_i^2 \right] \quad (3.56)$$

$$f(r) = k \left(\frac{D-3}{D+z-4} \right)^2 \frac{l^2}{r^2} + 1 - mr^{2-D-z} + \sum_{n=2}^{N-k} \frac{q_n^2 \mu^{-\sqrt{\frac{2(z-1)}{D-2}}} l^{2z}}{2(D-2)(D+z-4)} r^{-2(D+z-3)} \quad (3.57)$$

$$A'_{t,1} = l^{-z} \sqrt{2(D+z-2)(z-1)} \mu^{\sqrt{\frac{D-2}{2(z-1)}}} r^{D+z-3}, \quad (3.58)$$

$$A'_{t,n} = q_n \mu^{-\sqrt{\frac{2(z-1)}{D-2}}} r^{3-D-z}, \quad (3.59)$$

$$A'_{t,N} = l^{1-z} \frac{\sqrt{2k(D-2)(D-3)(z-1)}}{\sqrt{D+z-4}} \mu^{\frac{(D-3)}{\sqrt{2(D-2)(z-1)}}} r^{D+z-5}, \quad (3.60)$$

$$e^\phi = \mu r^{\sqrt{2(D-2)(z-1)}} \quad (3.61)$$

where there are N Maxwell fields $A_{t,n}$ coupled to a scalar ϕ (the dilaton). We can see that a number of the Maxwell fields are fixed in order to obtain the solution; the free fields are $n \in [2, N-k]$, when $N \geq 2+k$, and in addition all of the λ_i couplings between the Maxwell fields and the dilaton are fixed by the field equations. The additional field for $k=1$ as opposed to $k=0$ is because an extra gauge field is needed to support the near-horizon geometry; the first field is used to give the Lifshitz asymptotics. As a final note, $k=-1$ is allowed as a solution but has an imaginary charge density unless $z=1$, so we do not consider it here.

The temperature, entropy, and pressure can be computed via the usual methods,

$$T = \frac{r_h^z}{4\pi l^{z+1}} \left((D+z-2) + k \frac{l^2(D-3)^2}{r_h^2(D+z-4)} - \sum_{n=2}^{N-k} \frac{q_n^2 \mu^{-\sqrt{\frac{2(z-1)}{D-2}}} l^{2z}}{2(D-2)} r_h^{-2(D+z-3)} \right), \quad (3.62)$$

$$S = \frac{\omega_{D-2,k}}{4} r_h^{D-2}, \quad (3.63)$$

$$P = \frac{(D+z-2)(D+z-3)}{16\pi l^2} \quad (3.64)$$

and we comment that the computation of the Maxwell charge can be performed to yield

$$Q_i = \frac{1}{16\pi} \int e^{\lambda_i \phi} * F = \frac{q_i \omega_{D-2,k} l^{z-1}}{16\pi} \quad (3.65)$$

so we can obtain the electric potential with our method, in this case.

The metric function has $N + 1 - k$ independent lengthscales; q_n as well as l and r_h . The Smarr relation (2.51) and first law (2.50) constrain the thermodynamic mass, volume, and electric potential to be

$$M = \frac{(D-2)\omega_{D-2,k}}{16\pi} \left[\left(1 + k \frac{(D-3)^2 l^2}{(D+z-4)^2 r_h^2} \right) l^{-z-1} r_h^{D+z-2} + \sum_{n=2}^{N-k} \frac{q_n^2 \mu^{-\sqrt{\frac{2(z-1)}{D-2}}}}{2(D-2)(D+z-4)} l^{z-1} r_h^{4-D-z} \right], \quad (3.66)$$

$$V = \frac{(D-2)\omega_{D-2,k}}{(D+z-3)(D+z-2)} \left[\left(\frac{(z+1)}{2} + k \frac{(D-3)^2 (z-1) l^2}{2(D+z-4)^2 r_h^2} \right) l^{1-z} r_h^{D+z-2} - \sum_{n=2}^{N-k} \frac{(z-1) q_n^2 \mu^{-\sqrt{\frac{2(z-1)}{D-2}}}}{4(D-2)(D+z-4)} l^{z+1} r_h^{4-D-z} \right], \quad (3.67)$$

$$\Phi_n = - \frac{q_n \mu^{-\sqrt{\frac{2(z-1)}{D-2}}}}{(D+z-4)} r_h^{4-D-z}. \quad (3.68)$$

In fact, this mass is simply obtained by solving $f(r_h) = 0$ for m ; then the mass is

$$\mathcal{M} = \frac{\omega_{D-2,k}}{16\pi} m l^{-1-z} (D-2) \quad (3.69)$$

This result, along with our electric potential from (3.68), agrees with those found in [135] and [106]; [135] computed mass through a Komar prescription whilst [106] used a Wald method for the $k = 0$ case.

3.2.6 $z = 2(D-2)$, $k = 0$

The final case we shall consider here is a planar black brane solution in arbitrary dimension [136, 140]. This solution is interesting because it requires a the Maxwell field, a cosmological constant, and a Proca field to support a single exact solution with only one free parameter.

The action and solution is

$$\mathcal{S} = \frac{1}{16\pi} \int d^D x \sqrt{-g} \left(R - 2\Lambda - \frac{1}{4} H^2 - \frac{1}{2} m^2 B^2 - \frac{1}{4} F^2 \right) \quad (3.70)$$

$$f(r) = 1 - \frac{q^2 l^2}{2(D-2)^2 r^z} \quad (3.71)$$

$$B_t = \sqrt{\frac{2(z-1)}{z}} \frac{r^z}{l^z} f(r), \quad F_{rt} = ql^{1-z} r^{-D+z+1} \quad (3.72)$$

$$(3.73)$$

where the solution is found for $z = 2(D-2)$, and H is the Proca field strength while F is the Maxwell field strength.

The temperature, entropy, and pressure of this black hole are

$$T = \frac{l^{5-2D} q^2}{4\pi(D-2)}, \quad S = \frac{r_h^{D-2}}{4} \omega_{D-2,0}, \quad (3.74)$$

$$P = \frac{7D^2 - 30D + 32}{16\pi l^2}, \quad (3.75)$$

and the Maxwell charge can be found from an integral

$$Q = \frac{1}{4\pi} \int *F = \frac{q}{4\pi} \omega_{D-2,0} \quad (3.76)$$

This solution is particularly difficult to constrain thermodynamically, because we again have a dependence among our lengthscales. We choose q as the completely independent parameter in order for our method of splitting charge apart from the r_h, l power series to apply, leaving $r_h = r_h(l)$, and we make use of the aforementioned techniques to make some educated guesses at a thermodynamic mass and volume. There are not yet any unambiguous alternative derivations of the mass for this black hole, so while we can make suggestions about this black hole's mass we cannot find another work with which to agree or disagree.

Using the fictitious mass approach, where the metric function is

$$f^2(r) = 1 + m \left(\frac{l}{r} \right)^p - \frac{q^2 l^2}{2(D-2)^2 r^z} \quad (3.77)$$

yields

$$M = \frac{(6(D-2) - 2p)\omega_{D-2,0}r_h^{3D-6}}{48\pi l^{2D-3}}$$

$$PV = \frac{(6D^2 - 27D + 30 + 2p(3-D))\omega_{D-2,0}r_h^{3D-6}}{48\pi l^{2D-3}}$$

so we can see that for $p = (D + z - 2)$, $M = 0$.

The other interesting case, when r_h and l are assumed to be independent in the entropy and temperature, gives a mass that is finite for nonzero r_h and q , and obeys

$$M = \frac{1}{2}\Phi Q$$

which seems sensible because it simply reflects the fact that this solution necessarily requires a finite Maxwell field in order to generate a black hole solution; linking the mass and charge in this manner is plausible. If we were to neglect entropy and pressure as dynamical thermodynamic variables, the Eulerian scaling argument on the remaining lengthscale $[q]$ would give us this relationship.

3.2.7 Summary

The table 3.3 shows the Lifshitz black holes we have considered in this section, where the masses were thermodynamically ambiguous, and it counts the instances in which other approaches' masses agree with our approaches. Interestingly the HIM mass with the extended action returns the same result as assuming a fictitious mass term with the dimensional scaling that is conjectured in (2.45). Further study might give better insight into exactly why this is, but on the surface it seems plausible that a method designed to carefully build independence of the various lengthscales in the problem should agree with a thermodynamic approach that is carefully designed to also allow for complicated relationships between lengthscales.

In addition, in the instances when the mass was not thermodynamically ambiguous, our approach has agreed with multiple methods, including the Wald, Komar, and Brown-York methods.

Apparently the task of varying the Proca field independently of the metric tensor yields problems only when additional lengthscales are mixed, such as those of the horizon radius

method	$p = (D - 3)$	$p = (D + z - 2)$	$M = 0$	r_h, l independent
Brown-York	0	0	0	✓
HIM	0	0	0	0
HIM-extended	✓	0	0	0
Topological (zero mass)	0	✓✓	✓✓	0

Table 3.3: Comparison of alternative methods of obtaining the mass in section 3.1.4 with our thermodynamic methods of section 3.1.3 for the solutions considered here.

and cosmological constant. When these lengthscales are independent, counterterms can be fixed using the thermodynamics, and this gives a prescription for mass that always agrees with ours. To strengthen this conclusion, applying the HIM and Brown-York methods to some of the black holes considered here remains an interesting endeavour.

3.3 A Specific Smarr Relation

Here I show a derivation of the Smarr relation (3.6) as arising from the more general Smarr relation (2.51). The former is an alternative Smarr relation for anisotropic black holes which depends on the critical parameter z [106, 107, 108, 109, 110, 111, 112] and appears to hold. The question is whether and how this Smarr relation is related to (2.51), and which of them is more fundamental. As shown below, our relation (2.51) can be shown to simplify to (3.6) in some specific cases, such as when $k = 0$ for some planar Lifshitz black holes. We propose [3] that the relation (3.6) be used instead, as it is more widely applicable.

In order to show equivalence, we have to make a number of restrictive assumptions, which is why this former Smarr relation is less general than (2.51). First of all, we assume that the parameters l and r_h are independent and that the thermodynamic parameters $S = S(r_h)$ and $P = P(l)$. The latter is an important restriction as it does not necessarily hold when higher curvature terms are added to the action, for example in (2.40). If the higher curvature couplings are made dimensionless by adding them to the action in a way that depends on the cosmological lengthscale, one then has an entropy that is not independent of l , and in the context of an extended Smarr relation the entropy can take the form $S = S(r_h, \lambda, \mu, \dots)$.

Nonetheless, with this assumption the first law of thermodynamics greatly simplifies, yielding two equations

$$\frac{\partial M}{\partial l} = V \frac{\partial P}{\partial l} \quad \frac{\partial M}{\partial r_h} = T \frac{\partial S}{\partial r_h} \quad (3.78)$$

We then make the simplification that the entropy depends only on r_h^{D-2} . Since the cosmological constant $[\Lambda] = 1/l^2$, (3.78) simplifies to

$$r_h \frac{\partial S}{\partial r_h} = (D-2)S \quad \frac{\partial P}{\partial l} = -\frac{2P}{l} \quad (3.79)$$

Finally, we assume that the temperature depends on the horizon radius and cosmological lengthscale in a very simple way, namely that the dimensionality of temperature is

$$[T] = \frac{r_h^z}{l^{z+1}} \quad (3.80)$$

This tends to hold for simple forms of the metric function $f^2(r)$, usually just for planar black holes (when $k = 0$), as then the metric function takes the form

$$f(r) = 1 + m \left(\frac{l}{r} \right)^\Xi$$

for some constant power Ξ , which yields temperatures of the form (3.80) when the formula (2.31) is applied.

The dimensional scaling of the mass in this case is

$$[M] = \frac{r_h^{z+D-2}}{l^{z+1}} \quad (3.81)$$

and the relevant equation for the thermodynamic mass is

$$M = \frac{T \cdot r_h}{\beta} \frac{\partial S}{\partial r_h} = \frac{(D-2)}{(D+z-2)} TS \quad (3.82)$$

We therefore see that in these specific contexts the Smarr relation may appear to be dependent on the Lifshitz parameter z when in fact a more general interpretation where the asymptotic behaviour is accounted for as a pressure term will yield a Smarr relation that is more similar to the traditional form.

3.4 The Reverse Isoperimetric Inequality

One question which this work enables us to answer is whether the reverse isoperimetric inequality holds for asymptotically Lifshitz symmetric black holes. Fundamentally a geometric relationship between the area and volume of a closed surface, the isoperimetric

inequality says that the ratio

$$\mathcal{R} = \left(\frac{(D-1)\mathcal{V}}{\omega_{D-2,1}} \right)^{\frac{1}{D-1}} \left(\frac{\omega_{D-2,1}}{\mathcal{A}} \right)^{\frac{1}{D-2}} \quad (3.83)$$

is less than or equal to one for a connected domain in Euclidean space, where \mathcal{V} is the volume enclosed by the subject and \mathcal{A} is its surface area [70].

For black holes in general relativity, however, the relationship is reversed, and it was conjectured [70] that instead, a reverse isoperimetric inequality will hold for black holes. For example, the Schwarzschild-AdS black hole saturates the inequality, with $\mathcal{R} = 1$, while Kerr-AdS black holes have $\mathcal{R} \geq 1$, with saturation only when non-rotating.

The Lifshitz case was examined in [3] and we found that for a number of $z \geq 2$ black holes (all of them for which we computed this quantity), the isoperimetric inequality can be violated ($\mathcal{R} < 1$) in certain regimes. Furthermore, we showed that increasing the charge of the black hole can act to increase the isoperimetric ratio, eventually yielding $\mathcal{R} > 1$.

These results join another work on “super-entropic” black holes [83] in providing examples where the reverse isoperimetric inequality is violated. This leads us to believe that this relationship is more complicated than previously thought. Because volume is not a covariant quantity, it is likely possible to better understand this inequality by carefully studying prescriptions for volume in asymptotically Lifshitz symmetric spacetimes.

3.5 Numerical Solutions

Numerical methods are quite important in the study of these anisotropic black holes because as we have seen, the exact solutions often have parameters which are not independent, making the thermodynamics challenging to interpret.

The first step in tackling this problem is in obtaining the field equations given a spherically symmetric metric ansatz. The method of Appendix A will be used to perform a functional variation of the action (3.4) under the metric (3.5).

In this description of the method, I will use a cubic quasitopological theory without a Maxwell field to discuss the details, and then I will examine the thermodynamics from this theory (in subsection 3.5.2) followed by a discussion of the changes that need to be made to account for a quartic quasitopological term (in subsection 3.5.3). The Maxwell field can be added with relative ease; its field equation can be solved and its contributions to the field equations accounted for; no substantial changes to the methodology are required.

The current state of GRTensor [141] does not yet provide an easy method for obtaining dimension-independent quantities in general relativity, so for each dimension the variation of the action with respect to the metric functions N , g , and h is performed. These results were checked by hand for a dimension-independent calculation in order to obtain the dimensionally independent field equations, which are related to the equations (2.65)-(2.67), but with modifications due to the Lifshitz parameter and the mass of the Proca field; for example, the field equation (2.66) is

$$\left[(D-2)r^{D-1} \left(\frac{-2\Lambda L^2}{(D-1)(D-2)} - \kappa + \frac{\tilde{\lambda}}{L^2} \kappa^2 - \frac{\tilde{\mu}}{L^4} \kappa^3 \right) \right]' = \frac{q^2 r^{D-2}}{2N^2} [((rh)' + zh)^2 + m^2 L^2 h^2] \quad (3.84)$$

where the coupling constants of (3.4) are redefined in order to produce a simplification of the field equations:

$$\tilde{\lambda} \equiv (D-3)(D-4)\mu_2 \quad \tilde{\mu} \equiv \frac{(3D^4 - 42D^3 + 205D^2 - 414D + 288)}{(16D - 24)} \mu_3$$

and $\kappa \equiv (g^2(r) - \frac{L^2}{r^2} k)$. In the numerical work provided in this thesis, we use redefinitions $\mu \equiv \tilde{\mu} L^4$ and $\lambda \equiv \tilde{\lambda} L^2$ to remove dimensionality from the higher curvature coefficients. However, for complete extended phase space thermodynamics (as mentioned in 4.2), the above definitions are required, so the implementation of this method will be performed using the dimensional definitions $\tilde{\mu}, \tilde{\lambda}$. Furthermore, the extension to quartic quasitopological terms is algebraically very lengthy, so it is discussed in section 3.5.3.

In order to replicate these results without relying on symbolic algebra packages, it is often useful to simplify the action before the functional variation;

$$\mathcal{S} \sim \frac{1}{L^{z+1}} \int d^D x \sqrt{\frac{f}{g}} \frac{r^{z-1}}{k^{(D-3)/2}} \left(\left\{ (D-2)r^{D-1} \left(1 - \kappa + \frac{\tilde{\lambda}}{L^2} \kappa^2 - \frac{\tilde{\mu}}{L^4} \kappa^3 \right) \right\}' + r^{D-2} \frac{q^2}{2f} \{ [(rh)' + zh]^2 + m^2 L^2 h^2 \} \right) \quad (3.85)$$

which is a lengthy algebraic procedure; the easiest approach is to expand the derivatives in the integrand of this action and compare term-by-term with the action (3.4) after using the integration by parts utility from appendix A to remove all second order derivatives in $f(r)$ and $g(r)$.

Adding a Maxwell field yields an additional set of terms; the same ansatz as for the Proca field means the terms are the same up to a substitution $h(r) \rightarrow \gamma(r)$ although there

is no mass term present for the Maxwell; inside the round brackets of (3.85) the additional terms will appear as

$$r^{D-4} \frac{Q^2}{2f} [(r\gamma)' + z\gamma]^2 \quad (3.86)$$

An ansatz is made for the vector potential of the Proca field, implicitly bringing out the scaling that it requires to form an interesting numerical solution [108],

$$A_t = q \frac{r^z}{L^z} h(r) \quad (3.87)$$

where a $r \rightarrow \infty$, $h(r) \rightarrow 1$. The higher curvature terms do allow for an asymptotically Lifshitz solution to be obtained when $h(r)$ vanishes, but this is typically a highly constrained type of solution and is not thermodynamically interesting; the cosmological constant and higher curvature couplings are fixed in terms of a single parameter, and the equations of motion are solvable to yield an exact solution for $g^2(r)$ [4, 108, 142]. I will not consider these solutions any further here.

The decision for the cosmological constant typically amounts to ensuring that the metric functions are asymptotically equal to one, which makes the numerical procedure much easier. The case when we are in $D = 5$ yields a solution

$$\Lambda_{5D} = - \frac{-48 \tilde{\mu} z - 32 L^2 \tilde{\lambda} z - 24 \tilde{\mu} + 16 L^4 z - 16 \tilde{\lambda} z^2 L^2 - 24 \tilde{\mu} z^2 - 48 L^2 \tilde{\lambda} + 72 L^4 + 8 L^4 z^2}{16L^6} \quad (3.88)$$

while the case of $D = 4$ yields

$$\Lambda_{4D} = \frac{1}{2} \frac{(-4 - z - z^2)}{L^2} \quad (3.89)$$

where it should be noticed that since we are in four dimensions, the quasitopological and Gauss-Bonnet term are not active, so the cosmological constant is only dependent on the Lifshitz parameter z .

In addition, the asymptotic requirements that $f^2(r), g^2(r), h(r)$ all equal one also provides restrictions on the Proca field's mass and charge. These turn out to be

$$q^2 = \frac{2(z-1)(1-2\lambda+3\mu)}{z} \quad m^2 = \frac{3z}{L^2} \quad (3.90)$$

We now have a coupled set of nonlinear differential equations, which are first order in $f(r)$ and $g(r)$ (a simple substitution $j(r) = dh(r)/dr$ yields completely first order equations at the cost of one additional equation). This problem is well posed when the horizon

boundary condition is interpreted as an initial value, which is evolved out to infinity by setting up a discretization in the radial direction, and evolving the metric functions with a finite difference form of the differential equations. The free parameters are tuned to obtain convergence to the appropriate asymptotics. The metric functions $f(r) = g(r) = 0$ at the horizon r_h (more importantly, they are regular and linearly go to zero the horizon, so that $f^2(r) = (r - r_h)\tilde{f}(r)$ and $g^2(r) = (r - r_h)\tilde{g}(r)$ imply finite and nonzero $\tilde{f}(r), \tilde{g}(r)$ - this ensures that the expected sign change in the metric functions occurs across the horizon).

Note that there exists the possibility of allowing for solutions where the metric functions do not go to zero linearly, but instead with some power, provided that the horizon is only a saddle point. This scenario is not considered in this work since, within numerical error, it is likely that both ansätze for the near-horizon metric function will yield the same convergent numerical solution.

The series ansätze can be formed:

$$\begin{aligned} f^2(r) &= f_1 \left\{ (r - r_0) + f_2(r - r_0)^2 + f_3(r - r_0)^3 + \dots \right\}, \\ g^2(r) &= g_1(r - r_0) + g_2(r - r_0)^2 + g_3(r - r_0)^3 + \dots, \\ h(r) &= f_1^{1/2} \left\{ h_0 + h_1(r - r_0) + h_2(r - r_0)^2 + h_3(r - r_0)^3 + \dots \right\} \end{aligned} \quad (3.91)$$

The complete series expansion of these metric functions is given by first checking that after substitution of the cosmological constant, Proca mass, and charge, the field equations are all solved when the metric functions equal one. Two of the field equations reduce to the same condition, that

$$6(z - 1) f_1 h_0^2 (-1 + 2\lambda - \mu) r_0^6 = 0 \quad (3.92)$$

which is satisfied by having the Proca field potential linearly tend to zero at the horizon, $h_0 = 0$.

The differential equations are then solved to first order in $(r - r_h) \equiv \epsilon$ by taking derivatives with respect to ϵ and then setting $\epsilon = 0$, yielding one nontrivial equation

$$\begin{aligned} & -12 \frac{f_1}{z} \left(\frac{1}{2} h_1^2 (z - 1) g_1 \left(-\frac{1}{3} + \frac{2}{3} \lambda - \mu \right) r_0^8 - \frac{1}{2} z g_1 r_0^7 - \frac{1}{2} \right. \\ & \left. \left(\left(-\frac{1}{3} + \frac{2}{3} \lambda - \mu \right) z^2 + \left(\frac{4}{3} \lambda - 2\mu - \frac{2}{3} \right) z - 3 + 2\lambda - \mu \right) \right. \\ & \left. z r_0^6 - L^2 \lambda k z g_1 r_0^5 + L^2 k z r_0^4 - \frac{3}{2} L^4 \mu k^2 z g_1 r_0^3 + z((- \mu) L^6 k) \right) = 0 \end{aligned} \quad (3.93)$$

which is an expression in f_1, h_1, g_1 , and has a solution in g_1 . We find that this coefficient can be fixed in terms of the other two, as

$$\begin{aligned}
g_1 = & -\frac{z}{2} \left(12L^2kr_0^4 + 2z^2r_0^6 - 4z^2\lambda r_0^6 - 6(-\mu)z^2r_0^6 \right. \\
& - 8z\lambda r_0^6 - 12(-\mu)zr_0^6 + 4zr_0^6 + 18r_0^6 - 12r_0^6\lambda - 6r_0^6(-\mu) + 12(-\mu)L^6k) \\
& \times \left(r_0^3(-3zr_0^4 - 6L^2\lambda k z r_0^2 - h_1^2r_0^5z + 2h_1^2r_0^5z\lambda + 3h_1^2r_0^5(-\mu)z \right. \\
& \left. \left. + h_1^2r_0^5 - 2h_1^2r_0^5\lambda - 3h_1^2r_0^5(-\mu) + 9L^4(-\mu)k^2z \right) \right)^{-1} \tag{3.94}
\end{aligned}$$

If a Maxwell field is added for charged solutions, a new field equation is obtained from the Maxwell potential ansatz

$$\mathcal{A}_t = \frac{r^z}{L^z} \psi(r) \tag{3.95}$$

which takes the form

$$\frac{r^z}{r} \psi(r) + r^z (\psi'(r)) = \frac{Qf(r)}{r^{4-z}g(r)} \tag{3.96}$$

where Q is a constant of integration (related to the Maxwell charge) and new expressions for (3.93), (3.94) are required:

$$\begin{aligned}
& -12\frac{f_1}{z} \left(\frac{1}{2}h_1^2(z-1)g_1 \left(-\frac{1}{3} + \frac{2}{3}\lambda - \mu \right) r_0^8 - \frac{1}{2}z g_1 r_0^7 - \frac{1}{2} \right. \\
& \left(\left(-\frac{1}{3} + \frac{2}{3}\lambda - \mu \right) z^2 + \left(\frac{4}{3}\lambda - 2\mu - \frac{2}{3} \right) z - 3 + 2\lambda - \mu \right) \\
& \left. z r_0^6 - L^2\lambda k z g_1 r_0^5 + L^2k z r_0^4 - \frac{3}{2}L^4\mu k^2 z g_1 r_0^3 + z((-\mu)L^6k - \frac{1}{12}Q^2) \right) = 0 \tag{3.97} \\
g_1 = & -\frac{z}{2} \left(12L^2kr_0^4 + 2z^2r_0^6 - 4z^2\lambda r_0^6 - 6(-\mu)z^2r_0^6 \right. \\
& - 8z\lambda r_0^6 - 12(-\mu)zr_0^6 + 4zr_0^6 + 18r_0^6 - 12r_0^6\lambda - 6r_0^6(-\mu) + 12(-\mu)L^6k - Q^2) \\
& \times \left(r_0^3(-3zr_0^4 - 6L^2\lambda k z r_0^2 - h_1^2r_0^5z + 2h_1^2r_0^5z\lambda + 3h_1^2r_0^5(-\mu)z \right. \\
& \left. \left. + h_1^2r_0^5 - 2h_1^2r_0^5\lambda - 3h_1^2r_0^5(-\mu) + 9L^4(-\mu)k^2z \right) \right)^{-1} \tag{3.98}
\end{aligned}$$

It can be seen that the Maxwell field does not qualitatively alter this method.

In the case where there is no Maxwell field, the second order near-horizon field equations

can be solved for solutions for f_2, g_2, h_2 yielding

$$\begin{aligned}
f_2 = & \left(-6g_1r_0^8 \left(z \left(\lambda g_1 - \frac{2}{3}h_1^2L_0 \right) + \frac{2}{3}h_1^2L_0 \right) + 12zr_0^7 \left(z \left(g_1 + \frac{1}{2}L_0h_1^2 \right) + \frac{3}{4}g_1 - \frac{1}{4}L_0h_1^2 \right) \right. \\
& + 18zr_0^6 \left(\frac{1}{9}L_0z^2 + \frac{2}{9}L_0z + \frac{1}{3}L_0 + (-\mu)L^2kg_1^2 \right) + 24kL^2g_1\lambda zr_0^5 \left(z - \frac{1}{4} \right) \\
& - 36k^2L^4g_1z(-\mu)r_0^3 \left(z - \frac{5}{4} \right) + 24z(-\mu)L^6k^3 \Big) \\
& \times \left(r_0 \left(L_0h_1^2g_1r_0^8 - 9zr_0^7g_1 - zr_0^6 \left(L_0z^2 + 2L_0z + 3(-\mu) + 6\lambda - 9 \right) \right. \right. \\
& \left. \left. - 18z\lambda L^2kg_1r_0^5 + 6zL^2kr_0^4 + 27L^4k^2(-\mu)zr_0^3g_1 + 6z(-\mu)L^6k^3 \right) \right)^{-1}
\end{aligned}$$

$$\begin{aligned}
g_2 = & \left(2g_1r_0^{12} \left(L_0 \left(g_1 + h_1^2 \left(z^2 + 1 \right) L_0 \right) \right. \right. \\
& + z \left(-3g_1^2\lambda - 2h_1^2g_1L_0 - 2h_1^4L_0^2 \right) - 3zg_1r_0^{11} \left(z \left(2g_1 + 5L_0h_1^2 \right) - 13g_1 + 5h_1^2L_0 \right) + \\
& + r_0^{10} \left(-2z^4L_0 \left(g_1 + h_1^2L_0 \right) + 2z^3L_0 \left(2g_1 - h_1^2L_0 \right) \right. \\
& + z^2 \left(4L_0L^2k\lambda h_1^2g_1^2 + g_1 \left(42(-\mu) + 20\lambda + 2 \right) + 2h_1^2L_0 \left(3(-\mu) - 2\lambda + 7 \right) \right) \\
& + z \left(6g_1^3L^2k \left(-3\mu - 2\lambda^2 \right) - 8L^2k\lambda h_1^2g_1^2L_0 \right. \\
& + g_1 \left(-24\mu + 48\lambda - 72 \right) + 6h_1^2L_0 \left(-\mu + 2\lambda - 3 \right) \Big) + 4L^2k\lambda h_1^2g_1^2L_0 \\
& - 6L^2kzg_1\lambda r_0^9 \left(z \left(4g_1 + 5h_1^2L_0 \right) - 22g_1 + 5h_1^2 \right) \\
& - 4L^2kr_0^8 \left(z^4\lambda g_1L_0 - 2z^3\lambda g_1L_0 + z^2 \left(-\frac{3}{2}\mu L^2kh_1^2g_1^2L_0 + g_1 \left(-3 - \lambda - 10\lambda^2 + 21\lambda\mu \right) - 3h_1^2L_0 \right) \right. \\
& + z \left(-\frac{27}{2}kL^2g_1^3\lambda(-\mu) - 3L_0(-\mu)L^2kh_1^2g_1^2 + 3g_1 \left(-8\lambda^2 - 4(-\mu)\lambda + 12\lambda + 3 \right) + 3h_1^2L_0 \right) \\
& \left. + \frac{3}{2}L_0(-\mu)L^2kh_1^2g_1^2 \right) \\
& + 9L^4zk^2g_1r_0^7 \left(z \left(g_1 \left(4(-\mu) - \frac{8}{3}\lambda^2 \right) + 5(-\mu)h_1^2L_0 \right) + g_1 \left(-18(-\mu) + 12\lambda^2 \right) - 5(-\mu)h_1^2L_0 \right) \\
& + 6L^4zk^2g_1r_0^6 \left(z^3(-\mu)L_0 - 2z^2(-\mu)L_0 + z \left(-21(-\mu)^2 - (-\mu) - 10\lambda(-\mu) + 4\lambda \right) \right. \\
& - 9kL^2(-\mu)^2g_1^2 - 12(-\mu)^2 + (-\mu) \left(36 - 24\lambda \right) - 12\lambda \Big) \\
& + 36(-\mu)L^6zk^3g_1^2\lambda r_0^5 \left(2z - 7 \right) - 12(-\mu)L^6zk^3r_0^4 \left(z \left(2g_1 - L_0h_1^2 \right) - 8g_1 + h_1^2L_0 \right) \\
& + 27(-\mu)^2L^8zk^4g_1^2r_0^3 \left(2z - 5 \right) + 24zg_1(-\mu)L^8k^4\lambda r_0^2 \left(z - 1 \right) - 36zg_1(-\mu)^2L^10k^5 \left(z - 1 \right) \\
& \times \left(r_0 \left(-r_0^4 - 2\lambda L^2kr_0^2 + 3L^4k^2(-\mu) \right) \left(-L_0g_1 \left(z - 1 \right) h_1^2r_0^8 + 9zg_1r_0^7 \right. \right. \\
& \left. \left. + zr_0^6 \left(z^2L_0 + 2zL_0 - 3\mu - 9 + 6\lambda \right) + 18z\lambda L^2kg_1r_0^5 - 6zL^2kr_0^4 + 27L^4k^2\mu zr_0^3g_1 + 6z\mu L^6k^3 \right) \right)^{-1}
\end{aligned}$$

$$\begin{aligned}
h_2 = & -h_1 \left(r_0^5 \left(z \left(-2g_1 - h_1^2 L_0 \right) - 3g_1 + h_1^2 L_0 \right) + 3zr_0^4 - 4L^2 k g_1 \lambda r_0^3 (2z + 3) \right. \\
& + 6z\lambda L^2 k r_0^2 + 3(-\mu)L^4 k^2 g_1 r_0 (2z + 3) - 9L^4 k^2 (-\mu)z \left. \right) \\
& \cdot \left(r_0^2 g_1 \left(-2r_0^4 - 4\lambda L^2 k r_0^2 + 6L^4 k^2 (-\mu) \right) \right)^{-1}
\end{aligned}$$

where we define the constant $L_0 \equiv -1 + 2\lambda - 3\mu$ for a bit of algebraic simplicity. After substituting the solution for g_1 from equation (3.94), we notice that these expressions become dependent only on f_1, h_1 .

The procedure is performed yet again to solve for f_3, h_3, g_3 and ultimately these solutions are found in terms of f_1, h_1 . This forms a third order near-horizon series expansion that we can use to set up initial conditions for the shooting method, given free parameters f_1, L, r_0 , and h_1 .

The remaining boundary condition is much easier; the metric functions must all approach unity as $r \rightarrow \infty$. Reducing the field equations (3.84) to first order requires a new parameter

$$j(r) \equiv \frac{dh(r)}{dr} \quad (3.99)$$

and comes at the cost of one additional equation to numerically solve.

Upon making this substitution, as well as the substitution of the cosmological constant, Proca charge, and mass, our set of first order differential equations is (under the simplifying notation $f \equiv f^2(r)$, $g \equiv g^2(r)$, $h \equiv h(r)$, and $j \equiv j(r)$)

$$\frac{dj}{dr} = \frac{zh(3-2g) - z^2hg - rjg(2z+3)}{gr^2} - L_0 \frac{r^2h^2(zh+rj)(z-1)}{fgH}$$

$$\begin{aligned}
\frac{df}{dr} = & \frac{1}{3zr^3gH} \left\{ 3[4+6(z-1)]z(-\mu)r^6fg^3 \right. \\
& + 3zr^4 \left[-3k(-\mu)L^2(4z-2) + (4z)\lambda r^2 \right] fg^2 \\
& - 3zr^2 \left[3(2z-2)k^2(-\mu) + 4zk\lambda L^2r^2 + (2z+2)r^4 \right] fg \\
& - z(-\mu) \left\{ [3(z-1)^2 + 12z]r^6 - 6k^3L^6 \right\} f \\
& - z\lambda r^2 \left\{ [2(z-1)^2 + 8z+4]r^4 \right\} f \\
& + zr^4 \left\{ [(z-1)^2 + 4z+8]r^2 + 6kL^2 \right\} f \\
& + (z-1)L_0r^6 \left[(zh+rj)^2g - 3zh^2 \right] \left. \right\}
\end{aligned}$$

$$\begin{aligned}
\frac{dg}{dr} = \frac{1}{3zr^3 f H} & \left\{ 12z(-\mu)r^6 f g^3 + 3zr^4 [-6L^2 k(-\mu) + 4\lambda r^2] f g^2 \right. \\
& - 3zr^2 [4k\lambda L^2 r^2 + 4r^4] f g \\
& - z(-\mu) \{ [3(z-1)^2 + 12z] r^6 - 6k^3 L^6 \} f \\
& - z\lambda r^2 \{ [2(z-1)^2 + 8z + 4] r^4 \} f \\
& + zr^4 \{ [(z-1)^2 + 4z + 8] r^2 + 6kL^2 \} f \\
& \left. + (z-1)L_0 r^6 [(zh + rj)^2 g + 3zh^2] \right\} \tag{3.100}
\end{aligned}$$

with the simplifying substitutions

$$\begin{aligned}
L_0 & \equiv -1 + 2\lambda - 3\mu \\
H & \equiv r^4 + 2\lambda r^2 (kL^2 - r^2 g) + 3\mu (kL^2 - r^2 g)^2
\end{aligned}$$

We now have a well-posed first order boundary-value problem and so I will outline how it can be numerically solved in the following subsections.

3.5.1 Shooting Method

To solve these equations, we use a shooting method [143]. This is a very simple numerical method for solving nonlinear boundary value problems. If the numerical algorithm is appropriately chosen, the error in the numerical approximation to the metric functions will be bounded. In practise, we do see some numerical issues with this method, but in our approach to the black hole thermodynamics the simple shooting method is able to yield solutions which are enough to properly describe the interesting behaviour.

Furthermore, the simplicity of this method means that we can flexibly handle singular differential equations; we expect that our set of metric functions become singular as the horizon radius goes to zero as the temperature should diverge, but we also know that the metric functions will have zeroes on the horizon and so the coupled set of differential equations should be singular there as well. We can simply avoid this region in the shooting method by setting up our boundary sufficiently far from the horizon so that the seed values for the free parameters will hopefully generate a physical solution.

The most pressing problem that this approach suffers from is the potential lack of a solution for poor initial guesses. A nonlinear initial value problem may only have a solution on a subset of the radial coordinate domain, which means our numerical evolution towards

$r \rightarrow \infty$ could fail for poor initial guesses. There are a number of ways to mitigate this; many solutions require the introduction of substantially more complexity and sometimes they imply substantially more computational time, even in the case when solutions can be readily obtained via the simple shooting method. This is especially true when dealing with the lengthy and complicated coupled differential equations which we have obtained.

For reference, some of the techniques that could be used to tackle these issues include the bidirectional shooting, multi-shooting and stabilized marching methods [143]. In this thesis I will focus on solving this problem with the simple shooting method alone.

We first have to identify our initial conditions. The boundary conditions for this problem are the series solutions to the differential equations to third order ($\mathcal{O}^3(\epsilon)$ where the boundary is $r_h + \epsilon$). The fourth-order and higher series solutions can be readily built from these equations but we find that the third order solution is enough for good numerical behaviour. Because this is a first order set of differential equations, we need only the value of these metric functions at $r_h + \epsilon$ to generate a solution.

The free parameters that remain from this procedure can be seen in (3.93) and they are the derivative of $f(r)$ at the horizon (f_1) and the derivative of $h(r)$ at the horizon (h_1); these relate to the lengthscale of the horizon radius and the strength of the Proca field. We make an initial guess at these values and update the guess with the asymptotic behaviour of the numerical solution.

Then, the exact equations are solved using Maple's dsolve:

```
dsolve(diffeqns union IVs,numeric,output=listprocedure,maxfun=mffun):
```

This uses a Runge-Kutta method to evolve the initial conditions from the horizon radius to a very large radius in a convergent and stable manner, specifically, the default is the RKF45 method.

The functions $f^2(r), g^2(r), h(r)$ are then evaluated at a very large radius and the free parameters are tuned using this value in an iterative manner, until the metric and gauge field functions converge to unity. Typically this tuning is performed through a Newton-Raphson method or the like, but in practise for the $z = 2$ Lifshitz symmetric black holes simply dividing the derivatives at the horizon by the evaluation of the functions $f^2(r), h(r)$ at large radius results in convergence within three iterations if the initial guesses are well chosen.

Generally we can not expect that both of the parameters f_1 and h_1 will always converge to values that yield a valid solution; for this reason deeper analysis is required when

convergence is not obtained. Fortunately, it was shown that in $z = 2$ Einsteinian gravity, the large-radius expansion of the field equations features modes that are all decaying when $D > z + 2$ [144]. This was further discussed for the higher curvature solutions in [145] and in the appendix of [4]. In this case, the functions f_1 and h_1 together yield the horizon radius, with an additional degree of freedom allowing for a family of black hole solutions.

In the case where $z = 3, D = 5$ we have a zero mode that can be problematic [144, 146]. This results in a fine-tuning problem where h_1 will need to take certain specific values, and a family of $z = 3$ solutions will arise which correspond to the values of f_1 that satisfy asymptotics for a given h_1 . For this reason it is quite uncommon to see $z > 2$ considered in the literature. In [144], it was seen in the Einsteinian case that the two needed degrees of freedom could be separated from one another, and one could be used to correctly fix the asymptotics while the other could be used to set the horizon radius.

The aforementioned analysis involves an expansion

$$\begin{aligned} f &= 1 + \epsilon f_{L1} \\ g &= \frac{1}{1 + \epsilon g_{L1}} \\ \tilde{h} &= 1 + \epsilon h_{L1} \\ \tilde{j} &= 1 + \epsilon j_{L1} \end{aligned} \tag{3.101}$$

that is performed to first order in ϵ after a redefinition of h, j so that the falloff of all functions is the same, and they can be compared to one another in the same matrix expression. The field equations become a matrix equation relating the derivatives of the vectors of $(f_{L1}, g_{L1}, h_{L1}, j_{L1})$ to the values $(f_{L1}, g_{L1}, h_{L1}, j_{L1})$. This matrix is diagonalized to yield a set of solutions

$$s_{Li} = c \cdot e^{\lambda_i r} \tag{3.102}$$

for $i \in \{1, 2, 3, 4\}$ and some constant c ; the sign of the eigenvalues determines the stability of the mode. It ends up being slightly more complicated than this, as the eigenvalues are dependent on r , so integrating the resultant differential equation can have solutions with a different form such as $s_{Li} \sim r^{\lambda_i}$ for example, but ultimately the stability is determined by examining whether the resultant solution set decays or grows at large r . Growing solution modes will, pending appropriate free parameters, require a degree of freedom to fix to zero.

The more challenging aspect of the numerical technique when $z = 2$ is evaluating the metric functions at small horizon radius with fixed precision. The seed values for the free parameters must be chosen correctly to yield a reasonable initial guess at the solution, otherwise we may accidentally guess at a large black hole, where the differential equations

are singular in our domain because $r_h + \epsilon$ is smaller than r_h^* , the horizon radius of the black hole solution in the seed values. The way in which we solve this problem is somewhat empirical, and it is done by setting the constants to values proportional to the inverse of the initial horizon radius. Provided that we are able to evaluate solutions at a small enough radius to yield the interesting thermodynamics, we are satisfied with this approach.

Although this is ultimately just a guess, we can provide some physical justification - when we study small black holes, and the temperature rises with a small horizon radius, we will typically have a larger derivative at the horizon for smaller black holes. We want to underestimate the size of the black hole slightly, while still being able to handle black holes for which the temperature increases with horizon radius, so multiplicative factors are guessed at until the algorithm runs properly over the range of horizon radii in which we are interested.

To achieve autonomous operation as well as substantial speedup, `try` and `catch` statements are used to handle cases where the horizon radius is too small to find a convergent numerical solution. When probing the parameter space (running this routine multiple times for varying higher curvature coupling constants, other horizon topologies, or differing cosmological constants), this minimum convergent radius is re-used to avoid the massive slowdown that occurs when `dsolve` begins seeing divergent functions.

3.5.2 $z = 2$ 3^{rd} order quasitopological black hole

In [4] we obtained solutions for Lifshitz symmetric black hole solutions with cubic quasitopological terms. Recall that the cubic terms are given by (2.61).

The (higher dimensional AdS Schwarzschild) Einsteinian solution as well as the exact Gauss-Bonnet black hole solution for $z = 1$ were used in comparison with the numerical method to provide a careful test that we were converging to good solutions. In addition, the exact cubic quasitopological solution later published in [5] was used to perform a check of the $z = 1$ quasitopological terms. Finally, since the numerical routine was independently written, results were compared with those of [144] to ensure that the $z = 2$ Einsteinian behaviour was accurate.

For example, the cubic quasitopological $D = 5$ solution from section 2.2.2 with $k = 0, r_h = 0.9, \lambda = 0.04, \mu = 0.001$ was compared to the output of the numerical solver and it was found that values for the metric functions were identical to within 10^{-7} .

Then, new results showing how the quasitopological term affects the thermodynamic stability in asymptotically $z = 2$ Lifshitz spacetimes were obtained. It was seen that the

cubic quasitopological term acts similarly in $z = 2$ to $z = 1$: if the negative slope on a temperature-entropy plot is indicative of a valid phase transition, the quasitopological term can act to control the radius at which this phase transition can occur. This effect is apparently analogous to the charge in the AdS Reissner-Nordström black hole, where an uncharged spherical $D = 4$ black hole solution will always have a phase transition at some finite radius, but where introducing a charge means that there are some temperatures for which no phase transition will ever occur. Of course, further investigation is required (and will be performed in this thesis) to see that this is indeed the case - for now it is only suggestive. Knowing where phase transitions occur is an important step in identifying the critical point.

In figure 3.1 we see that at the level of small r_h to which our numerical routines can probe (smaller r_h corresponds to the left-hand side of the figure), there is not yet any evidence of instability for the spherical black holes, while figure 3.2 shows that for a slightly smaller value of the cubic quasitopological coupling constant, we can recover the instability (and therefore phase transition) that occurs in the Einsteinian solution, at a small black hole horizon radius.

3.5.3 $z = 2$ 4th order quasitopological black hole

In [1] we published thermodynamics for asymptotically Lifshitz symmetric solutions with the quartic quasitopological terms. In these cases the quartic term is given explicitly by (2.62).

For these solutions we define the coupling constants in a similar fashion to (3.5), with the extension

$$\mu_4 = \frac{L^6 \xi}{(D-1)(D-2)(D-4)(D-8)(D-3)^2(D^5 - 20D^4 + 142D^3 - 472D^2 + 743D - 436)} \quad (3.103)$$

This solution yields the most general expression for the cosmological constant presented in this thesis;

$$\Lambda = -\frac{1}{2L^2} \left[(1 - 2\lambda - 3\mu - 4\xi) (D^2 + (z-4)D + z^2 - 3z + 4) + (D-1)(D-2)(\lambda + 2\mu + 3\xi) \right] \quad (3.104)$$

which we can see simplifies in the case of $\mu = \xi = 0$ and $D = 5$ to $-6(1-\lambda)/L^2$ as desired.

The numerical procedure illustrated above is followed for $D = 5$ solutions here, obtaining

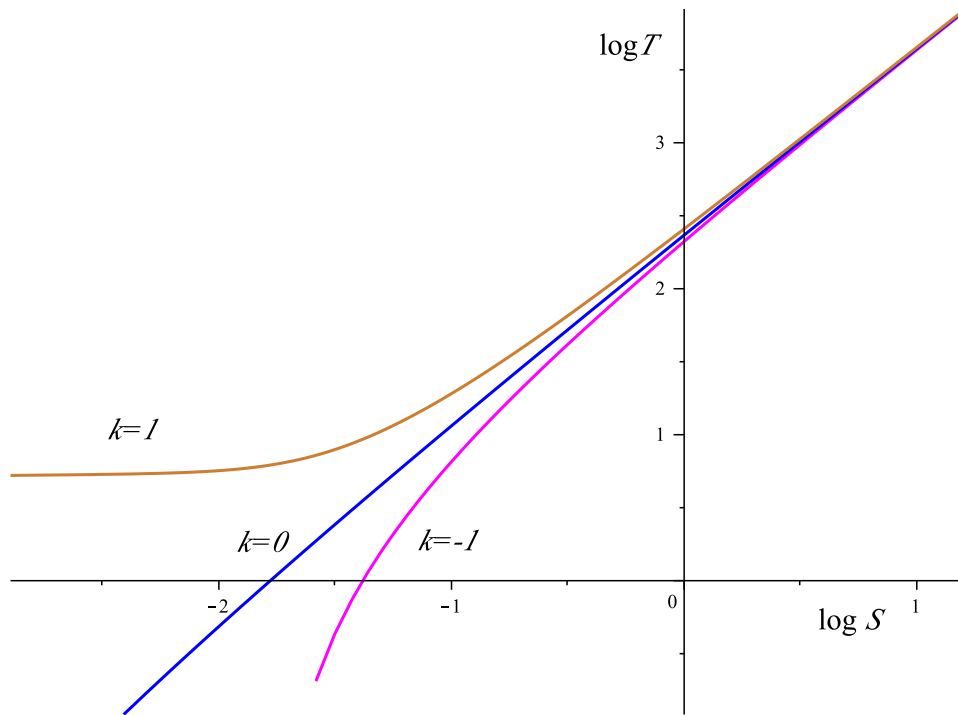


Figure 3.1: The log-log plot of temperature versus entropy for asymptotically anti-de Sitter cubic quasitopological uncharged numerical black holes where $k = -1, 0, 1$ (pink, blue, brown). Here the higher curvature couplings take the values $\lambda = 0.04, \mu = 0.001$, while the cosmological constant is fixed using (3.88) in order to ensure that the metric functions have the same asymptotics.

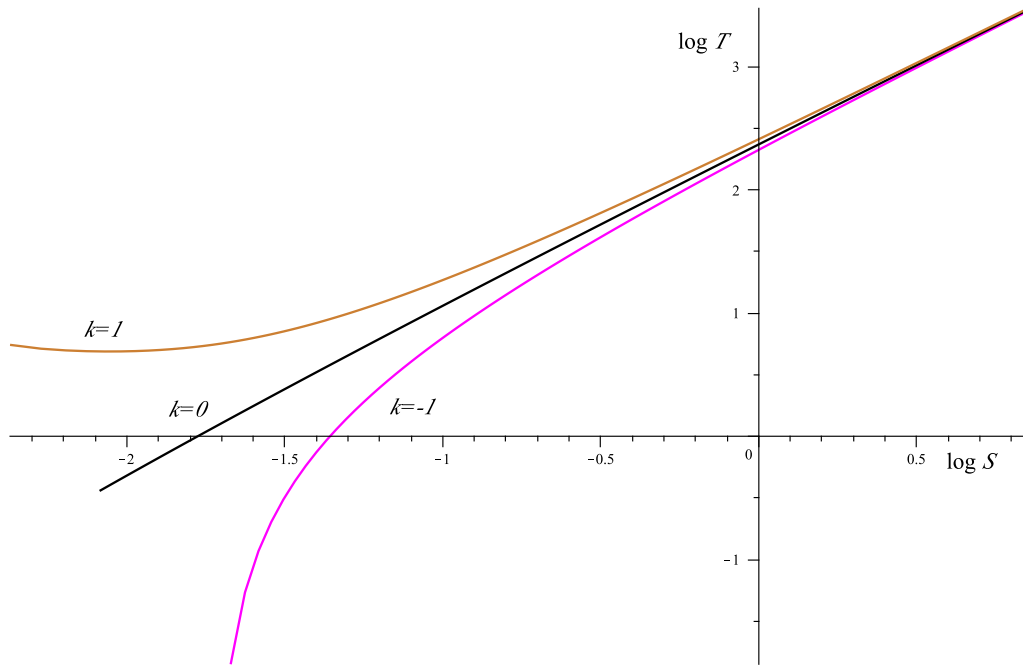


Figure 3.2: The log-log plot of temperature versus entropy for asymptotically anti-de Sitter cubic quasitopological uncharged numerical black holes where $k = -1, 0, 1$ (pink, black, brown). Here the higher curvature couplings take the values $\lambda = 0.04, \mu = 0.0003$, while the cosmological constant is fixed using (3.88) in order to ensure that the metric functions have the same asymptotics.

values for the Proca charge and mass of

$$q^2 = \frac{2(z-1)(1-2\lambda+3\mu-4\xi)}{z} \quad m^2 = \frac{3z}{L^2} \quad (3.105)$$

which allow the correct asymptotics, and the first, second, and third order series expansions in the metric functions are performed. Again, f_1 and h_1 are the free parameters that are found using a shooting method.

We can plot the results of this routine to show that the effect of the quartic quasitopological term is as expected. From figure 3.3, we can see that there is a very subtle instability for small horizon radius; probing this small of a radius was challenging and computationally slow. This leads us to suspect that, as with the cubic quasitopological black holes, the phase transition can survive with small quartic quasitopological terms, and so the additional parameter space gained by adding a quartic term could also be used to formulate a richer, more complex thermodynamic model.

3.6 Discussion

In this chapter we have examined black hole thermodynamics in a wide variety of cases where the spacetime asymptotically obeys Lifshitz symmetries.

In order to do this, we needed to develop an array of specific techniques for dealing with these solutions. There are relatively few exact solutions in asymptotically Lifshitz gravity, and in order to perform an exploration where the parameters z , L , and r_h are relatively unconstrained, we had to introduce the numerical apparatus of 3.5 in order to find numerical solutions to these black holes. The development of these approaches has led to an understanding about how the critical exponent z influences the stability of shooting-method approaches to numerically solving the field equations.

Another glaring obstacle that needed to be overcome was the lack of an agreed-upon mass for asymptotically Lifshitz solutions. Various methods were illustrated for a number of exact solutions, and ultimately we developed the thermodynamic method of obtaining a mass in 3.2, which has the benefit of being easily applicable to numerical solutions as well as exact ones. I highlighted the weaknesses as well as the strengths of this method, importantly, its inability to deal with constrained scenarios where the cosmological lengthscale is tied to the horizon radius. Understanding these problematic solutions remains an open problem in determining a mass for Lifshitz black holes.

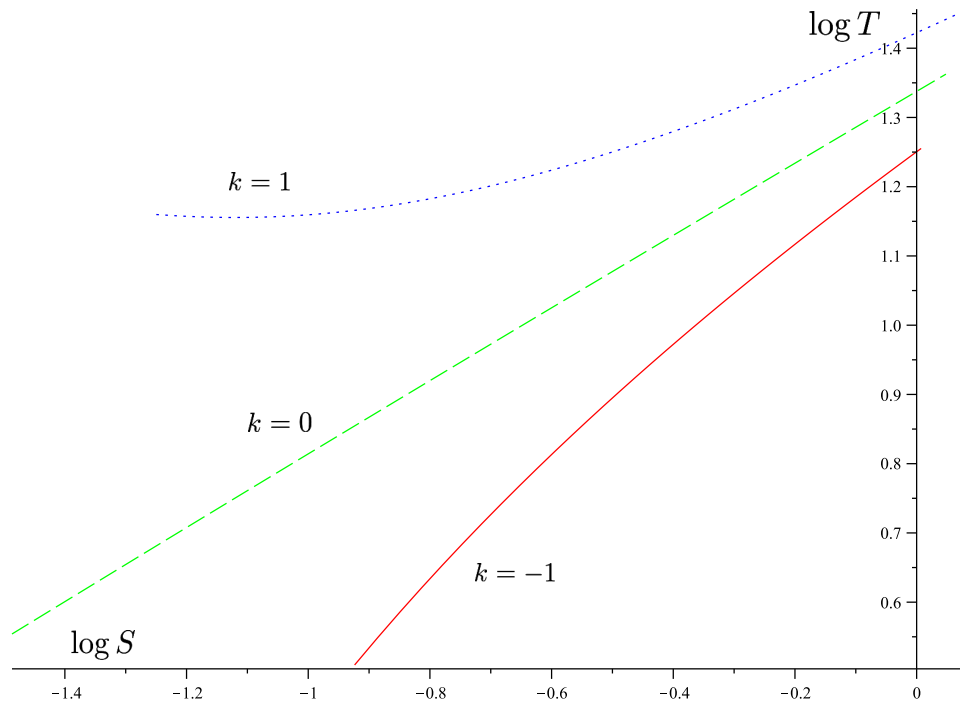


Figure 3.3: The log-log plot of temperature versus entropy for asymptotically anti-de Sitter five-dimensional quartic quasitopological uncharged numerical black holes where $k = -1, 0, 1$ (red/solid, green/dashed, blue/dotted, respectively). Here the higher curvature couplings take the values $\lambda = 0.04, \mu = 0.001, \xi = 0.0003$, while the cosmological constant is fixed using (3.104) in order to ensure that the metric functions have the same asymptotics.

This endeavour has helped us set the stage for future investigations into Lifshitz thermodynamics. In the next section, I will build up the background needed to find the universality class of black hole critical behaviour. This section provides the necessary ingredients to apply both numerical and analytic techniques of extracting critical exponents to Lifshitz black holes, as long as they have independent lengthscales. As such, finding the universality class of the numerical solutions presented here is now theoretically possible although it has not yet been done because in practise, the venture is predicted to be time consuming, as many numerical solutions are required to identify the critical point and to obtain high quality, convergent Padé models for the temperature.

Chapter 4

Universality Classes and Black Holes

4.1 The Universality Class

The universality class is studied here as an avenue to understanding the gauge/gravity correspondence. If this conjecture holds, thermodynamic quantities in the gravity bulk will be analogous to thermodynamic quantities in some gauge theory. The universality class can be thought of as a coarse-grained test of the gauge/gravity correspondence.

The key observation inspiring renormalization group theory and critical exponents was that systems near criticality obey characteristic behaviour, namely the divergence of various derivatives of their thermodynamic potentials. Upon further inspection, it was found that disparate materials could be grouped into relatively few “universality classes” based on the set of exponents which characterize the divergence of their thermodynamic properties.

For the purpose of holography, if a bulk theory experiences criticality and shares its thermodynamics (namely its temperature, entropy, etc.) with a gauge theory, we expect that the two theories will fall into the same universality class. Because of the maturity of the condensed matter physics, and the development of powerful renormalization group techniques like the lattice methods of Kadanoff (c.f. [23]) and the divide-and-conquer approaches of Wilson (for example, [147]), universality classes of many gauge theories have been calculated, so when we write down the universality class of the gravity theory it is plausible that we can immediately identify the group of potential gauge theories to focus on as gravitational duals.

Only recently, with the description of the cosmological constant as a thermodynamic pressure, has the field of black hole thermodynamics started seeing success in the computation of the universality class of asymptotically AdS black holes. Studying this relationship

may yield insight on both sides of the duality; for example, higher dimensional black holes have been shown to have a critical point with the same universality class as $D = 4$ charged black holes [2], which is somewhat counterintuitive given the strong dependence of the universality class on dimension in, for example, the Ising model [23]. Understanding this more deeply could yield insight into exactly what dimension the “boundary theory” must take in general, for some theory of gravity. More study on the black hole side may also yield a relationship to the higher-dimensional Ising system (for reasons we shall later see), which would be a substantial contribution to the condensed matter physics community as computations of e.g. critical exponents in three-dimensional Ising models are challenging in a computational sense [148].

4.1.1 Critical Exponents and Universality

The essential principle is to begin with an action or Hamiltonian that describes a physical system.

Since we do not focus strongly on lattice-spin systems in this thesis, I will not spend a lot of time on the Kadanoff scaling or renormalization group. For a review of the theory behind these universality classes see any good textbook on condensed matter physics, such as [23]. Instead, I will focus on obtaining the critical exponents supposing we have a complete thermodynamic potential (internal energy, enthalpy, Gibbs free energy, etc.) along with an equation of state. As is well known, we then have access to all of the remaining thermodynamic potentials.

The critical exponents arise as the only relevant lengthscale becomes the correlation length of the theory; when the theory approaches criticality the renormalization group becomes an important tool as the theory is otherwise scale invariant. The thermodynamic functions for the theory will have scaling based on this lengthscale; in practise it is common to express the scaling of the main group of critical exponents as a function of reduced temperature, $(T - T_c)/T_c$ or $(T_c - T)/T_c$, depending on whether criticality is approached from the disordered ($T > T_c$) or ordered ($T < T_c$) phase.

Essentially this amounts to examining the power-law scaling of the expansion of thermodynamic functions near criticality, to first order. For example,

$$C = \frac{dS(T)}{d\log(T)} \sim A \left(\frac{T_c - T}{T_c} \right)^{-\alpha} + \mathcal{O} \left(\left(\frac{T_c - T}{T_c} \right)^{-\alpha+1} \right) \quad (4.1)$$

where α is the critical exponent corresponding to the divergence of the specific heat.

Common critical exponents are denoted $\alpha, \beta, \gamma, \nu$ and correspond to the power-law behaviour of the specific heat C , order parameter $\langle \phi \rangle$, susceptibility of an external field χ , and correlation length ξ . Additionally, critical scaling can also be seen precisely at the critical temperature, when other thermodynamic quantities are not at their critical values, if this is allowed by the degrees of freedom of the system. A common critical exponent at the critical temperature is that of the order parameter at constant temperature while approaching criticality through changing some external field; in practise this exponent is denoted δ and is related to the scaling of the order parameter with reduced pressure, $(P_c - P)/P_c$.

The precise relationships are, for $T_R \equiv (T_c - T)/T_c$ and $P_R \equiv (P_c - P)/P_c$:

$$C \sim (T_R)^{-\alpha} \quad \langle \phi \rangle|_{T=T_c} \sim (P_R)^{1/\delta} \quad \chi \sim (T_R)^{-\gamma} \quad \langle \phi \rangle \sim (T_R)^\beta \quad (4.2)$$

I will note that using a zero for a critical exponent is the convention given when the function of interest has a discontinuity at the critical point, or when it has a logarithmic divergence [149].

Later I will provide a table of some common values of these critical exponents, for comparison with the black hole results.

4.1.2 Application to the Van der Waals Model

In section 4.1.3 we shall see why I chose the Van der Waals gas as the subject of renormalization group scaling, but for now we treat it as an entirely pedagogical example. The Van der Waals gas is typically described by an equation of state such as [150, 78]

$$\left(p + \frac{a}{v^2}\right)(v - b) = T \quad (4.3)$$

where p and v are the pressure per particle and volume per particle of the gas. The parameter a empirically measures the attraction between gas particles, while b is related to the size of the particles. Both are dimensionful lengthscales in the theory of the Van der Waals gas. The use of the specific pressure and volume, as opposed to ‘regular’ pressure and volume, will not affect the universality class.

The extreme popularity of this model arises from its simplicity, combined with the appearance of a critical point between what are denoted as “liquid” and “gas” phases. In the Van der Waals model the critical point will exhibit scale invariance, namely, the

equation of state at the critical point should have quantities defined by T_R , and these quantities will be independent of the lengthscales generated by the parameters a and b .

With some algebra, the equation of state (4.3) becomes [78]

$$v^3 - \left(b + \frac{T}{p}\right)v^2 + \frac{a}{p}v + \frac{ab}{p} = 0 \quad (4.4)$$

and at criticality, $v = v_c$ so $(v - v_c)^3 = 0$ which expanded, means

$$v^3 - 3v^2v_c + 3vv_c^2 - v_c^3 = 0 \quad (4.5)$$

so by comparison, the critical parameters are found by solving the equations

$$p_c v_c^3 = ab \quad 3p_c v_c^2 = a \quad 3v_c p_c = bp_c + T_c \quad (4.6)$$

and therefore

$$v_c = 3b \quad p_c = \frac{a}{27b^2} \quad T_c = \frac{8a}{27b} \quad (4.7)$$

from which we can substitute the reduced temperature T_R , specific pressure p_R , and specific volume v_R into the equation of state to obtain a scale-independent equation (featuring only p_R, T_R, v_R with no a, b in appearance), as expected.

The Helmholtz free energy of the Van der Waals gas is known to be [151, 152]

$$F_{vdw} = -T \left[\log \left(\frac{v-b}{\Phi T^{-3/2}} \right) + 1 \right] - \frac{a}{v} \quad (4.8)$$

which yields the Gibbs free energy through $G = H - TS = F + Pv$ of [78]

$$G_{vdw} = -T \left[\log \left(\frac{v-b}{\Phi T^{-3/2}} \right) + 1 \right] - \frac{a}{v} + Pv \quad (4.9)$$

These potentials can be used to extract the critical exponents; for example, to obtain the isothermal compressibility, one knows that

$$\left(\frac{\partial^2 F}{\partial V^2} \right)_T = \left(\frac{\partial p}{\partial V} \right)_T = -\frac{1}{V\kappa_T} \quad (4.10)$$

and we can evaluate the scaling of this term by examining

$$\left(\frac{\partial^2 F}{\partial V^2} \right)_{T, V=V_c} = \frac{T}{\xi_1} - \xi_2 \quad (4.11)$$

critical exponent	value
α	0
β	$\frac{1}{2}$
γ	1
δ	3

Table 4.1: A table of critical exponents, computed for the Van der Waals gas.

where \mathfrak{k}_1 and \mathfrak{k}_2 are constants independent of temperature (in this case they are somewhat messy functions of $V = V_c$). This implies that

$$\kappa_T \sim c|T - T_c|^{-1} \quad (4.12)$$

since the expression (4.11) will have a zero, corresponding to the divergence of the isothermal compressibility, when $T = T_c = \mathfrak{k}_2 \cdot \mathfrak{k}_1 = 2a(v_c - b)^2/v_c^2$.

Similar analysis is performed in [78] to ascertain the critical exponents of the Van der Waals gas, illustrated in table 4.1. In this context the order parameter is the difference between the volume of the gas phase and liquid phase; $\langle \phi \rangle \equiv v_g - v_l$. The critical exponents therefore take the form

$$\begin{aligned} C_v &\sim |T - T_c|^{-\alpha} & \langle \phi \rangle &\sim |T - T_c|^\beta \\ \kappa_T &\sim |T - T_c|^{-\gamma} & |P - P_c| &\sim |v - v_c|^\delta \end{aligned} \quad (4.13)$$

In the following, I will try to identify similar sets of critical exponents for black hole systems. At the moment, it is relevant to note that the critical exponents for the Van der Waals gas are equal to those for the Ising model in four spatial dimensions. This is also the mean-field theory, where only one-body interactions are allowed. I will discuss the implications of this on gravitational systems in 4.2.

4.1.3 AdS Reissner-Nordström Black Hole

In 3+1 dimensions, the AdS Reissner-Nordström black hole has the solution with no higher curvature coefficients ($\mu_2 = \mu_3 = \dots = 0$) and one Maxwell field, but with a cosmological constant $\Lambda = -3/l^2$, meaning the pressure from (2.46) is

$$P = \frac{3}{8\pi l^2} \quad (4.14)$$

The metric functions from the ansatz (3.5) are explicitly

$$f^2(r) = g^2(r) = 1 - k\frac{l^2}{r^2} - 2m\frac{l^2}{r^3} + q^2\frac{l^2}{r^4} \quad (4.15)$$

where $k = 1$, $z = 1$ for the solution we consider. Here m is a parameter related to the mass of the black hole while q is the parameter corresponding to the Maxwell charge. This solution can also be obtained by the $D = 4$ simplification with $\mu_2 = \lambda = 0$ of the Gauss-Bonnet exact solution presented in (2.13).

The temperature and entropy of this solution can be computed in the manner of sections 2.1.1 and 2.1.2:

$$T = \frac{3r_h}{4\pi l^2} + \frac{k}{4\pi r_h} - \frac{q^2}{4\pi r_h^3} \quad S = \frac{\omega_{2,k} r_h^2}{4} \quad (4.16)$$

We can solve for the mass through our thermodynamic method from section 3.1.3 and obtain a thermodynamic mass and volume of

$$M_{RN} = \frac{\omega_{2,k} r_h^3}{8\pi l^2} + \frac{k\omega_{2,k} r_h}{8\pi} + \frac{q^2 \omega_{2,k}}{8\pi r_h} \quad V_{RN} = \frac{\omega_{2,k} r_h^3}{3} \quad (4.17)$$

Following the same procedure as for the Van der Waals gas, the Gibbs free energy is now defined (since M is interpreted as the enthalpy) by

$$G = M - TS = \frac{\omega_{2,k} r_h^3}{8\pi l^2} + \frac{k\omega_{2,k} r_h}{8\pi} + \frac{q^2 \omega_{2,k}}{8\pi r_h} - \left(\frac{3r_h}{4\pi l^2} + \frac{k}{4\pi r_h} - \frac{q^2}{4\pi r_h^3} \right) \frac{\omega_{2,k} r_h^2}{4} \quad (4.18)$$

$$= -\frac{\omega_{2,k} r_h^3}{16\pi l^2} + \frac{k\omega_{2,k} r_h}{16\pi} + \frac{q^2 \omega_{2,k}}{16\pi r_h} \quad (4.19)$$

while the Helmholtz free energy is

$$F = G - PV = -\frac{5\omega_{2,k} r_h^3}{16\pi l^2} + \frac{k\omega_{2,k} r_h}{16\pi} + \frac{q^2 \omega_{2,k}}{16\pi r_h} \quad (4.20)$$

Since this function depends on r_h and l rather than T, V , in order to find the isothermal compressibility we are better off performing the derivative

$$\left(\frac{\partial P}{\partial V} \right)_T$$

directly; since $P = P(l)$ and $V = V(r_h)$ we can substitute these functions into (4.16) to obtain an equation of state. This yields

$$P = \left(\frac{\omega_{2,k}}{24\sqrt[3]{3\pi} V^{4/3}} \right) \left(-12\pi TV - \sqrt[3]{3}\omega_{2,k}^{2/3} q^2 V^{1/3} + 3^{2/3} k \omega_{2,k}^{1/3} V^{2/3} \right) \quad (4.21)$$

which we can differentiate to find

$$\left(\frac{\partial P}{\partial V}\right)_T = -\frac{\omega_{2,k} \left(-2\sqrt[3]{3}k\sqrt[3]{\frac{V}{\omega_{2,k}}} + 4 \cdot 3^{2/3}\pi T \left(\frac{V}{\omega_{2,k}}\right)^{2/3} + 3q^2\right)}{72\pi V^2} \quad (4.22)$$

from which we see that $\kappa_T = c|T - T_c|^{-1}$ where T_c is given by the zero of (4.22),

$$T_c = \frac{2\sqrt[3]{3}k\sqrt[3]{\frac{V_c}{\omega_{2,k}}} - 3q^2}{4 \cdot 3^{2/3}\pi \left(\frac{V_c}{\omega_{2,k}}\right)^{2/3}} \quad (4.23)$$

Other critical exponents can be computed in a similar fashion [78], and they take the exact same values as table 4.1, the table of critical exponents for the Van der Waals gas.

This relationship between the Van der Waals gas, mean field theory, and AdS Reissner-Nordström black hole was first noticed in the late 1990s [153, 154] where charge was varied (with no pressure) to obtain criticality. However, this approach required treating extensive variables as intensive variables and vice versa, which is an issue that was resolved by treating pressure as a dynamical variable. In this case, criticality was found to occur in closer correspondence to the Van der Waals system as volume, entropy, and charge are all treated extensively [78].

4.1.4 Techniques for Numerical Black Holes

In this subsection the procedure of obtaining the universality class of a simple numerical black hole is developed. The general outline of this procedure is to take a set of temperatures for different values of the horizon radius and cosmological constant and fit them onto some function that closely matches the analytic expression for the temperature; because of singularities in the temperature the Padé approximant is used as a model function (this can be thought of as an extension of power series to rational functions).

Then, the model function can be used to generate an accurate power series near the point where criticality is expected to occur. The other thermodynamic quantities such as mass and volume can be generated from this power series using the method introduced in 3.1.3.

Padé Approximants

A much more well suited function to fit to a temperature (as compared to a series in r, L) is a Padé approximant. This is because the Padé approximants can handle singular functions much more readily than a polynomial series expansion, due to the possibility for their denominator to have roots. The temperature is expected to have divergent behaviour for small r_h and one can check for oneself that the fit to a polynomial will be ill-behaved for the region in which we are interested.

The Padé approximant is canonically defined as a function

$$\mathcal{P}_A(r) = \frac{a_0 + a_1r + a_2r^2 + \dots + a_Lr^L}{1 + b_1r + b_2r^2 + \dots + b_Mr^M} \quad (4.24)$$

where a notational convention commonly used is simply $[L/M]$ [155]. For this thesis, my notation indicates that $A(r)$ is the function we are interested in approximating, and we assume that A also has a power series expression

$$A(r) = \sum_{i=0}^{\infty} c_i r^i \quad (4.25)$$

The Padé approximants have a number of highly useful mathematical properties which make them popular in a broad array of disciplines. Given a truncated power series, a conversion into a Padé approximant can have surprisingly improved accuracy in representing a function using the same number of coefficients as the power series.

Particularly relevant is their use in finding a critical point and identifying critical exponents. The Padé approximants remain quite feasible as an improvement to the standard series expansions and linear fitting that can be used to extract the power of divergence of a function. It is relatively simple; D-log type Padé approximants are used when there is an expectation that the function for which you have a truncated series expansion takes a specific form, e.g.

$$f(T) = A(T) \left(\frac{T_c - T}{T} \right)^{-\gamma} \quad (4.26)$$

where $A(T)$ does not change rapidly at the singularity compared to the term in brackets. In this case a specific set of Padé approximants can be used to obtain information about γ and T_c [155, 156]. Since we will eventually produce a truncated series expansion of the Gibbs free energy, this method should be highly applicable.

Nonlinear Fitting

From our shooting method, in order to obtain a temperature from the numerical data we require a fitting method. As justified in section 4.1.4, I have made the choice to fit to a Padé approximant model. Because this is not a simple linear fit we need to apply some methods that are more complicated than linear regression (commonly with a least-squares fit). For the purposes of this work, the `Automatic` specification in Mathematica's `NonlinearModelFit` package was sufficient; this chooses between a number of nonlinear methods including (conjugate) gradient, (quasi) Newton, and interpolations between the two, like the Levenberg-Marquardt methods [157, 158]. In the case of the models we fit to, the automatic choice is Levenberg-Marquardt which has performed well.

The Levenberg-Marquardt method [159] falls into the field of nonlinear regression methods for rational function modelling. The details of this method focus on the update step of an iterative least-squares fit, where from our set of numerical data we have N equations

$$y_i = f(x_i, \vec{\theta}) \quad (4.27)$$

The objective is to minimize the least-squares error for our best guess at the model parameters $\vec{\theta}^*$,

$$S(\vec{\theta}^*) = \sum_{i=1}^N (y_i - f(x_i, \vec{\theta}^*))^2 \quad (4.28)$$

We make use of the Jacobian matrix of the function $f(\vec{x}, \vec{\theta})$ where derivatives are taken with respect to elements of $\vec{\theta}$; define this matrix when evaluated at $\vec{\theta}^*$ to be simply denoted \mathbf{F} .

Then, an exact solution to the linear least-squares error equation $S(\vec{\theta}^*) = 0$ is given by

$$(\mathbf{F}^T \mathbf{F})^{-1} \mathbf{F}^T \vec{\epsilon} = 0 \quad (4.29)$$

where $\vec{\epsilon} \equiv \vec{y} - \vec{f}(\vec{\theta}^*)$, $\vec{f}(\vec{\theta}) \equiv (f(x_1, \vec{\theta}), \dots, f(x_N, \vec{\theta}))^T$, and \mathbf{F}^T is the transpose of \mathbf{F} . For further details, see the Appendix B.

This is an equation which we can attempt to solve for nonlinear models in an iterative fashion. One method (the Gauss-Newton method) takes a linearized Taylor expansion of the function f , and uses (4.29) as an solution to the least-squares minimization, updating the guess for $\vec{\theta}^*$ correspondingly. Other methods, like steepest descent, compute gradients of the least-squares minimization (4.28) and update $\vec{\theta}^*$ along that direction such that (4.28) is minimized.

For the method I describe here, the replacement of $\vec{\theta}_{(i)}^*$ with a better guess $\vec{\theta}_{(i+1)}^*$ governed by the equation

$$\vec{\theta}_{(i+1)}^* = \vec{\theta}_{(i)}^* + \left(\mathbf{F}_{(i)}^\top \mathbf{F}_{(i)} - \eta_{(i)} \mathbb{I} \right)^{-1} \mathbf{F}_{(i)}^\top \vec{\epsilon} \quad (4.30)$$

which is the Levenberg-Marquardt method. There, \mathbb{I} is the identity matrix.

The method essentially interpolates between the Gauss-Newton method and the method of steepest descent (a gradient method), and η is a parameter that is updated between each step which governs this interpolation. The exact algorithm used to update this parameter varies, and in the Mathematica implementation we use it is proprietary.

Extraction of Critical Exponents

The critical exponents can finally be extracted. Naïvely one can apply a simple linear regression least-squares fit to the logarithm of the data of interest, near criticality. The slope of this line yields an approximation of the critical exponent. However, this is highly undesirable! Most importantly, the logarithm of the data is linear only as we are approaching criticality. This means that a finite grid over the initial input r_h, l will be stretched out considerably when the logarithm is taken and criticality is approached, and so the resolution of the data may make an accurate fit unachievable.

As mentioned in section 4.1.4, this can be improved through the clever use of Padé approximants. I will show in section 4.3 how these tools can be applied to probe the nature of the divergence in the functions of interest, extracting the information about the power of the divergence from the series expansion, where the said information is ‘hidden’ because of the poor fit of the polynomial to the singular behaviour.

First, we will examine a more complicated exact solution, before we apply these numerical methods. This will give us a sense of the algebraic complexity that the numerical procedure will eventually need to be able to handle.

4.2 An Exact Quasitopological Black Hole

As an example of the power of this technique we examined [2] the universality class of the exact quasitopological black hole with a Maxwell charge in multiple dimensions, as first derived in [5]. The thermodynamics of this black hole has been discussed in 2.2.2. In this thesis I will use the solution given there, with the added constraint of

$$\Lambda = -\frac{(D-1)(D-2)}{2L^2} \quad (4.31)$$

and the quasitopological and Gauss-Bonnet couplings are defined so that their lengthscale is implicit;

$$\frac{\tilde{\lambda}}{(D-3)(D-4)} = \mu_2 \quad \frac{(16D-24)\tilde{\mu}}{(3D^4-42D^3+205D^2-414D+288)} = \mu_3 \quad (4.32)$$

This is important for any future extensions to extended-phase-space thermodynamics where the couplings may be varied to generate new thermodynamic potentials. Furthermore, it is useful to use this convention as it makes this work comparable to the cubic Lovelock gravity thermodynamics investigated in [160, 161].

As in the case of the Van der Waals fluid, we begin by finding the equation of state and thermodynamic potentials of the black hole. Using our thermodynamic temperature and entropy (2.2.1), the mass and thermodynamic volume can be computed through the technique from section 3.1.3.

The extended first law and Smarr relation are given by

$$dM = TdS + VdP + \Phi dQ + \Psi_{\tilde{\lambda}} d\tilde{\lambda} + \Psi_{\tilde{\mu}} d\tilde{\mu} \quad (4.33)$$

$$(D-3)M = (D-2)TS - 2PV + (D-3)\Phi Q + 2\tilde{\lambda}\Psi_{\tilde{\lambda}} + 4\tilde{\mu}\Psi_{\tilde{\mu}} \quad (4.34)$$

where the latter has been obtained using Eulerian scaling justifications, and where the conjugate potentials to the higher curvature couplings are

$$\Psi_{\tilde{\lambda}} = \frac{\omega_{D-2,k}(D-2)}{16\pi} k r_h^{D-5} \left(k - \frac{8\pi r_h T}{D-4} \right), \quad \Psi_{\tilde{\mu}} = \frac{\omega_{D-2,k}(D-2)}{16\pi} k^2 r_h^{D-7} \left(k - \frac{12\pi r_h T}{D-6} \right) \quad (4.35)$$

In this study we did not consider the thermodynamic details of the variation of $\tilde{\mu}$ or $\tilde{\lambda}$ so we set $d\tilde{\mu}$ and $d\tilde{\lambda}$ to zero.

Some $\tilde{\mu}$ -dimensionless thermodynamic quantities are introduced for ease of computation as well as for comparison with other works. The association of these quantities to “specific volume”, “specific charge”, “specific temperature”, and “specific pressure” will be used to form an equation of state where $\tilde{\mu}$ has been scaled out. The rescalings we have performed here take the positive signs for positive values of $\tilde{\mu}$ while for negative values of $\tilde{\mu}$ we perform the sign flip $\tilde{\mu} \rightarrow -\tilde{\mu}$, allowing the rescalings to stay real and allowing us to examine thermodynamics in all regimes of the higher curvature parameter space shown in

figure 2.3.

$$\begin{aligned}
r_h &= v\tilde{\mu}^{1/4} \\
\mathbf{q} &= q\sqrt{\frac{(D-2)(D-3)}{\pi}}\tilde{\mu}^{-(D-3)/4} \\
t &= (D-2)\tilde{\mu}^{1/4}T \\
\alpha &= \frac{\tilde{\lambda}}{\sqrt{\tilde{\mu}}} \\
p &= 4\sqrt{\tilde{\mu}}P \\
g &= \frac{\tilde{\mu}^{(3-D)/4}}{\omega_{D-2,k}}G
\end{aligned} \tag{4.36}$$

As has been the trend in this field, the specific volume is not actually proportional to the thermodynamic volume V . This originated with the work in [78], where the specific volume was defined proportional to the horizon radius because it facilitates comparison with the Van der Waals thermodynamics. This does not affect the results we obtain regarding the universality class.

The equation of state is found by substituting these redefinitions into the expression for the temperature (2.80). This yields

$$\begin{aligned}
p = \frac{t}{v} - \frac{(D-2)(D-3)k}{4\pi v^2} + \frac{2kt\alpha}{v^3} - \frac{(D-2)(D-5)k^2\alpha}{4\pi v^4} + \frac{3k^2t}{v^5} \\
- \frac{(D-2)(D-7)k}{4\pi v^6} + \frac{\mathbf{q}^2}{v^{2(D-2)}}
\end{aligned} \tag{4.37}$$

in the case where $\tilde{\mu} > 0$ and

$$\begin{aligned}
p = \frac{t}{v} - \frac{(D-2)(D-3)k}{4\pi v^2} + \frac{2kt\alpha}{v^3} - \frac{(D-2)(D-5)k^2\alpha}{4\pi v^4} - \frac{3k^2t}{v^5} \\
+ \frac{(D-2)(D-7)k}{4\pi v^6} + \frac{\mathbf{q}^2}{v^{2(D-2)}}
\end{aligned} \tag{4.38}$$

when $\tilde{\mu} < 0$. To find the Gibbs free energy, the mass is obtained most easily from the cubic equation (2.73), which now takes the form

$$1 - \kappa + \frac{\tilde{\lambda}}{L^2}\kappa^2 - \frac{\tilde{\mu}}{L^4}\kappa^3 = \frac{mL^2}{r^{D-1}} - \frac{q^2L^2}{r^{2(D-2)}} \tag{4.39}$$

as we have explicitly fixed Λ , have altered the dimensionality of μ, λ , and have redefined parameters q, m (which are not exactly equal to the mass and Maxwell charge of the solution). Solving for the mass and evaluating $G = M - TS$ yields

$$\begin{aligned}
g = & -\frac{1}{16\pi(v^4 + 2\alpha kv^2 + 3)} \left[-\frac{3(D-2)kv^{D-7}}{(D-6)} - \frac{3(D-2)(D-8)\alpha v^{D-5}}{(D-6)(D-4)} + \frac{4(D+3)kv^{D-3}}{D-6} \right. \\
& - \frac{2(D-2)\alpha^2 kv^{D-3}}{D-4} - \frac{\alpha(D-8)v^{D-1}}{D-4} + \frac{60\pi pv^{D-1}}{(D-1)(D-6)} \\
& \left. - kv^{D+1} + \frac{24\pi\alpha kpv^{D+1}}{(D-1)(D-4)} + \frac{4\pi pv^{D+3}}{(D-1)(D-2)} \right] \\
& + \frac{q^2}{4(D-3)(v^4 + 2\alpha kv^2 + 3)v^{D-3}} \left[\frac{(2D-5)v^4}{D-2} + \frac{2(2D-7)\alpha kv^2}{D-4} + \frac{3(2D-9)}{(D-6)} \right] \quad (4.40)
\end{aligned}$$

when $\tilde{\mu} > 0$ and

$$\begin{aligned}
g = & -\frac{1}{16\pi(v^4 + 2\alpha kv^2 - 3)} \left[-\frac{3(D-2)kv^{D-7}}{(D-6)} + \frac{3(D-2)(D-8)\alpha v^{D-5}}{(D-6)(D-4)} - \frac{4(D+3)kv^{D-3}}{D-6} \right. \\
& - \frac{2(D-2)\alpha^2 kv^{D-3}}{D-4} - \frac{\alpha(D-8)v^{D-1}}{D-4} - \frac{60\pi pv^{D-1}}{(D-1)(D-6)} \\
& \left. - kv^{D+1} + \frac{24\pi\alpha kpv^{D+1}}{(D-1)(D-4)} + \frac{4\pi pv^{D+3}}{(D-1)(D-2)} \right] \\
& + \frac{q^2}{4(D-3)(v^4 + 2\alpha kv^2 - 3)v^{D-3}} \left[\frac{(2D-5)v^4}{D-2} + \frac{2(2D-7)\alpha kv^2}{D-4} - \frac{3(2D-9)}{(D-6)} \right] \quad (4.41)
\end{aligned}$$

when $\tilde{\mu} < 0$.

These expressions are rather tedious to deal with, and the relevant paper on the subject is long and sufficiently elaborates on the required considerations in ensuring that the solutions are asymptotically AdS - essentially we have to carefully work only in regions where the solutions we obtain are guaranteed to have AdS asymptotics because checking this requirement for all parameters is very arduous. While the form of the metric that we used here was required to compare with the Lovelock solutions [160], this trouble motivates future use of a cosmological constant that ensures the correct asymptotics such as (2.81), though I should mention that the metric function is then a function of the higher curvature couplings, and in that case it is not entirely clear to me how the extended phase space thermodynamics should be phrased since Λ now mixes together L, λ, μ , *et cetera*. Either the cosmological constant is to be associated with the pressure, or the lengthscale generated by the cosmological constant L is directly associated with the pressure.

We also discuss restricting the solutions to positive entropy, and cover some very interesting thermodynamic behaviour which had been observed in higher dimensional Lovelock gravity, but which was observed for the first time in five dimensional quasitopological gravity. Cataloguing the thermodynamic phase structure is important because it can further narrow our investigations into how a holographic dual theory should behave.

The phase transition can be seen through a plot of the Gibbs free energy versus temperature, where we look for the key “swallowtail” that vanishes at the critical point. An example, for $\alpha = 4$, $\mathfrak{q} = 0$, $k = 1$, $D = 5$ can be seen in figure 4.1. This particular phase transition is quite interesting, since first of all it culminates in a critical point which occurs for uncharged black holes, whereas in the four-dimensional Reissner-Nordström black hole of section 4.1.3, we saw that the critical point requires a finite charge to exist. That the critical point does not require a charge is also a feature of other higher curvature theories such as Lovelock gravity [160]. However, it is not so general as to survive for all higher curvature theories; we find that for negative $\tilde{\mu}$, for example, a value of $\alpha < \sqrt{225 + 120\sqrt{15}}/9$ means that no critical point(s) can exist.

Secondly, this phase transition is actually part of a larger phenomenon called a reentrant phase transition [81], where one can observe the swallowtail crossing over from the lower to the upper branch of the Gibbs free energy, resulting in a combination of two phase transitions - the system will undergo a first transition to a different state, and then it can undergo a second, different, phase transition which returns it to the original phase.

In this thesis we are interested in the universality class at the critical point in $k = 1$ five-dimensional quasitopological gravity; we investigated this in scenarios with a nonzero Maxwell charge, by requiring that the first and second derivatives of the pressure with respect to the volume are both zero:

$$\frac{\partial p}{\partial v} = 0 \quad \frac{\partial^2 p}{\partial v^2} = 0 \quad (4.42)$$

These two equations can be readily solved using the equations of state (4.37) and (4.38) to yield the critical values t_c, p_c, v_c .

The expansion of the equation of state can then be made in terms of t_R, p_r, v_R as per (4.2), to yield

$$\frac{p}{p_c} = 1 + At_R + Bt_R v_R + Cv_R^3 + \mathcal{O}(t_R v_R^2, v_R^4) \quad (4.43)$$

in the limit near criticality. Then, to compute the critical exponent of the isothermal compressibility (4.10), for example, we take

$$\left(\frac{\partial p}{\partial v}\right)_t \approx Bt_R + \mathcal{O}(v_R t_R, v_R^2) \quad (4.44)$$

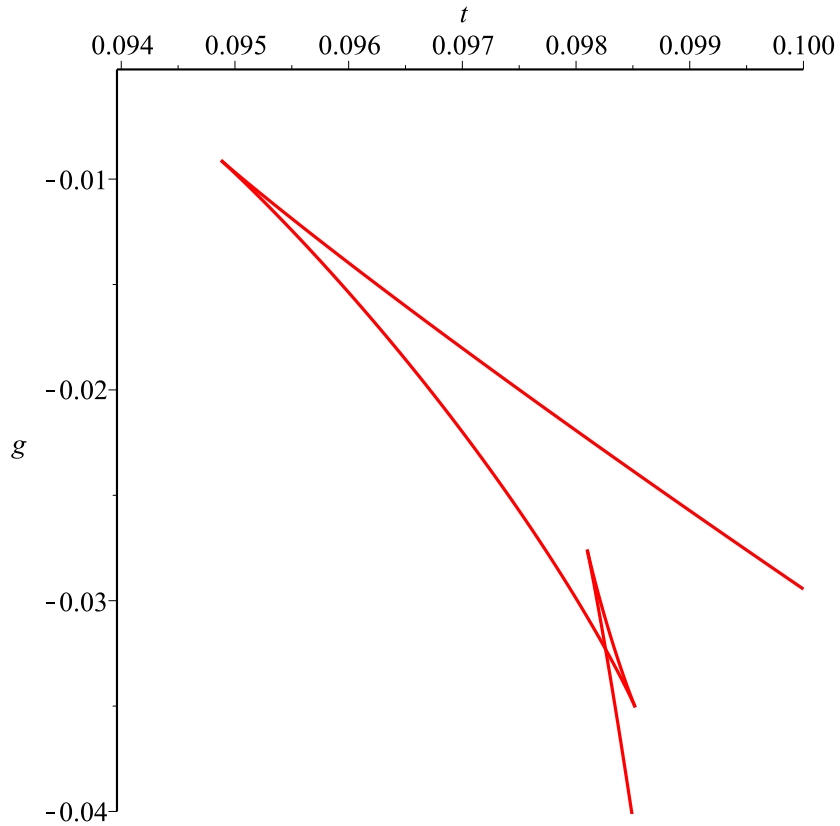


Figure 4.1: A plot of the μ -dimensionless Gibbs free energy g versus μ -dimensionless temperature t where μ is negative. In this figure, we are in five dimensions, looking at a set of spherical uncharged black holes, with the parameter $\alpha = 4$. We see a characteristic “swallowtail” on the lower branch of the free energy, corresponding to a phase transition.

which, when evaluated at $v = v_c$, becomes

$$\left(\frac{\partial p}{\partial v}\right)_t \rightarrow Bt_R \tag{4.45}$$

and therefore $\gamma = 1$ for this black hole. A similar procedure can be performed for the other critical exponents [2, 160] which again yields the universality class of table 4.1.

The interesting result here is that the universality class is the same for arbitrary dimension. Since having all higher dimensional gravity theories dual to gauge theories of a single, fixed dimension runs counter to the general holographic proposal that the D -dimensional bulk theory corresponds to a $(D - 1)$ -dimensional gauge theory, it is much more likely is that the static, higher curvature, higher dimensional black holes that we have examined all are governed by a mean field theory [149] near criticality. In retrospect this may not be unexpected; I should not overspeculate but it is indeed possible that the upper critical dimension of four spatial dimensions implies that the mean field theory is quite plausible as the descriptor of our black hole systems, provided that there is no spontaneous symmetry breaking. That said, it should not be this simple - there is evidence of a gravitational critical point that does not share the Van der Waals universality class [161]; a similar point also occurs in these quasitopological solutions but for parameters which make the black hole unphysical. In addition, holography suggests that a three-dimensional gauge theory should have a dual four-dimensional gravitational theory; if we want to extend this relationship to generic field theories on the boundary, where non-mean-field-theory criticality has been observed, how can we make this change in the gravitational theory? Not through higher curvature corrections alone, it would appear!

4.3 A Numerical Black Hole

Due to the results in section 3.5.2 indicating interesting phase behaviour and potential criticality with anisotropy, I have also been motivated towards investigating other types of gravitational theories to try to obtain a black hole with a different universality class. The one that was the most relevant to my work is the asymptotically Lifshitz black hole; its anisotropy should certainly have an effect on the criticality of the system. In condensed matter physics, we expect that this only manifests itself in the dynamic universality class, so our expectation would be to initially obtain the same universality class as that of section 4.1.

In order to find the universality class of an asymptotically Lifshitz black hole, I turned to the numerical solution found in [4]. I chose this solution because known exact asymp-

totically Lifshitz black holes often have a dependency of lengthscales which makes their thermodynamic parameters difficult to separate [3].

Furthermore, these numerical solutions are easy to modify by adding a Maxwell charge or alternative higher curvature terms, which means that the methodology proposed here is applicable to a very broad set of solutions.

My path here involves extracting the form of the Gibbs free energy from the numerical solution, then identifying a critical point along the line of phase transitions. Another reason for choosing this black hole solution is that the phase transition we are interested in has been observed in [1]. After identifying this critical point, derivatives of the free energy are taken to obtain the specific heat and the thermal compressibility. Taking the logarithm of these quantities near criticality, a linear fit will then yield the critical exponent as its slope.

In principle this formalism is well defined when the metric functions are exactly known. However, in this context an approximating polynomial is used and so we will need to characterize the error that this introduces and show that it does not affect this final result.

Difficulties arise, however, particularly when modelling the profile for the temperature, as obtaining good convergence without a sensible ansatz can be difficult when fitting non-linearly. In addition, the amount of time required to generate numerical data means that this work is not yet finished. Therefore, below I present a proof of concept, a numerical derivation of the universality class for the Reissner-Nordström black hole.

Note that here I again use the conventions of section 3.1 for the cosmological lengthscale ($L \rightarrow l$).

We begin with the equations of motion for the $D = 4$ Reissner-Nordström black hole. The exact solution is given by (4.15), but we can obtain a numerical solution through our shooting method of section 3.5 as a specific case of the $z = 1$, $D = 4$ simplification of the equations (3.84) with the higher curvature terms and Proca charge set to zero.

I first checked that the numerical method yields the same solution as the exact case, and then in the interest of computation time I created a mock dataset from the exact metric function, exactly as we obtain from the numerical method - it consists of the horizon radius, cosmological lengthscale, temperature, entropy, and derivative of the entropy.

In Mathematica this can be achieved with

```
rnK1D4Data =
Table[{cosmLength, horRad,
temperatureRN /. {l -> cosmLength, rh -> horRad, k -> 1},
```

```

entropyRN /. {rh -> horRad, omegak2 -> 4 \[Pi], k -> 1},
diffEntropyRN /. {rh -> horRad, omegak2 -> 4 \[Pi], k -> 1},
3/(8 \[Pi]*cosmLength^2)}, {cosmLength,
2.01, 9, 0.05}, {horRad, 0.01, 15, 0.05}];

```

In fact, we generate two datasets, the first using the $q = 0$ case and the second with charge; in this example I use $q = 1.0$:

```

rnK1D4DataQ =
Table[{cosmLength,
horRad, (temperatureRN + temperatureRNQ) /. {l -> cosmLength,
rh -> horRad, k -> 1, q -> 1.0},
entropyRN /. {rh -> horRad, omegak2 -> 4 \[Pi], k -> 1},
diffEntropyRN /. {rh -> horRad, omegak2 -> 4 \[Pi], k -> 1},
3/(8 \[Pi]*cosmLength^2)}, {cosmLength,
2.01, 9, 0.05}, {horRad, 0.01, 15, 0.05}];

```

where `temperatureRN` is the Reissner-Nordström black hole temperature (4.16) with $q = 0$ and `temperatureRNQ` is the temperature (4.16) when $q = 1.0$ minus the temperature when $q = 0$ (it is the “charge part” of the temperature).

This data is generated with an evenly spaced grid of size 0.05; the procedure below is completely independent of this spacing size and so once we obtain a critical point and begin attempting to extract critical exponents, we will want a higher resolution dataset with r_h, l taking values near criticality. Obtaining the location of this critical point is part of the challenge here; an initially broad sweep over many values of r_h, l may be required.

We then strive to compute the Gibbs free energy numerically. Because we emulate the scenario where we do not exactly know the mass of the black hole, we must implement the procedure in section 3.1.3. This requires a power expansion of the temperature and entropy. The entropy is exactly known (as is assumed for the Lifshitz case as well), so we only need the temperature’s expansion.

Taking only the temperature subset of our datasets, we fit constant coefficients to a Padé approximant (with the dynamic dimensionless variable of r_h/l). Note that we can use a general form for the temperature; with an uncharged black hole, each term in the metric function is dimensionless so the temperature must have a dimensionality of $1/L$; this means that we can consider terms of r_h/l only. For nonzero q , we understand that typically the term(s) added to the metric function go as q^2 , so there is an added $1/L^2$ in the approximant (as the numerical method takes q to be a dimensionless constant).

The approximants are in the canonical form, but there is an overall prefactor of C/r_h^D where C and D are dimension- and charge-dependent constants, which we absorb into the denominator of the approximant.

```

temperatureDataForFit = Flatten[rnK1D4Data, 1][[All, {1, 2, 3}]];
temperatureDataForFitQ = Flatten[rnK1D4DataQ, 1][[All, {1, 2, 3}]];
nlmCoeffsPade = {{a, 1.0}, {b, 0.0}, {c, 0.0}, {d, 1.0}, {e, 0.0}};
fitModel = (a*x/y + b + c*x^2/y^2)/(d*x + e*x^2/y);
fullFit =
  FindFit[temperatureDataForFit, fitModel, nlmCoeffsPade, {y, x},
    MaxIterations -> 5000];
fullFitNLM = fitModel /. fullFit
fitModelQ = (a*x/y + b + c*x^2/y^2)/(d*y*x^2 + e*x^3);
fullFitQ =
  FindFit[temperatureDataForFitQ, fullFitNLM + fitModelQ,
    nlmCoeffsPade, {y, x}, MaxIterations -> 5000];
fullFitNLMQ = fitModelQ /. fullFitQ

```

Each fit uses only four parameters. In this case we already have a good idea for initial values for the coefficients, where a, d are set to unity while the rest are zero as a starting value. However, in general this needs consideration. Fortunately, when fitting to a rational model such as this, it is known that a good choice of initial values for the Padé expression [162] is to first perform an initial linear least-squares fit on the model,

$$T_{RN-Pade} = \left(a \frac{x}{y} + b + c \frac{x^2}{y^2} \right) - T_{RN-Pade} (dx^2y + ex^3) \quad (4.46)$$

to obtain initial guesses for $\{a, b, \dots, e\}$.

After fitting, the temperature approximants are

$$T_{RN-Pade}|_{q=0} = \frac{\frac{(6.75801 \times 10^{-1})x^2}{y^2} - \frac{(5.07022 \times 10^{-17})x}{y} + 2.25267 \times 10^{-1}}{2.83079x - \frac{(9.17017 \times 10^{-16})x^2}{y}} \quad (4.47)$$

$$T_{RN-Pade}|_{q=1.0} - T_{RN-Pade}|_{q=0} = \frac{-\frac{(1.71879 \times 10^{-12})x^3}{y^3} + \frac{(1.75748 \times 10^{-12})x^2}{y^2} - 3.59126 \times 10^{-1}}{4.51291x^3 + (6.78043 \times 10^{-20})yx^2} \quad (4.48)$$

We can ensure that these approximants are good by examining both the numerical evaluation of these temperature approximants and the original values, as well as through a

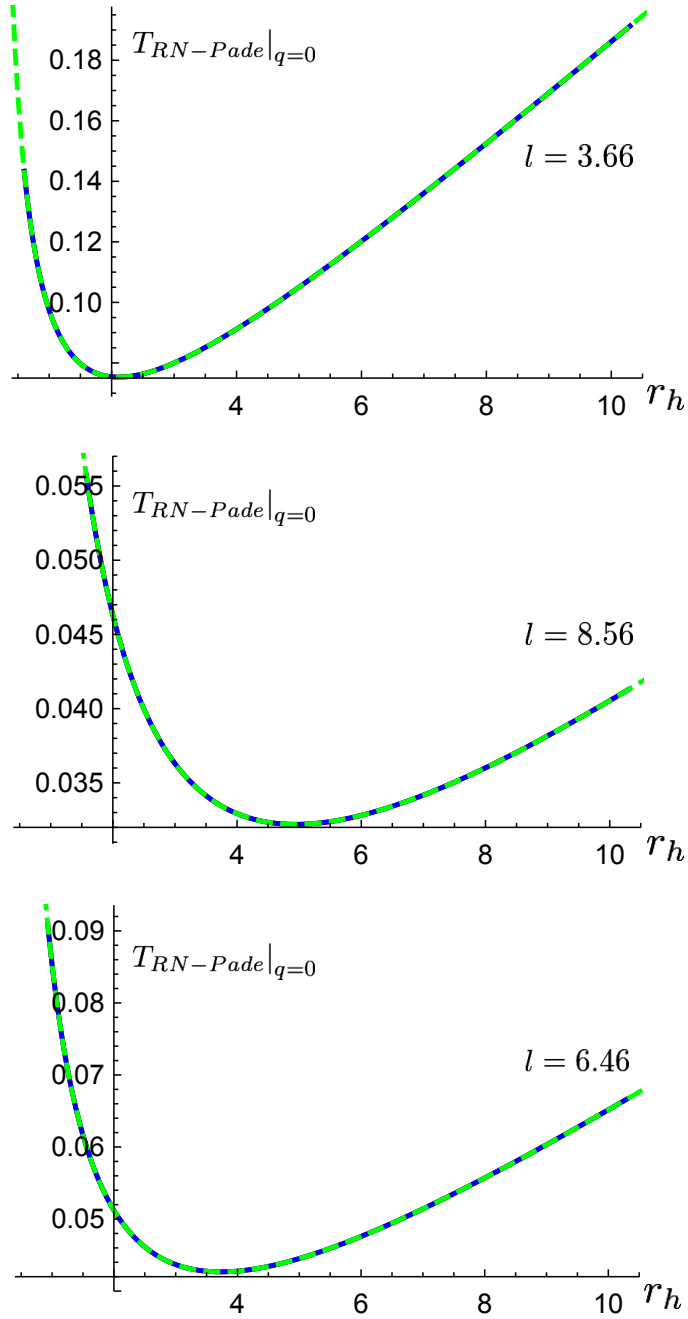


Figure 4.2: Three plots of $T_{RN-Pade}$ when $q = 0$ (solid blue) compared with the dataset generated from the exact temperature (4.16) (dashed green). The horizontal axis is the horizon radius r_h and the plots encompass values of $l = 3.66$, $l = 8.56$, and $l = 6.46$ respectively.

plot of both quantities over the regions of interest. We see from figure 4.2 that in the $q = 0$ case, these two functions have very good overlap; the same is true for the $q = 1.0$ solution.

In order to apply our thermodynamic method to obtain a mass, it is easiest to use a series solution for the temperature. We have extracted the usefulness of the Padé method by requiring a relatively small number of fit parameters, and now we can use a (potentially much) larger series expansion in order to obtain a mass in powers of r_h and l .

```

fullFitNLMSeries =
  Normal[Series[
    Series[fullFitNLM /. y -> 1/yinv, {x, 0, 10}], {yinv, 0, 4}] /.
  yinv -> 1/y;
fullFitNLMSeriesQ =
  Normal[Series[
    Series[fullFitNLMQ /. {y -> 1/yinv, x -> 1/xinv}, {xinv, 0,
      20}], {yinv, 1, 15}]] /. {yinv -> 1/y, xinv -> 1/x};
Block[{r, l},
  TemperatureFunctionQ0[{r_, l_}] = fullFitNLMSeries /. {y -> l, x -> r};
  TemperatureFunctionQ[{r_, l_}] = fullFitNLMSeriesQ /. {y -> l, x -> r};
]
tempListQ0 = List @@ Expand[TemperatureFunctionQ0[{r, l}]];
tempListQ = List @@ Expand[TemperatureFunctionQ[{r, l}]];

```

Because we seek expansions that are accurate for relatively large numerical values of l (we know from [78] that the criticality should be somewhere near $l = 6$), we expand in powers of the inverse of the cosmological lengthscale.

We therefore now have a series function for the $q = 0$ and q part, as well as a list of each of these terms. The list form will be very useful in our thermodynamic method, as each of the terms in the power series is processed individually.

We must also check the goodness-of-fit of our series solution to the original data. This is plotted for the entire temperature function ($q = 1.0$) in figure 4.3.

In our last step manipulating the temperature, we map the temperature over the values of r_h and l in the dataset, discretizing this series approximation. We can again check that there is very good overlap.

```

TemperatureListQ0 = Map[TemperatureFunctionQ0, temperatureDataForFit[[All, {2, 1}]];
TemperatureListQ = Map[TemperatureFunctionQ, temperatureDataForFitQ[[All, {2, 1}]];

```

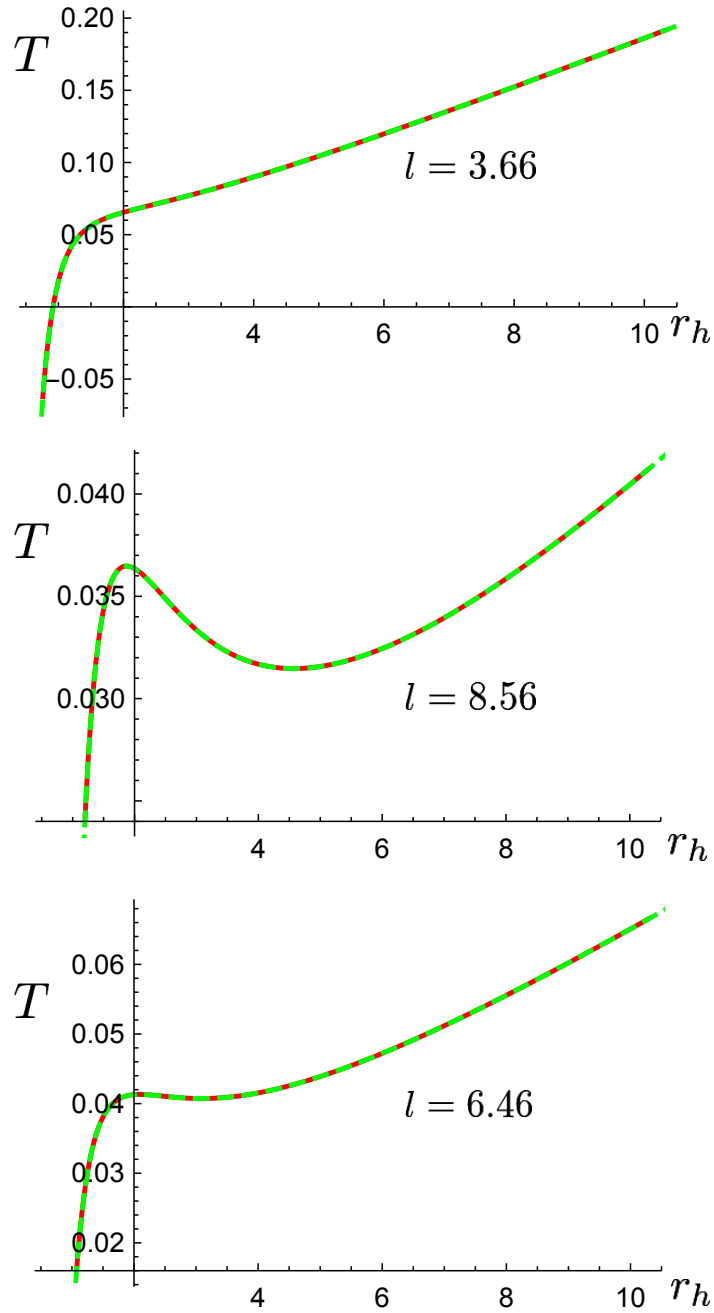


Figure 4.3: Three plots of the series expansion of $T_{RN-Pade}$ when $q = 1.0$ (solid red) compared with the $T_{RN-Pade}$ (solid blue) and the dataset generated from the exact temperature (4.16) (dashed green). The horizontal axis is the horizon radius r_h and the plots encompass values of $l = 3.66$, $l = 8.56$, and $l = 6.46$ respectively.

Using the method provided in Appendix C.3, we obtain a list of mass values as well as thermodynamic volume. We can again check that there is good overlap between the numerically determined mass and the mass of the exact solution.

Next, the Gibbs free energy is computed from $G = M - TS$. Here we build a function and map it over the dataset, similar to temperature. Having a functional form is important because the derivatives of the free energy are useful in obtaining the universality class.

The Gibbs free energy can be parametrically plotted against the numerically obtained temperature for $q = 1.0$ as seen in figure 4.4. We can see the swallowtail behaviour of a critical point in great detail, and we can see from higher resolution in l that criticality occurs somewhere around 6.00.

Now, we extract the critical exponents. First, we plot the Gibbs free energy in much higher resolution to obtain a value of $l_c \approx 6.005$. As a pedagogical example, here we will focus on the critical exponent corresponding to the isothermal compressibility,

$$\kappa_T \equiv -\frac{1}{V} \left(\frac{\partial V}{\partial P} \right)_T \quad (4.49)$$

We first need to convert this expression to a form that we can work with - remember that I only have $V = V(r_h, l)$. We can make use of the pressure depending on only one lengthscale, $P = P(l)$, such that

$$dV = \left(\frac{\partial V}{\partial P} \right)_T dP + \left(\frac{\partial V}{\partial T} \right)_P dT \quad (4.50)$$

$$dT = \left(\frac{\partial T}{\partial r_h} \right)_l dr_h + \left(\frac{\partial T}{\partial l} \right)_{r_h} dl \quad (4.51)$$

$$dP = \left(\frac{\partial P}{\partial l} \right) dl \quad (4.52)$$

This means that we can expand

$$\left(\frac{\partial V}{\partial P} \right)_T = \left[\left(\frac{\partial V}{\partial l} \right)_{r_h} - \left(\frac{\partial V}{\partial r_h} \right)_l \left(\frac{\partial T}{\partial l} \right)_{r_h} \left(\frac{\partial T}{\partial r_h} \right)_l^{-1} \right] \left(\frac{\partial P}{\partial l} \right)^{-1} \quad (4.53)$$

which allows us to compute the isothermal compressibility directly:

```

dVolumedPressure[r_, l_] := ((1/D[pressure[lvar], lvar] )*(D[VolumeFunctionQ[{r, lvar}], lvar]
  ↳ lvar]
  - D[VolumeFunctionQ[{rvar, l}], rvar]*D[TemperatureFunction[{r, lvar}], lvar] /
  D[TemperatureFunction[{rvar, l}], rvar])) /. {lvar -> l, rvar -> r};
\[\Kappa]T[r_, l_] := -(1/VolumeFunctionQ[{r, l}])*dVolumedPressure[r, l];

```

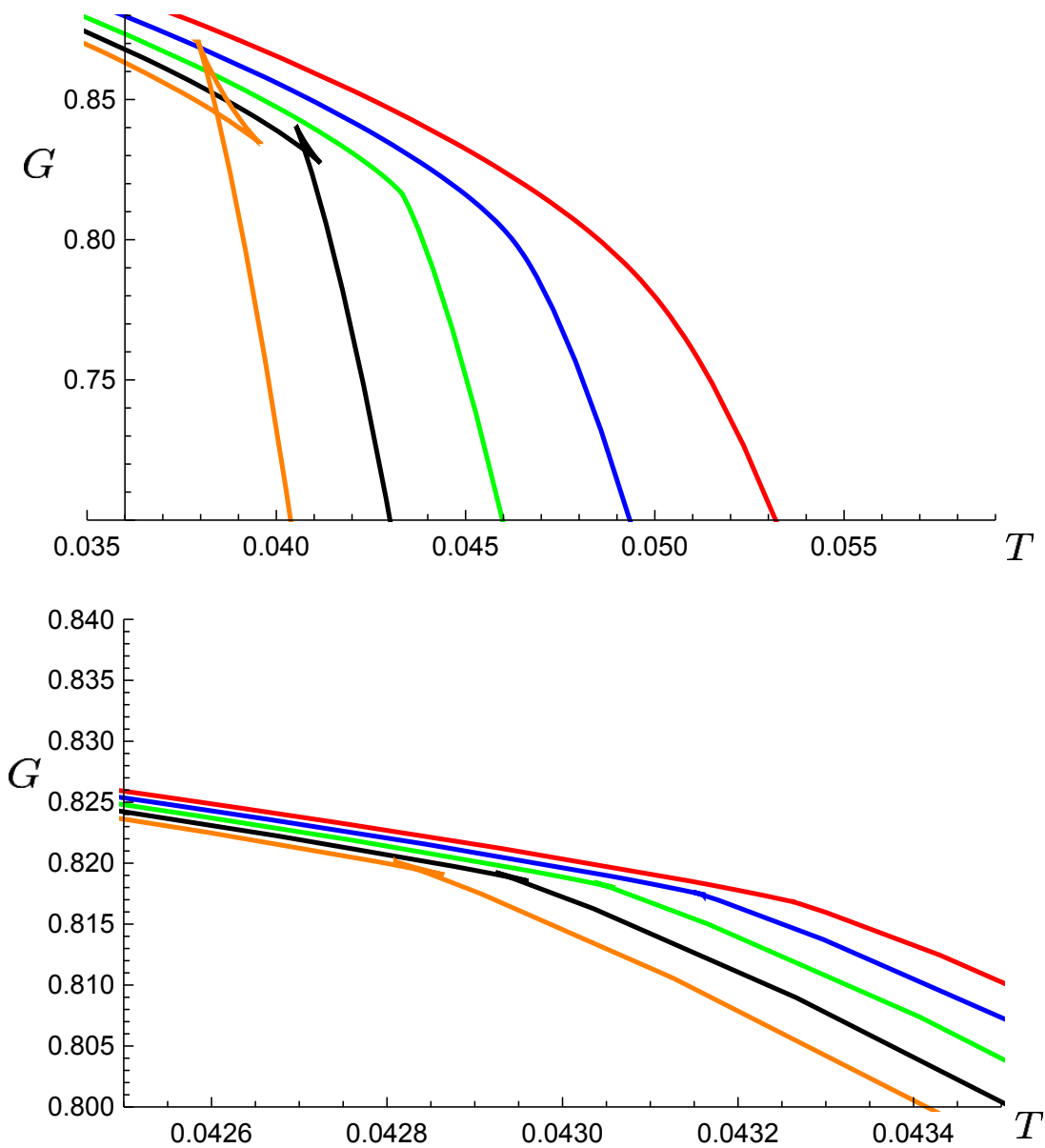


Figure 4.4: Two plots of the Gibbs free energy (obtained from numerical data) versus the series expansion of the temperature. On the top we have a larger range of cosmological constant considered, where the values of l are in the range $\{5.0, 5.5, 6.0, 6.5, 7.0\}$ ($\{\text{Red, Blue, Green, Black, Orange}\}$) while the figure on the bottom has l taking the range $\{6.01, 6.03, 6.05, 6.07, 6.09\}$, with the same colour profile.

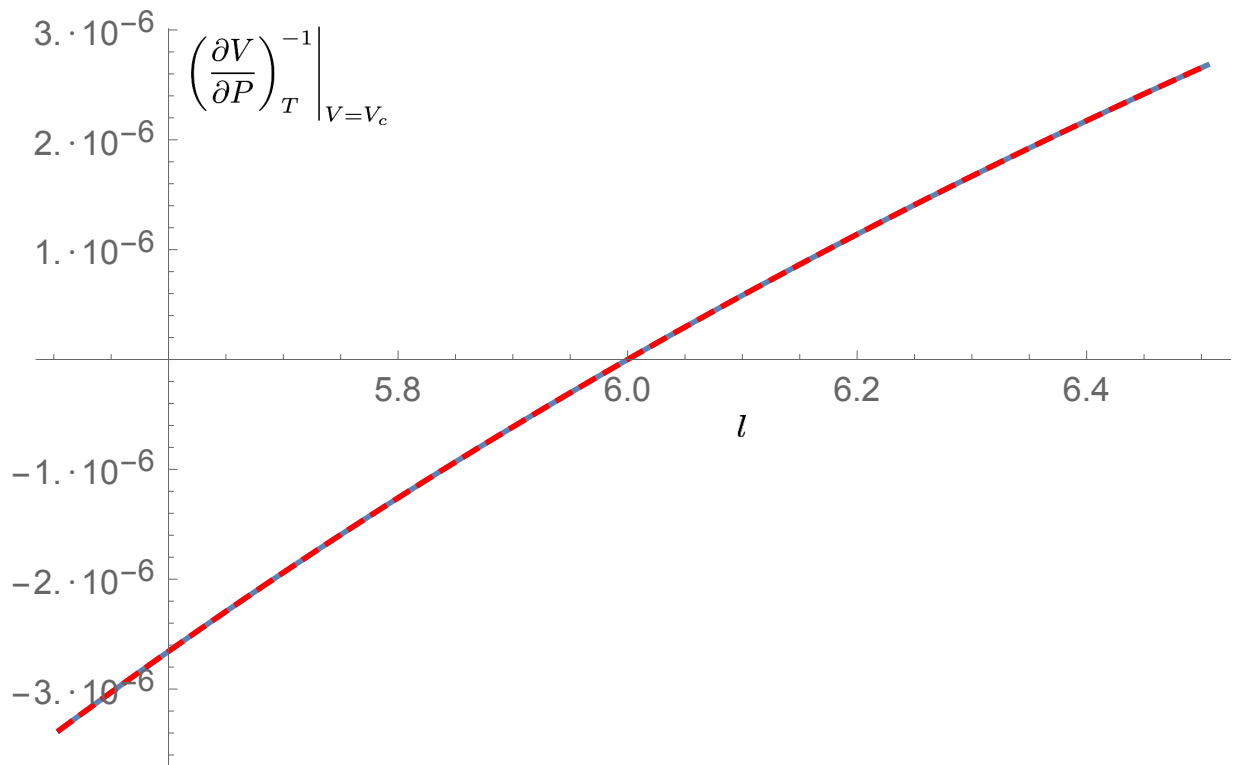


Figure 4.5: The analytic (blue, solid) and series (red, dashed) inverse of $(\partial V/\partial P)_T$ is plotted versus l when $V = V_c$. We see a very good match near the critical point (when the inverse reaches zero).

Since we have an exact solution, we can compute this derivative exactly and ensure that our series expansion remains accurate near criticality (where the inverse of this function will reach zero). Plotted in figure 4.5 is the inverse of $(\partial V/\partial P)_T$ versus l when $r_h = r_h^{(c)}$ (the horizon radius takes its critical value, i.e. $V = V_c$ in this context).

Now, near criticality the isothermal compressibility is expected to take the form

$$\kappa_T \rightarrow c |T - T_c|^{-\gamma} \quad (4.54)$$

where γ is the critical exponent for the isothermal compressibility and c is some constant. This limit is taken by varying temperature while holding V constant, $V = V_c$. We can exploit the knowledge of the singular structure to extract both the critical exponent and the critical cosmological length.

As in [155, 156, 163], consider a function

$$f(z) = A(z) (1 - uz)^{-\gamma} + B(z) \quad (4.55)$$

where z is the dynamical parameter of interest (in this context it is the temperature), an $A(z), B(z)$ are some functions that are not singular at $z = u^{-1}$. Then,

$$\frac{d(\log f(z))}{dz} = \frac{-\gamma}{1 - uz} (-u) + \text{nonsingular terms} \quad (4.56)$$

Furthermore,

$$(u^{-1} - z) \frac{d(\log f(z))}{dz} = \gamma + \text{terms multiplied by zero} \quad (4.57)$$

If we were to take the [1/1] Padé approximant of the left-hand side of (4.56), we can obtain unbiased values of both γ and u . Using u as a refinement of the inverse critical temperature, we can take the [1/1] Padé approximant of the left-hand side of (4.57), which will give a biased estimate of the critical exponent.

For our case, the parameter $T = T(l)$, since we have evaluated temperature at fixed horizon radius (since $V = V(r_h)$) and so we can develop the method of obtaining a critical exponent.

Suppose instead of (4.56), we therefore have

$$\frac{d(\log f(T(l)))}{dl} = \frac{-\gamma}{1 - uT(l)} (-u) \left(\frac{\partial T}{\partial l} \right)_{r_h=r_h^{(c)}} + \text{nonsingular terms} \quad (4.58)$$

We can modify this to give an estimate of the critical exponent by taking

$$(T_c - T(l)) \left(\frac{\partial T}{\partial l} \right)_{r_h=r_h^{(c)}}^{-1} \frac{d(\log f(T(l)))}{dl} = \gamma \quad (4.59)$$

Perhaps a deeper understanding of the proper boundaries for black hole thermodynamics in anisotropic spacetimes will yield notions of volume that only depend on the horizon radius of the black hole. In principle this will mean that the above method will be directly applicable to e.g. Lifshitz solutions. Otherwise, more analysis is needed to determine the appropriate expression to convert to a Padé approximant in order to extract the critical cosmological lengthscale and the isothermal compressibility's critical exponent.

In this case, however, computing the critical exponent is as simple as evaluating

```
PadéApproximant[(1/dTempPadéCritRh)*(criticalTemperature - tempPadéCritRh)*
D[Log[dVolumedPressure[criticalHorizon, l]], l], {l, 5, 0}]
```

which yields $\gamma = 0.99998$, in agreement with the theoretical value of $\gamma = 1.0$ for the $D = 4$ Reissner-Nordström black hole, after equation (4.58) was used to refine the critical temperature (in precise agreement with the analytic solution).

Due to the impressive performance of this model, future work involves the extension to other critical exponents in a wide variety of numerical black hole spacetimes. Namely, an interesting problem is to use this procedure to find the previously-undiscovered universality class of the $D = 5$ numerical cubic quasitopological asymptotically Lifshitz black hole of section 3.5.2.

4.4 Discussion

In this section I began by presenting the universality class as motivated by thermodynamics of simple physical theories that arise from a Hamiltonian. The Van der Waals gas was used as an example; after writing down the equation of state, I showed how to find critical behaviour, and how the thermodynamic potentials can be used to obtain quantities which diverge at criticality. I used the isothermal compressibility κ_T as our quantity of interest, and found the related critical exponent γ , ultimately finishing by presenting the other common critical exponents for this system.

Then, I presented the first gravitational analogue of the Van der Waals gas, the four-dimensional Reissner-Nordström black hole. I showed how the universality class could be found for this system, including an explicit derivation of the isothermal compressibility, when the cosmological constant is interpreted as a pressure.

The universality class of a five-dimensional exact cubic quasitopological black hole was presented, both with and without Maxwell charge. This was used to show how the extended

phase space thermodynamics can yield new behaviour through the additional parameter space arising from the quasitopological terms that were added to the action.

The compelling result was that the universality class of the main large black hole - small black hole phase transition remains the same as that of the four-dimensional Reissner-Nordström black hole, even though new features such as reentrant phase transitions and isolated critical points emerge. This has exciting implications for holography, namely the relationship of all of these black hole solutions to mean field theory thermodynamics.

I also provided an introduction to computational techniques that can be of assistance when finding the universality class of numerical black holes. The application of nonlinear fitting methods and Padé approximants was then shown to be effective in an example whereby a mock dataset was constructed for the $D = 4$ AdS Reissner-Nordström black hole whose universality class we already extracted. A complete derivation of the critical exponent for the isothermal compressibility was detailed, when the only prior data were tuples consisting of the cosmological constant, horizon radius, temperature, and entropy.

This approach is essentially the culmination of this thesis; it is applicable to the higher curvature theories and makes use of the insights into thermodynamics from studying black holes with AdS asymptotics. Studying asymptotically Lifshitz black holes has given us a technique for determining mass and volume from the power series for temperature and entropy, which is crucial to this numerical procedure, and this method of numerically obtaining the universality class applies directly to the output from the aforementioned shooting method numerical solutions. For an accurate result, finding the universality class numerically also required the use of the computational techniques described above.

This section also leads us to a set of important questions regarding the universality class of black holes, and presents us with some ideas of where to turn. An obvious next step is to obtain the universality class for the asymptotically Lifshitz black holes. If the Lifshitz parameter does turn out to be the dynamic critical exponent, this represents an important verification of what was hoped to be true with the introduction of anisotropy in this fashion. Primarily, I posit that the asymptotically Lifshitz black holes are likely to be models of mean field theory criticality with different dynamical universality classes. This represents the first step of fine-graining that we can do after formulating the universality class.

Chapter 5

Conclusion

This thesis examined the thermodynamic behaviour of higher curvature and anisotropic black holes in five dimensions. Higher curvature theories were motivated by the desire to keep the resultant field equations to second derivatives of the metric tensor or fewer, and both the Lovelock theories and the quasitopological theories were examined.

I presented the general Lovelock theory, and examined the second-order Lovelock gravity (arising through the addition of the Lanczos-Gauss-Bonnet term to the action). Black hole solutions in this theory were studied, and seen to offer a more rich solution space than in the $D = 5$ Einsteinian case; in particular, there existed two valid black hole solutions, each of which have the same temperature and entropy, along with a new parameter corresponding to the Lanczos-Gauss-Bonnet term which affects the asymptotic behaviour of solutions of the theory.

The Euclidean regularization technique was presented as a framework to obtain a temperature of black holes in this theory, as well as the use of the Wald method to obtain an entropy for these black holes. The higher curvature contributed to nontrivial corrections to the entropy.

Quasitopological theories were introduced, which allow us the benefit of the higher dimensional Lovelock theories (second order field equations) in only five dimensions, at the cost of requiring spherical symmetry. To explore gravity theories that should have a four-dimensional dual, this was a trade that we were willing to make. It was seen that these theories have solutions that are very similar to the Lovelock theories; the field equations change only in terms of constants proportional to the number of dimensions. Furthermore, the temperature and entropy were computed using the same methodology as for the Lovelock case.

Holographic arguments were presented which guide us into a range of parameters that allow for positivity of energy flux in the dual field theories and contribute to the stability of the bulk theory (essentially the higher curvature couplings are constrained to be sufficiently small). The extended phase space thermodynamics was applied, which interprets dimensional parameters in the action as new thermodynamic quantities. For anti-de Sitter spacetimes, the Eulerian scaling argument was used to justify using the cosmological constant as a pressure, since mass has dimensionality to the power $(D - 3)$ while entropy is like an area, of dimensionality $(D - 2)$. Intuitive notions of volume allows the remaining constant factor needed to specify the pressure term completely to be fixed.

Then, we were able to begin the thermodynamic examination of black hole solutions in these theories. The temperature and entropy can be used to graphically see transitions in the sign of the specific heat via the second law of thermodynamics, and plots were used to show that higher curvature terms can be used to control the stability of the black hole solutions. An intuitive notion of the way higher curvature terms affect thermodynamic behaviour is important in investigations into deeper concepts like the universality class, because knowing which sign and magnitude of coupling constants will correspond to black holes with a critical point allows one to more quickly home in on criticality (or even gives insight into whether criticality exists), especially for black holes which can only be obtained numerically.

A Maxwell charge was then introduced into the cubic quasitopological solution, and we were able to see its effect from both plots of temperature and entropy as well as from looking at the specific heat itself. Some important possible pitfalls were discussed - for example, it appears that the charge can cause instability in the otherwise-stable planar black hole from looking at the specific heat. However, an examination of the conditions for extremality in these higher curvature solutions (the algebraic complexity makes this a greater challenge) showed that such a transition in the sign of the specific heat will not take place for non-extremal black holes.

The Lifshitz symmetric black holes were discussed next, which arise by breaking the usual scaling of time and space through the introduction of a parameter which governs “how much more” time will scale by. This type of modification was motivated in this thesis by the predicted dynamical scaling that it will induce in the theory, which splits the universality class into a set of dynamical universality classes.

In order for these black holes to be thermodynamically useful, however, we needed a notion of mass (as enthalpy) which obeys a first law and Smarr relation. For some time we worked to understand how mass should scale in anisotropic spacetimes, and here I presented the result of that work, through a plausible Smarr relation whose scaling depends only on

the dimensionality (not the Lifshitz exponent z) and reduces to forms of the Smarr relation that have been previously used in the literature (presumably found by comparison with non-anisotropic solutions, but presented without justification, and specific to the parameter z and the topology of the black hole k). That is, all other Smarr relations can be regarded as special cases of the one which we proposed.

The knowledge of the Smarr relation turned out to be enough to specify most of the thermodynamic quantities of the system, given a certain number of independent parameters for the solution. We proposed a method to yield mass, volume, and work terms given the temperature, entropy, and pressure of any solution in a power series, and I presented that method in this thesis, along with some analysis for a set of exact Lifshitz solutions.

The attempt was designed to allow for solutions where the lengthscale from the cosmological constant was mixed with lengthscale of the horizon radius in a nontrivial way, and to build a method to obtain a mass and volume that was robust to that. Ultimately this was not successful as solutions where the cosmological constant and horizon radius are completely dependent result in a reduction of rank in our set of equations, and we were not able to propose a single method that explained the results of all of the other approaches towards obtaining a mass. However, our method was shown to perform well for black holes where horizon radius and length are independent, and new lengthscales (such as a dimensionful charge from a Maxwell field) remain independent as well.

In addition, the method did offer insight into the differences between the Brown-York and Hollands-Ishibashi-Marolf masses in asymptotically Lifshitz spacetimes. The HIM approach with an action that was constructed to allow for independent variation of parameters such as the metric tensor and Proca field agreed with a fictitious approach that had a mass term with $(D - 1)$ scaling, the form of the scaling that we conjecture in our Smarr relation. Conversely, the Brown-York mass agreed with our thermodynamic mass when we ignored the dependence of the cosmological lengthscale on the black hole horizon.

A clear path of development for this method was towards the numerical Lifshitz solutions, so the five-dimensional cubic and quartic quasitopological asymptotically $z = 2$ Lifshitz numerical black hole solutions were presented. No exact solution is known for an anisotropic black hole that is quite this general, with control over the parameter z (fractional powers could be examined if desired) as well as independence of the horizon radius and cosmological lengthscale. The entropy and temperature of these solutions were plotted to examine whether they had suitable phase transition behaviour for studying potential criticality and it was seen that indeed, there is evidence that there are unstable and stable black holes, and a divergent specific heat, for certain values of the higher curvature couplings.

The endgame of this thesis was then presented - the black hole universality class. This allowed us to characterize an entire ensemble of black holes (of varying cosmological constant, horizon radius, and charge) by a set of a few parameters corresponding to the power with which a set of functions describing the system thermodynamically diverge, as a critical point is approached.

The basic procedure to find these parameters was shown for the Van der Waals gas as well as for the four-dimensional asymptotically AdS Reissner-Nordström black hole. The latter is an important case study as it was the first black hole found to share its universality class with the Van der Waals gas.

I presented the procedure used to find the universality class of the five dimensional asymptotically AdS cubic quasitopological black hole, upon which it was seen that it falls into the same universality class as the Van der Waals gas. Other works provide additional evidence that this is not coincidental, that the mean field theory critical exponents describe all of these theories for a reason, though the physics that explains this reason remains to be completely understood.

In light of this, I presented techniques which could be used to eventually examine the universality class of numerical black holes, in the hopes that they can lend insight into the nature of the universality class. On the one hand, if time is playing a role in the thermodynamics, causing the mean field theory to be applicable to the black hole criticality for $D \geq 4$, the Lifshitz anisotropy should represent a substantial change to the behaviour of the universality class. On the other, if as expected the Lifshitz critical exponent will correspond to the dynamic universality class only, then perhaps it can be used as a more finely grained gauge/gravity duality. Either way, the result is interesting.

Therefore, a method using data from numerical solutions needed to be developed. Here it was tested for the simplest case, a $D = 4$ asymptotically AdS Reissner-Nordström black hole. It was seen that through careful use of the Padé approximant and series expansions, a rational function model of temperature could be constructed that yields a correct mass and volume via our thermodynamic method. Close agreement with the exact solution was ensured at each step of this process. The critical exponent for the isothermal compressibility was extracted and found to agree with the exact analysis.

A driving goal of theoretical physics is to take the complexity that we observe and reduce it to models which are well understood and have predictive power. In that sense, this thesis is very representative of this goal. Beginning with the algebraically complex higher curvature gravity, we have taken a journey through black hole thermodynamics that ultimately allowed us to develop a set of numerical methods that reduce all of the complexity of these theories to an important single number, and that number happens to

be 1. Beautiful!

The promise of this method means that future work with the goal of obtaining the universality class for the asymptotically Lifshitz black holes is coming in the near future. My hope is that this approach is able to play a part in the final understanding of the gauge/gravity duality and the deep mathematics that this conjecture surely represents.

References

- [1] M. Ghanaatian, A. Bazrafshan, and W. G. Brenna, “Lifshitz Quartic Quasitopological Black Holes,” *Phys. Rev. D* **89** (Feb., 2014) 124012, [1402.0820](#).
- [2] R. A. Hennigar, W. G. Brenna, and R. B. Mann, “P-V Criticality in Quasitopological Gravity,” *JHEP* **2015** no. 7, (July, 2015), [1505.05517](#).
- [3] W. G. Brenna, R. B. Mann, and M. Park, “Mass and Thermodynamic Volume in Lifshitz Spacetimes,” *Phys. Rev. D* **92** (May, 2015) 044015, [1505.06331](#).
- [4] W. G. Brenna, M. H. Dehghani, and R. B. Mann, “Quasi-Topological Lifshitz Black Holes,” *Phys. Rev. D* **84** (Jan., 2011) 024012, [1101.3476](#).
- [5] W. G. Brenna and R. B. Mann, “Quasi-topological Reissner-Nordström Black Holes,” *Phys. Rev. D* **86** (June, 2012) 064035, [1206.4738](#).
- [6] W. G. Brenna, E. G. Brown, R. B. Mann, and E. Martin-Martinez, “Universality and thermalization in the Unruh Effect,” *Phys. Rev. D* **88** (July, 2013) 064031, [1307.3335](#).
- [7] W. G. Brenna, R. B. Mann, and E. Martin-Martinez, “Anti-Unruh Phenomena,” *Phys. Lett. B* **757** (June, 2016) 307–311, [1504.02468](#).
- [8] W. G. Brenna and C. Flori, “Complex Numbers, One-Parameter of Unitary Transformations and Stone’s Theorem in Topos Quantum Theory.” June, 2012. [1206.0809](#).
- [9] M. Natsuume, *AdS/CFT Duality User Guide*, vol. 903. Springer Japan, 1 ed., Sept., 2014. [1409.3575](#).
- [10] V. Frolov and A. Zelnikov, *Introduction to Black Hole Physics*. OUP Oxford, 2011. https://books.google.ca/books?id=r_l5AK9DdXsC.

- [11] J. M. Maldacena, “The Large N Limit of Superconformal Field Theories and Supergravity,” *Adv. Theor. Math. Phys.* **2** (1998) 231–252, [hep-th/9711200](#).
- [12] S. Stotyn, *Exact Solutions and Black Hole Stability in Higher Dimensional Supergravity Theories*. PhD thesis, University of Waterloo, Sept., 2012. [1209.2726](#).
- [13] E. Witten, “Anti De Sitter Space And Holography,” *Adv. Theor. Math. Phys.* **2** (1998) 253–291, [hep-th/9802150](#).
- [14] S. S. Gubser, I. R. Klebanov, and A. M. Polyakov, “Gauge Theory Correlators from Non-Critical String Theory,” *Phys. Lett. B* **428** (1998) 105–114, [hep-th/9802109](#).
- [15] G. Policastro, D. T. Son, and A. O. Starinets, “Shear Viscosity of Strongly Coupled $N = 4$ Supersymmetric Yang-Mills Plasma,” *Phys. Rev. Lett.* **87** no. 8, (Aug., 2001).
- [16] A. Strominger, “The dS/CFT correspondence,” *JHEP* **2001** no. 10, (Oct., 2001) [034–034](#).
- [17] V. Balasubramanian, J. de Boer, and D. Minic, “Mass, Entropy and Holography in Asymptotically de Sitter Spaces,” *Phys. Rev. D* **65** (2002) 123508, [hep-th/0110108](#).
- [18] A. M. Ghezelbash and R. B. Mann, “Action, Mass and Entropy of Schwarzschild-de Sitter black holes and the de Sitter/CFT Correspondence,” *JHEP* **0201** (2002) 005, [hep-th/0111217](#).
- [19] M. Guica, T. Hartman, W. Song, and A. Strominger, “The Kerr/CFT Correspondence,” *Phys. Rev. D* **80** (Sept., 2008) 124008, [0809.4266](#).
- [20] R. B. Mann and D. Marolf, “Holographic Renormalization of Asymptotically Flat Spacetimes,” *Class. Quant. Grav.* **23** (2006) 2927–2950, [hep-th/0511096](#).
- [21] S. A. Hartnoll, C. P. Herzog, and G. T. Horowitz, “Building an AdS/CFT superconductor,” *Phys. Rev. Lett.* **101** (Mar., 2008) 031601, [0803.3295](#).
- [22] P. Kovtun, D. T. Son, and A. O. Starinets, “Viscosity in Strongly Interacting Quantum Field Theories from Black Hole Physics,” *Phys. Rev. Lett.* **94** (2005) 111601, [hep-th/0405231](#).
- [23] P. Chaikin and T. Lubensky, *Principles of Condensed Matter Physics*. Cambridge University Press, 1995. <https://books.google.ca/books?id=P9YjNjzr90IC>.

- [24] V. Iyer and R. M. Wald, “Some Properties of Noether Charge and a Proposal for Dynamical Black Hole Entropy,” *Phys. Rev. D* **50** (1994) 846–864, [gr-qc/9403028](#).
- [25] Volunteers and Macsyma Group, *Maxima*. version 5.34.1 ed. maxima.sourceforge.net, 2014.
- [26] Waterloo Maple, Inc., *Maple*. version 13.0 ed. Maplesoft, 2009.
- [27] Wolfram Research, Inc., *Mathematica*. version 10.4 ed. Wolfram Research, Inc., 2016.
- [28] R. Wald, *General relativity*. Physics/Astrophysics. University of Chicago Press, 1984.
<http://books.google.ca/books?id=9S-hzg6-moYC>.
- [29] M. V. Ostrogradski, *Mémoire sur les équations différentielles relatives au problème des isopérimètres. Lu le 17 (29) novembre 1848*, vol. 4 of 6. l’Académie impériale des sciences, Nov., 1850.
<http://babel.hathitrust.org/cgi/pt?id=mdp.39015038710128;view=1up;seq=405>.
- [30] T. jun Chen, M. Fasiello, E. A. Lim, and A. J. Tolley, “Higher derivative theories with constraints : Exorcising Ostrogradski’s Ghost,” *JCAP* **1302** (Sept., 2012) 042, [1209.0583](#).
- [31] A. D. Felice and S. Tsujikawa, “f(R) Theories,” *Living Reviews in Relativity* **13** no. 3, (2010).
<http://www.livingreviews.org/lrr-2010-3>.
- [32] C. de Rham, G. Gabadadze, and A. J. Tolley, “Resummation of Massive Gravity,” *Phys. Rev. Lett.* **106** (Nov., 2010) 231101, [1011.1232](#).
- [33] A. G. Riess, A. V. Filippenko, P. Challis, A. Clocchiatti, A. Diercks, P. M. Garnavich, R. L. Gilliland, C. J. Hogan, S. Jha, R. P. Kirshner, and et al., “Observational Evidence from Supernovae for an Accelerating Universe and a Cosmological Constant,” *The Astronomical Journal* **116** no. 3, (Sept., 1998) 1009–1038.
- [34] R. C. Myers and J. Z. Simon, “Black-hole thermodynamics in Lovelock gravity,” *Phys. Rev. D* **38** no. 8, (Oct., 1988) 2434–2444.
- [35] P. Candelas, G. T. Horowitz, A. Strominger, and E. Witten, “Vacuum configurations for superstrings,” *Nucl. Phys. B* **258** (Jan., 1985) 46–74.

- [36] M. Duff, B. Nilsson, and C. Pope, “Gauss-Bonnet from Kaluza-Klein,” *Phys. Lett. B* **173** no. 1, (May, 1986) 69–72.
- [37] M. Visser, “Sakharov’s induced gravity: a modern perspective,” *Mod. Phys. Lett. A* **17** (2002) 977–992, [gr-qc/0204062](#).
- [38] A. Buchel, J. T. Liu, and A. O. Starinets, “Coupling constant dependence of the shear viscosity in N=4 supersymmetric Yang-Mills theory,” *Nucl. Phys. B* **707** (2005) 56–68, [hep-th/0406264](#).
- [39] Y. Kats and P. Petrov, “Effect of curvature squared corrections in AdS on the viscosity of the dual gauge theory,” *JHEP* **0901** no. 044, (Dec., 2007), [0712.0743](#).
- [40] R. C. Myers, M. F. Paulos, and A. Sinha, “Quantum corrections to η/s ,” *Phys. Rev. D* **79** (June, 2009) 041901, [0806.2156](#).
- [41] D. M. Hofman, “Higher Derivative Gravity, Causality and Positivity of Energy in a UV complete QFT,” *Nucl. Phys. B* **823** (July, 2009) 174–194, [0907.1625](#).
- [42] R. C. Myers, M. F. Paulos, and A. Sinha, “Holographic studies of quasi-topological gravity,” *JHEP* **2010** (Apr., 2010) 1–44, [1004.2055](#).
- [43] D. Lovelock, “The Einstein Tensor and Its Generalizations,” *J. Math. Phys.* **12** no. 3, (1971) 498–501.
<http://link.aip.org/link/?JMP/12/498/1>.
- [44] M. R. Mehdizadeh, M. H. Dehghani, and M. K. Zangeneh, “Counterterms for Static Lovelock Solutions,” *Eur. Phys. J. C* **75** (Jan., 2015) 276, [1501.05218](#).
- [45] R. A. Hennigar, R. B. Mann, and S. Mbarek, “Thermalon mediated phase transitions in Gauss-Bonnet gravity,” *JHEP* **02** (Dec., 2015) 034, [1512.02611](#).
- [46] C. Lanczos, “Elektromagnetismus als natürliche Eigenschaft der Riemannschen Geometrie,” *Z. Physik* **73** no. 3-4, (Mar., 1932) 147–168.
- [47] B. Zwiebach, “Curvature squared terms and string theories,” *Phys. Lett. B* **156** no. 5-6, (June, 1985) 315–317.
- [48] X. O. Camanho, *Lovelock gravity, black holes and holography*. PhD thesis, Universidade de Santiago de Compostela, Sept., 2015. [1509.08129](#).

- [49] H. S. Reall, N. Tanahashi, and B. Way, “Causality and Hyperbolicity of Lovelock Theories,” *Class. Quant. Grav.* **31** no. 20, (June, 2014) 205005, [1406.3379](#).
- [50] D. Kastor, S. Ray, and J. Traschen, “Enthalpy and the Mechanics of AdS Black Holes,” *Class. Quant. Grav.* **26** (Apr., 2009) 195011, [0904.2765](#).
- [51] A. Buchel, J. Escobedo, R. C. Myers, M. F. Paulos, A. Sinha, and M. Smolkin, “Holographic GB gravity in arbitrary dimensions,” *JHEP* **1003** (Nov., 2009) 111, [0911.4257](#).
- [52] D. G. Boulware and S. Deser, “String-Generated Gravity Models,” *Phys. Rev. Lett.* **55** (Dec., 1985) 2656–2660.
- [53] T. Clunan, S. F. Ross, and D. J. Smith, “On Gauss-Bonnet black hole entropy,” *Class. Quant. Grav.* **21** (2004) 3447–3458, [gr-qc/0402044](#).
- [54] V. P. Frolov and I. D. Novikov, *Black Hole Physics: Basic Concepts and New Developments*, vol. 96. Springer Netherlands, 1 ed., 1998.
- [55] R. C. Tolman, “On the Weight of Heat and Thermal Equilibrium in General Relativity,” *Phys. Rev.* **35** no. 8, (Apr., 1930) 904–924.
- [56] J. D. Brown, J. Creighton, and R. B. Mann, “Temperature, energy, and heat capacity of asymptotically anti-de Sitter black holes,” *Phys. Rev. D* **50** no. 10, (Nov., 1994) 6394–6403.
- [57] H. W. Braden, J. D. Brown, B. F. Whiting, and J. W. York, “Charged black hole in a grand canonical ensemble,” *Phys. Rev. D* **42** no. 10, (Nov., 1990) 3376–3385.
- [58] M. Atiyah and C. LeBrun, “Curvature, Cones, and Characteristic Numbers,” *Mathematical Proceedings of the Cambridge Philosophical Society* **155** no. 01, (Mar., 2013) 13–37, [1203.6389](#).
- [59] C. Krishnan and S. Kuperstein, “A comment on Kerr-CFT and Wald entropy,” *Phys. Lett. B* **677** no. 5, (June, 2009) 326–331.
- [60] S. W. Hawking, G. T. Horowitz, and S. F. Ross, “Entropy, Area, and Black Hole Pairs,” *Phys. Rev. D* **51** (1995) 4302–4314, [gr-qc/9409013](#).
- [61] V. Iyer and R. M. Wald, “A comparison of Noether charge and Euclidean methods for Computing the Entropy of Stationary Black Holes,” *Phys. Rev. D* **52** (1995) 4430–4439, [gr-qc/9503052](#).

- [62] R. M. Wald, “Black hole entropy is the Noether charge,” *Phys. Rev. D* **48** (Oct., 1993) R3427–R3431.
- [63] T. Jacobson and R. C. Myers, “Black hole entropy and higher curvature interactions,” *Phys. Rev. Lett.* **70** no. 24, (June, 1993) 3684–3687.
- [64] L. Smarr, “Mass Formula for Kerr Black Holes,” *Phys. Rev. Lett.* **30** (Jan., 1973) 71–73.
- [65] J. M. Bardeen, B. Carter, and S. W. Hawking, “The four laws of black hole mechanics,” *Communications in Mathematical Physics* **31** no. 2, (1973) 161–170.
- [66] P. Peebles and B. Ratra, “Cosmology with a time-variable cosmological ‘constant’,” *Astrophys. J.* **325** (1988) L17.
- [67] M. S. Berman, “Cosmological models with a variable cosmological term,” *Phys. Rev. D* **43** no. 4, (Feb., 1991) 1075–1078.
- [68] J. M. Overduin and F. I. Cooperstock, “Evolution of the scale factor with a variable cosmological term,” *Phys. Rev. D* **58** no. 4, (July, 1998).
- [69] J. D. E. Creighton and R. B. Mann, “Quasilocal Thermodynamics of Dilaton Gravity coupled to Gauge Fields,” *Phys. Rev. D* **52** (1995) 4569–4587, [gr-qc/9505007](#).
- [70] M. Cvetič, G. W. Gibbons, D. Kubiznak, and C. N. Pope, “Black Hole Enthalpy and an Entropy Inequality for the Thermodynamic Volume,” *Phys. Rev. D* **84** (Dec., 2011) 024037, [1012.2888](#).
- [71] M. M. Caldarelli, G. Cognola, and D. Klemm, “Thermodynamics of Kerr-Newman-AdS Black Holes and Conformal Field Theories,” *Class. Quant. Grav.* **17** (2000) 399–420, [hep-th/9908022](#).
- [72] B. P. Dolan, “Pressure and volume in the first law of black hole thermodynamics,” *Class. Quant. Grav.* **28** (June, 2011) 235017, [1106.6260](#).
- [73] B. P. Dolan, “Compressibility of rotating black holes,” *Phys. Rev. D* **84** (Sept., 2011) 127503, [1109.0198](#).
- [74] B. P. Dolan, “The cosmological constant and the black hole equation of state,” *Class. Quant. Grav.* **28** (Aug., 2011) 125020, [1008.5023](#).

- [75] B. P. Dolan, “Where is the PdV term in the first law of black hole thermodynamics?,” [1209.1272](#).
- [76] A. Larranaga and S. Mojica, “Geometric Thermodynamics of Kerr-AdS black hole with a Cosmological Constant as State Variable,” *The Abraham Zelmanov Journal* **5** (Apr., 2012) 68–77, [1204.3696](#).
- [77] G. W. Gibbons, “What is the Shape of a Black Hole?,” *AIP Conf. Proc.* **1460** no. 1, (Jan., 2012) 90–100, [1201.2340](#).
- [78] D. Kubiznak and R. B. Mann, “P-V criticality of charged AdS black holes,” *JHEP* **033** (May, 2012) 1207, [1205.0559](#).
- [79] S. Gunasekaran, D. Kubiznak, and R. B. Mann, “Extended phase space thermodynamics for charged and rotating black holes and Born-Infeld vacuum polarization,” *JHEP* **2012** no. 11, (Aug., 2012), [1208.6251](#).
- [80] B. P. Dolan, D. Kastor, D. Kubiznak, R. B. Mann, and J. Traschen, “Thermodynamic Volumes and Isoperimetric Inequalities for de Sitter Black Holes,” *Phys. Rev. D* **87** (Jan., 2013) 104017, [1301.5926](#).
- [81] N. Altamirano, D. Kubiznak, and R. B. Mann, “Reentrant Phase Transitions in Rotating AdS Black Holes,” *Phys. Rev. D* **88** (June, 2013) 101502, [1306.5756](#).
- [82] D. Kubiznak and R. B. Mann, “Black Hole Chemistry,” *Can. J. Phys.* **93** no. 9, (Apr., 2014) 999–1002, [1404.2126](#).
- [83] R. A. Hennigar, D. Kubiznak, and R. B. Mann, “Super-Entropic Black Holes,” *Phys. Rev. Lett.* **115** (Nov., 2014) 031101, [1411.4309](#).
- [84] N. Altamirano, D. Kubiznak, R. B. Mann, and Z. Sherkatghanad, “Thermodynamics of rotating black holes and black rings: phase transitions and thermodynamic volume,” *Galaxies* **2** (Jan., 2014) 89–159, [1401.2586](#).
- [85] M. Henneaux and C. Teitelboim, “Asymptotically anti-de Sitter spaces,” *Communications in Mathematical Physics* **98** no. 3, (1985) 391–424.
- [86] T. Padmanabhan, “Emergent perspective of Gravity and Dark Energy,” *Research in Astronomy and Astrophysics* **12** no. 8, (July, 2012) 891, [1207.0505](#).
- [87] S. W. Hawking and D. N. Page, “Thermodynamics of black holes in anti-de Sitter space,” *Communications in Mathematical Physics* **87** (1983) 577–588.

- [88] M. Brigante, H. Liu, R. C. Myers, S. Shenker, and S. Yaida, “Viscosity Bound Violation in Higher Derivative Gravity,” *Phys. Rev. D* **77** (Dec., 2007) 126006, [0712.0805](#).
- [89] A. Buchel and R. C. Myers, “Causality of Holographic Hydrodynamics,” *JHEP* **09** no. 08, (June, 2009) 016, [0906.2922](#).
- [90] R. C. Myers and B. Robinson, “Black Holes in Quasi-topological Gravity,” *JHEP* **2010** (Mar., 2010) 1–35, [1003.5357](#).
- [91] J. Oliva and S. Ray, “A new cubic theory of gravity in five dimensions: Black hole, Birkhoff’s theorem and C-function,” *Class. Quant. Grav.* **27** (Mar., 2010) 225002, [1003.4773](#).
- [92] M. Ghanaatian and A. Bazrafshan, “Nonlinear Charged Black Holes in Anti-de Sitter Quasi-Topological Gravity,” *International Journal of Modern Physics D* **1350076** no. 13, (Apr., 2013), [1304.2311](#).
- [93] S. Kachru, X. Liu, and M. Mulligan, “Gravity Duals of Lifshitz-like Fixed Points,” *Phys. Rev. D* **78** (Aug., 2008) 106005, [0808.1725](#).
- [94] S. F. Ross and O. Saremi, “Holographic stress tensor for non-relativistic theories,” *JHEP* **0909** (July, 2009) 009, [0907.1846](#).
- [95] D. T. Son, “Toward an AdS/cold atoms correspondence: a geometric realization of the Schroedinger symmetry,” *Phys. Rev. D* **78** (Apr., 2008) 046003, [0804.3972](#).
- [96] C. Hagen, “Scale and conformal transformations in Galilean-covariant field theory,” *Phys. Rev. D* **5** no. 2, (1972) 377.
- [97] T. Mehen, I. W. Stewart, and M. B. Wise, “Conformal Invariance for Non-Relativistic Field Theory,” *Phys. Lett. B* **474** (2000) 145–152, [hep-th/9910025](#).
- [98] P. Hořava, “Quantum gravity at a Lifshitz point,” *Phys. Rev. D* **79** no. 8, (Apr., 2009), [2009](#).
- [99] D. T. Son and M. A. Stephanov, “Dynamic universality class of the QCD critical point,” *Phys. Rev. D* **70** (2004) 056001, [hep-ph/0401052](#).
- [100] S. Lubeck, “Universal scaling behavior of non-equilibrium phase transitions,” *Int. J. Mod. Phys. B* **18**, (2004) 3977, [cond-mat/0501259](#).

- [101] H. Hinrichsen, “Nonequilibrium Critical Phenomena and Phase Transitions into Absorbing States,” *Adv.Phys.* **49** (2000) 815–958, [cond-mat/0001070](#).
- [102] J. Hartong, E. Kiritsis, and N. A. Obers, “Lifshitz Space-Times for Schroedinger Holography,” *Phys. Lett. B* **746** (June, 2015) 318–324, [1409.1519](#).
- [103] J. Hartong, E. Kiritsis, and N. A. Obers, “Schroedinger Invariance from Lifshitz Isometries in Holography and Field Theory,” *Phys. Rev. D* **92** (Sept., 2014) 066003, [1409.1522](#).
- [104] M. Baggio, J. de Boer, and K. Holsheimer, “Hamilton-Jacobi Renormalization for Lifshitz Spacetime,” *JHEP* **58** (July, 2012) 01058, [1107.5562](#).
- [105] R. Mann and R. McNees, “Holographic Renormalization for Asymptotically Lifshitz Spacetimes,” *JHEP* **129** no. 10, (July, 2011), [1107.5792](#).
- [106] H.-S. Liu and H. Lu, “Thermodynamics of Lifshitz Black Holes,” *JHEP* **12** (Oct., 2014) 071, [1410.6181](#).
- [107] G. Bertoldi, B. A. Burrington, and A. Peet, “Black holes in asymptotically Lifshitz spacetimes with arbitrary critical exponent,” *Phys. Rev. D* **80** (Dec., 2009) 126003, [0905.3183](#).
- [108] M. H. Dehghani and R. B. Mann, “Lovelock-Lifshitz Black Holes,” *JHEP* **07** (Apr., 2010) 019, [1004.4397](#).
- [109] P. Berglund, J. Bhattacharyya, and D. Mattingly, “Charged Dilatonic AdS Black Branes in Arbitrary Dimensions,” *JHEP* **08** (July, 2012) 042, [1107.3096](#).
- [110] M. H. Dehghani and S. Asnafi, “Thermodynamics of Rotating Lovelock-Lifshitz Black Branes,” *Phys. Rev. D* **84** (July, 2011) 064038, [1107.3354](#).
- [111] M. H. Dehghani, C. Shakuri, and M. H. Vahidinia, “Lifshitz black brane thermodynamics in the presence of a nonlinear electromagnetic field,” *Phys. Rev. D* **87** (June, 2013) 084013, [1306.4501](#).
- [112] B. Way, “Holographic Confinement/Deconfinement Transitions in Asymptotically Lifshitz Spacetimes,” *Phys. Rev. D* **86** (July, 2012) 086007, [1207.4205](#).
- [113] P. Basu, J. Bhattacharya, S. Bhattacharyya, R. Loganayagam, S. Minwalla, and V. Umesh, “Small Hairy Black Holes in Global AdS Spacetime,” *JHEP* **2010** no. 10, (Mar., 2010), [1003.3232](#).

- [114] O. J. C. Dias, P. Figueras, S. Minwalla, P. Mitra, R. Monteiro, and J. E. Santos, “Hairy black holes and solitons in global AdS 5,” *JHEP* **2012** no. 8, (Dec., 2011), [1112.4447](#).
- [115] R. Mann, L. Pegoraro, and M. Oltean, “Lifshitz Solitons,” *Phys. Rev. D* **84** no. 12, (Sept., 2011) 124047, [1109.5044](#).
- [116] A. Komar, “Covariant conservation laws in general relativity,” *Phys. Rev.* **113** no. 3, (1959) 934.
- [117] A. Komar, “Positive-definite energy density and global consequences for general relativity,” *Phys. Rev.* **129** no. 4, (1963) 1873.
- [118] E. Poisson, *A Relativist’s Toolkit*. Cambridge University Press, 2004.
- [119] R. Arnowitt, S. Deser, and C. W. Misner, “Dynamical Structure and Definition of Energy in General Relativity,” *Phys. Rev.* **116** no. 5, (Dec., 1959) 1322–1330.
- [120] J. Katz, D. Lynden-Bell, and W. Israel, “Quasilocal energy in static gravitational fields,” *Class. Quant. Grav.* **5** no. 7, (1988) 971.
- [121] J. D. Brown and J. W. York, “Quasilocal energy and conserved charges derived from the gravitational action,” *Phys. Rev. D* **47** (Feb., 1993) 1407–1419.
- [122] V. Balasubramanian and P. Kraus, “A Stress Tensor for Anti-de Sitter Gravity,” *Commun. Math. Phys.* **208** (1999) 413–428, [hep-th/9902121](#).
- [123] S. Hollands, A. Ishibashi, and D. Marolf, “Comparison between various notions of conserved charges in asymptotically AdS-spacetimes,” *Class. Quant. Grav.* **22** (2005) 2881–2920, [hep-th/0503045](#).
- [124] S. Hollands, A. Ishibashi, and D. Marolf, “Counterterm charges generate bulk symmetries,” *Phys. Rev. D* **72** no. 10, (2005) 104025, [hep-th/0503105](#).
- [125] H. Lu, C. N. Pope, and Q. Wen, “Thermodynamics of AdS Black Holes in Einstein-Scalar Gravity,” *JHEP* **1503** (Aug., 2014) 165, [1408.1514](#).
- [126] H.-S. Liu, H. Lu, and C. N. Pope, “Thermodynamics of Einstein-Proca AdS Black Holes,” *JHEP* **06** (Feb., 2014) 109, [1402.5153](#).
- [127] P. Kraus, F. Larsen, and R. Siebelink, “The Gravitational Action in Asymptotically AdS and Flat Spacetimes,” *Nucl. Phys. B* **563** (1999) 259–278, [hep-th/9906127](#).

- [128] R. B. Mann, “Misner String Entropy,” *Phys. Rev. D* **60** (1999) 104047, [hep-th/9903229](#).
- [129] R. Emparan, C. V. Johnson, and R. C. Myers, “Surface Terms as Counterterms in the AdS/CFT Correspondence,” *Phys. Rev. D* **60** (1999) 104001, [hep-th/9903238](#).
- [130] O. Hohm and E. Tonni, “A boundary stress tensor for higher-derivative gravity in AdS and Lifshitz backgrounds,” *JHEP* **93** no. 4, (Jan., 2010), [1001.3598](#).
- [131] R. B. Mann, “Lifshitz Topological Black Holes,” *JHEP* **0906** (May, 2009) 075, [0905.1136](#).
- [132] G. T. Horowitz, “Exactly soluble diffeomorphism invariant theories,” *Comm. Math. Phys.* **125** no. 3, (1989) 417–437. <http://projecteuclid.org/euclid.cmp/1104179527>.
- [133] R. B. Mann, “Black Holes of Negative Mass,” *Class. Quant. Grav.* **14** (1997) 2927–2930, [gr-qc/9705007](#).
- [134] S. Åminneborg, I. Bengtsson, S. Holst, and P. Peldan, “Making anti-de Sitter black holes,” *Class. Quant. Grav.* **13** no. 10, (1996) 2707.
- [135] J. Tarrío and S. Vandoren, “Black holes and black branes in Lifshitz spacetimes,” *JHEP* **1109** (May, 2011) 017, [1105.6335](#).
- [136] E. J. Brynjolfsson, U. H. Danielsson, L. Thorlacius, and T. Zingg, “Holographic Superconductors with Lifshitz Scaling,” *J. Phys. A* **43** (Aug., 2010) 065401, [0908.2611](#).
- [137] E. Ayon-Beato, A. Garbarz, G. Giribet, and M. Hassaine, “Analytic Lifshitz black holes in higher dimensions,” *JHEP* **30** no. 4, (Jan., 2010), [1001.2361](#).
- [138] Y. Gim, W. Kim, and S.-H. Yi, “The first law of thermodynamics in Lifshitz black holes revisited,” *JHEP* **07** (Mar., 2014) 002, [1403.4704](#).
- [139] E. Ayon-Beato, A. Garbarz, G. Giribet, and M. Hassaine, “Lifshitz Black Hole in Three Dimensions,” *Phys. Rev. D* **80** no. 104029, (Sept., 2009), [0909.1347](#).
- [140] D.-W. Pang, “On Charged Lifshitz Black Holes,” *JHEP* **2010** no. 1, (Nov., 2010) 1–20, [0911.2777](#).

- [141] Musgrave, P and Polleney, D and Lake, K, *GRTensor Version 1.79 (R4)*. Queens University, 1994.
- [142] G. Dotti, J. Oliva, and R. Troncoso, “Exact solutions for the Einstein-Gauss-Bonnet theory in five dimensions: Black holes, wormholes and spacetime horns,” *Phys. Rev. D* **76** no. 064038, (June, 2007), [0706.1830](#).
- [143] U. Ascher, R. Mattheij, and R. Russell, *Numerical Solution of Boundary Value Problems for Ordinary Differential Equations*. Classics in applied mathematics. Society for Industrial and Applied Mathematics (SIAM, 3600 Market Street, Floor 6, Philadelphia, PA 19104), 1988.
<https://books.google.ca/books?id=0Rv0rn04WgwC>.
- [144] M. H. Dehghani, R. Pourhasan, and R. B. Mann, “Charged Lifshitz Black Holes,” *Phys. Rev. D* **84** (Feb., 2011) 046002, [1102.0578](#).
- [145] R. B. Mann and R. Pourhasan, “Gauss-Bonnet Black Holes and Heavy Fermion Metals,” *JHEP* **1109** (May, 2011) 062, [1105.0389](#).
- [146] U. H. Danielsson and L. Thorlacius, “Black holes in asymptotically Lifshitz spacetime,” *JHEP* **0903** (Dec., 2009) 070, [0812.5088](#).
- [147] K. G. Wilson, “The renormalization group: Critical phenomena and the Kondo problem,” *Rev. Mod. Phys.* **47** no. 4, (Oct., 1975) 773–840.
- [148] Y. Deng and H. W. J. Blöte, “Simultaneous analysis of several models in the three-dimensional Ising universality class,” *Phys. Rev. E* **68** no. 3, (Sept., 2003).
- [149] N. Goldenfeld, *Lectures on Phase Transitions and the Renormalization Group*. Frontiers in physics. Addison-Wesley, Advanced Book Program, 1992.
https://books.google.ca/books?id=DdB1__n17CYC.
- [150] J. D. Van der Waals, *Over de Continuïteit van den Gas-en Vloeistofoestand*. PhD thesis, Leiden University, 1873.
- [151] D. C. Johnston, “Thermodynamic Properties of the van der Waals Fluid,” [1402.1205](#).
- [152] D. C. Johnston, *Advances in Thermodynamics of the van der Waals Fluid*. 2053-2571. Morgan & Claypool Publishers, 2014.

- [153] A. Chamblin, R. Emparan, C. V. Johnson, and R. C. Myers, “Holography, Thermodynamics and Fluctuations of Charged AdS Black Holes,” *Phys. Rev. D* **60** (1999) 104026, [hep-th/9904197](https://arxiv.org/abs/hep-th/9904197).
- [154] A. Chamblin, R. Emparan, C. V. Johnson, and R. C. Myers, “Charged AdS Black Holes and Catastrophic Holography,” *Phys. Rev. D* **60** (1999) 064018, [hep-th/9902170](https://arxiv.org/abs/hep-th/9902170).
- [155] G. Baker and P. Graves-Morris, *Padé Approximants: Basic theory*. Encyclopedia of mathematics and its applications. Addison-Wesley Pub. Co., 1981. <https://books.google.ca/books?id=EP4oAQAAAJ>.
- [156] G. Baker and P. Graves-Morris, *Padé Approximants: Extensions and applications*. No. v. 2 in Advanced book program. Addison-Wesley Publishing Company, 1981. https://books.google.ca/books?id=_F8VTS-noGwC.
- [157] K. Levenberg, “A method for the solution of certain non-linear problems in least squares,”.
- [158] D. W. Marquardt, “An algorithm for least-squares estimation of nonlinear parameters,” *Journal of the society for Industrial and Applied Mathematics* **11** no. 2, (1963) 431–441.
- [159] G. Seber and C. Wild, *Nonlinear Regression*. Wiley Series in Probability and Statistics. Wiley, 2003. https://books.google.ca/books?id=YBYlCpBNo_cC.
- [160] A. M. Frassino, D. Kubiznak, R. B. Mann, and F. Simovic, “Multiple Reentrant Phase Transitions and Triple Points in Lovelock Thermodynamics,” *JHEP* **09** (June, 2014) 080, [1406.7015](https://arxiv.org/abs/1406.7015).
- [161] B. P. Dolan, A. Kostouki, D. Kubiznak, and R. B. Mann, “Isolated critical point from Lovelock gravity,” *Class. Quant. Grav.* **31** no. 24, (July, 2014) 242001, [1407.4783](https://arxiv.org/abs/1407.4783).
- [162] J. Hauser, *Numerical Methods for Nonlinear Engineering Models*. Springer Netherlands, 2009. <https://books.google.ca/books?id=rdJvXG1k3HsC>.
- [163] G. A. Baker and J. M. Kincaid, “The continuous-spin Ising model, $g_0 : \phi^4 :_d$ field theory, and the renormalization group,” *J. Stat. Phys.* **24** no. 3, (Mar., 1981) 469–528.

Appendices

Appendix A

Obtaining the Einstein Field Equations

Substituting a metric function ansatz before functional variation of the action to obtain field equations is a technique to simplify Einstein's Field Equations for a theory in which the metric is restricted to obey certain symmetries. In some cases this method obtains a simpler set of coupled differential equations than substituting the form of the metric into the general Einstein Field Equations [28]

$$R_{\mu\nu} - \frac{1}{2}Rg_{\mu\nu} + \Lambda g_{\mu\nu} = 8\pi T_{\mu\nu} \quad (\text{A.1})$$

where the stress-energy-momentum tensor needs to be computed from the matter part of the action as

$$T_{\mu\nu} = -\frac{1}{8\pi\sqrt{-g}} \frac{\delta S_M}{\delta g^{\mu\nu}} \quad (\text{A.2})$$

where S_M is the matter part of the action, and g is the determinant of the metric tensor.

Our approach, made straightforward through computerized algebra software, will be to:

- compute the Ricci tensor and metric determinant for a specific form of the metric; here we will always assume static, spherically symmetric solutions so all dynamical functions will be functions of the radial coordinate only
- perform integration by parts in order to obtain the lowest-order differential equations possible
- propose an ansatz for the matter fields in terms of dynamical functions

- perform a functional variation of the expanded action in terms of the dynamical functions named above
- set these equations equal to zero and simplify; these are the Einstein Field Equations, constrained to the form for our particular metric

The functional variation and integration by parts go a little beyond the capability of most built-in CAS routines, so in [C.1](#) I provide a set of Maple packages which will do this task.

The snippet of code below will show these packages in practise. Here we find the field equations for third-order asymptotically Lifshitz quasitopological gravity in five dimensions, with a Maxwell field, with just a few Maple commands and the GRTensor package [141]. This method is simple to use for the reduction of a wide variety of algebraically lengthy actions to a set of differential equations when they are constrained by the metric (for example, to spherical symmetry).

Suppose we begin with the action after being constrained to the desired metric form;

```
grdef('action:=sqrt(-detg)*(-2*Lambda+RicciScalar+lambda/(dd-3)/(dd-4)*L2
-mu/(dd-3)/(dd-6)*L3 - 1/4*Fa{a b}*Fa^{a ^b} - 1/4*Ha{a b}*Ha^{a ^b}
- 1/2*m^2*B{a}*B^{a})');
actionInsideIntegral:=grcomponent(action);
```

This command has approximately fifteen lines of output (which I will not show here).

We can directly obtain the field equations with the commands

```
physicsdiff(actionInsideIntegral,h(r),r):ibp(%,2,r):
feqHr:=simplify(simplify(expand(simplify(
  subs(phi=Pi/2,theta=Pi/2/sqrt(k),%*(k)),size)),size))
assuming k>0, r>0, L>0, z>0;
physicsdiff(actionInsideIntegral,f(r),r):ibp(%,2,r):
feqFr:=simplify(simplify(expand(simplify(
  subs(phi=Pi/2,theta=Pi/2/sqrt(k),%*(k)),size)),size))
assuming k>0, r>0, L>0, z>0;
physicsdiff(actionInsideIntegral,kappa(r),r):ibp(%,2,r):
feqKr:=simplify(simplify(
  expand(simplify(subs(phi=Pi/2,theta=Pi/2/sqrt(k),%*(k)),size)),size))
assuming k>0, r>0, L>0, z>0;
physicsdiff(actionInsideIntegral,g(r),r):ibp(%,2,r):
feqGr:=simplify(simplify(
```

```

expand(simplify(subs(phi=Pi/2,theta=Pi/2/sqrt(k),%*(k)),size),size))
assuming k>0, r>0, L>0, z>0;

```

We can illustrate this method by focusing on the field equation for $f(r)$, given by `feqFr`. To obtain this quantity, the first command performs a functional variation of the action with respect to $f(r)$, and the second performs the necessary integration by parts (with respect to the dynamical variable r) to eliminate any second order derivatives in the expression. In order to obtain a field equation that agrees with the form (2.65), we evaluate the angular components at specific values (they can be grouped out of the expression because we have spherical symmetry, and then integrated over even though we didn't perform this part of the integral in the action, so they do not contribute to the equations of motion).

The equation obtained through this method yields the output

$$\begin{aligned}
\text{feqFr} := & -\frac{1}{16} \frac{1}{f(r)g(r)\sqrt{\frac{f(r)}{g(r)}}} \left(\left(72r^7 f(r) \left(\frac{d}{dr} g(r) \right) g^2(r) \mu - 48r^7 f(r) \left(\frac{d}{dr} g(r) \right) L^2 g(r) \lambda \right. \right. \\
& - 144r^5 f(r) \left(\frac{d}{dr} g(r) \right) L^2 g(r) \mu k + 48r^5 f(r) \left(\frac{d}{dr} g(r) \right) L^4 k \lambda + 24r^7 f(r) \left(\frac{d}{dr} g(r) \right) L^4 \\
& + 72r^3 f(r) \left(\frac{d}{dr} g(r) \right) L^4 k^2 \mu + 4r^8 L^4 g(r) \left(\frac{d}{dr} \kappa(r) \right)^2 + 8r^7 L^4 g(r) z \kappa(r) \left(\frac{d}{dr} \kappa(r) \right) \\
& + 4r^8 L^4 g(r) q^2 \left(\frac{d}{dr} h(r) \right)^2 + 8r^7 L^4 g(r) q^2 z h(r) \left(\frac{d}{dr} h(r) \right) + 96f(r)r^6 g^3(r) \mu \\
& - 96f(r)L^2 r^6 g^2(r) \lambda - 144f(r)L^2 r^4 g^2(r) \mu k + 96f(r)L^4 r^6 g(r) + 96f(r)L^4 r^4 g(r) k \lambda \\
& + 16f(r)L^6 \Lambda r^6 - 48f(r)L^6 r^4 k + 48f(r)L^6 k^3 \mu + 4L^4 r^6 z^2 g(r) q^2 h^2(r) \\
& \left. \left. + 4L^4 r^6 z^2 g(r) \kappa^2(r) + 4L^6 r^6 m^2 q^2 h^2(r) \right) r^{z-4} L^{-z-5} \right)
\end{aligned}$$

Evidence that this expression matches results derived by hand can be seen through some simple substitutions. For example, when $f(r) = g(r) = 1$ and $\kappa(r) = 0, k = 0, q = 0$, we expect a solution that is AdS (we have evaluated the asymptotic behaviour when $q = 0$, i.e., there is no Proca field). The terms corresponding to the Maxwell field κ have a faster falloff, along with those corresponding to k , so we set those to zero as well. This yields

$$-(6\mu - 6L^2\lambda + 6L^4 + L^6\Lambda) r^{z+2} L^{-z-5}$$

which has the solution

$$-6 \frac{\mu - L^2\lambda + L^4}{L^6}$$

Since this field equation used the definition of μ from [2], as well as the higher curvature terms being left dimensional, this is equivalent to (2.81) in the notation of this thesis.

Similar simplifications can be performed on these general field equations to show agreement with other works (at least with cubic quasitopological terms, this method has been extensively tested, c.f. [4, 5, 144, 145]).

These field equations can then be solved asymptotically for the completely general conditions on Λ , q , and m , and then they can be brought into a near-horizon series or a first order ODE form by using the procedures described in section 3.5.

Appendix B

Nonlinear Regression

We desire the minimization of the function

$$S(\vec{\theta}^*) = \sum_{i=1}^N (y_i - f(x_i, \vec{\theta}^*))^2 \quad (\text{B.1})$$

in the context of a linear least squares problem for some guess of parameters $\vec{\theta}^*$. Since the problem is assumed to be linear in the coefficients $\vec{\theta}$, perform a series expansion of

$$y_i = f(x_i, \vec{\theta}) = f(x_i, \vec{\theta}^*) + (\theta_j - \theta_j^*) \left(\frac{\partial}{\partial \theta_j} f(x_i, \vec{\theta}) \right)_{\theta_j = \theta_j^*} \quad (\text{B.2})$$

Here, the Jacobian for the function f is defined

$$\mathbf{F} = \begin{pmatrix} \left(\frac{\partial f(x_1, \vec{\theta})}{\partial \theta_1} \right)_{\vec{\theta} = \vec{\theta}^*} & \left(\frac{\partial f(x_1, \vec{\theta})}{\partial \theta_2} \right)_{\vec{\theta} = \vec{\theta}^*} & \cdots & \left(\frac{\partial f(x_1, \vec{\theta})}{\partial \theta_J} \right)_{\vec{\theta} = \vec{\theta}^*} \\ \left(\frac{\partial f(x_2, \vec{\theta})}{\partial \theta_1} \right)_{\vec{\theta} = \vec{\theta}^*} & \left(\frac{\partial f(x_2, \vec{\theta})}{\partial \theta_2} \right)_{\vec{\theta} = \vec{\theta}^*} & \cdots & \left(\frac{\partial f(x_2, \vec{\theta})}{\partial \theta_J} \right)_{\vec{\theta} = \vec{\theta}^*} \\ \vdots & \vdots & \ddots & \vdots \\ \left(\frac{\partial f(x_N, \vec{\theta})}{\partial \theta_1} \right)_{\vec{\theta} = \vec{\theta}^*} & \left(\frac{\partial f(x_N, \vec{\theta})}{\partial \theta_2} \right)_{\vec{\theta} = \vec{\theta}^*} & \cdots & \left(\frac{\partial f(x_N, \vec{\theta})}{\partial \theta_J} \right)_{\vec{\theta} = \vec{\theta}^*} \end{pmatrix} \quad (\text{B.3})$$

and so the equation (B.2) can be represented as

$$\vec{\epsilon} = \mathbf{F} (\vec{\theta} - \vec{\theta}^*) \quad (\text{B.4})$$

where $\vec{\epsilon} \equiv \vec{y} - \vec{f}(\vec{\theta}^*)$. It is important to realize that in the linear case the Jacobian takes the same values no matter where it is evaluated, but in the nonlinear case we make the

approximation that the Jacobian does not change (while recomputing it at each iteration) in the linearization of the system.

To account for errors in the data (or nonlinear functions f), we need to additionally impose minimization of (B.1), which means

$$\frac{\partial S(\vec{\theta})}{\partial \theta_j} = 0 \quad \rightarrow \quad 2(-\mathbf{F}^\top)(\vec{y} - \vec{f}(\vec{\theta})) = 0 \quad (\text{B.5})$$

and since

$$(\vec{y} - \vec{f}(\vec{\theta})) = \vec{\epsilon} + (\vec{f}(\vec{\theta}^*) - \vec{f}(\vec{\theta})) = \vec{\epsilon} - \mathbf{F}(\vec{\theta} - \vec{\theta}^*) \quad (\text{B.6})$$

we can obtain the equation obeyed by linear least squares as well as the iterative Gauss-Newton method by seeing that (B.4) satisfies the equation from substituting (B.6) into (B.5):

$$(\mathbf{F}^\top \mathbf{F})^{-1} \mathbf{F}^\top \vec{\epsilon} = \vec{\theta} - \vec{\theta}^* \quad (\text{B.7})$$

which is the basis for the iteration in the Gauss-Newton method.

The gradient method, instead of linearizing the function f , takes the approach of approximately solving (B.5) by minimizing \mathbf{f}^\top at each step, using a gradient descent

$$\vec{\theta} = \vec{\theta}^* - \boldsymbol{\eta} \mathbf{F}^\top \quad (\text{B.8})$$

which has strong guarantees on convergence for many problems when the matrix $\boldsymbol{\eta}$ is correctly determined at each step (with a line search approach), but the actual speed of convergence can be very slow since the line of descent can wind around the minimum, or when the model function is very flat around the minimum (having small derivatives).

Appendix C

Code

The following features some code snippets and complete routines for the work of this thesis.

C.1 Maple Packages

The first package is called with the command `physicsdiff(expression, f(r), r)` which will perform a functional differentiation of `expression` with respect to the function `f(r)`. It is able to handle derivatives with respect to `f(r)` through an integration by parts followed by a differentiation.

```
#This maple procedure does a functional variation, much like diff does when used
#with(Physics):, but with the added feature that it can vary simple derivatives
#with respect to that function, ie. vary(c*diff(f(r),r)^2,f(r)) using
#integration by parts.
global MAXIMUM_NUMBER_OF_DERIVATIVES := 10;

_physicsdiff_term := proc(expr,function,term,dparam)
  local counter,counter2,tmp,retterm,_physicsdiff_innervar;
  retterm := 0;

  if is(op(0,dparam)='list') then
    for counter from 1 to nops(dparam) do
      for counter2 from 1 to MAXIMUM_NUMBER_OF_DERIVATIVES do
        tmp := subs(diff(function,dparam[counter]$counter2)=_physicsdiff_innervar(dparam[
          ↵ counter]),term);
```

```

        retterm := retterm + (-1)^(counter2)*diff(subs(_physicsdiff_innervar(dparam[
        ↪ counter]) =
        diff(function,dparam[counter]$counter2),Physics:-diff(tmp, ↪
        ↪ _physicsdiff_innervar(dparam[counter]))),dparam[counter]$counter2);
    end do:
end do:
RETURN(retterm);
else
for counter2 from 1 to MAXIMUM_NUMBER_OF_DERIVATIVES do
    tmp := subs(diff(function,dparam$counter2)=_physicsdiff_innervar(dparam),term);
    retterm := retterm + (-1)^(counter2)*diff(subs(_physicsdiff_innervar(dparam) =
        diff(function,dparam$counter2),Physics:-diff(tmp,_physicsdiff_innervar(dparam)) ↪
        ↪ ),dparam$counter2);
    end do:
RETURN(retterm);
fi:

end proc:

physicsdiff := proc(expr,function,dparam)
    local expr2,newexpr,exprlength,term,tmp,counter;
    description "This Maple procedure will perform a physicists' functional differentiation, ↪
        ↪ neglecting boundary terms and integrating by parts to functionally vary an ↪
        ↪ expression with respect to a function, even if it contains powers of first ↪
        ↪ derivatives of that function. Written by W. Brenna, Sept 3 2012. Version 0.3.";

    if not(is(op(0,f(r)*g(r))='*')) then
        print("Error: Conflicting package detected! The '*' declaration has been redefined and ↪
            ↪ results are therefore unreliable. Make sure you have loaded physicsdiff before ↪
            ↪ running with(Physics).");
        RETURN(expr);
    fi:
    if assigned(makeg) then
        print("Error: Conflicting package detected! GRTensor overwrites a number of variables ↪
            ↪ that can cause physicsdiff to perform in unstable ways. Please use physicsdiff ↪
            ↪ before running grtw().");
        RETURN(expr);
    fi:

    expr2 := expand(expr);

```

```

exprlength := nops(expr2);
newexpr := 0;

if is(op(0,expr2)='+') then
  for counter from 1 to exprlength do
    term := op(counter,expr2);
#This just does the first order integration by parts.
    newexpr := newexpr + _physicsdiff_term(newexpr,function,term,dparam):
  end do:
else
  term := expr2;
  newexpr := newexpr + _physicsdiff_term(newexpr,function,term,dparam):
fi:

#Finally, we do the regular differentiation by parts to build up the final
#terms.
RETURN(newexpr + Physics:-diff(expr2,function));

end proc:

```

This second package performs integration by parts, neglecting boundary terms. It is called with `ibp(expression, 2, r, [f(r), g(r)]` and will integrate expression by parts to remove all derivatives of power 2, where the functions $f(r)$, $g(r)$ are the ones whose second order derivatives will be integrated out.

```

#This maple procedure will integrate an algebraic function by parts, neglecting
#boundary terms

#First, the helper procedures
_ibp_solveqn := proc(outexpr,oldterm,ibpcoeff,derivterm,dparam)
  local newterm, counter, myinteger;
#outexpr is the full expression that is returned by this procedure.
#oldterm is the original term that we are integrating by parts
#ibpcoeff is the coefficient which we treat as V in VdU
#derivterm is the term to integrate out...it needs to be in the form
  #diff(f(x),x$N)
#where n is some integer!
  newterm := expand(diff(ibpcoeff,dparam)*op(1,derivterm));
  if is(op(0,newterm) = '+') then
    for counter from 1 to nops(newterm) do:

```



```

        if is(op(counter,newterm)/oldterm,real) then
#If there exists a term in the IBP expansion equal to the original term up to a constant,
#solve the equation to get a closed-form solution for oldterm.
        myinteger := op(counter,newterm)/oldterm;
        newterm := ( newterm - myinteger*oldterm)/(1+myinteger);
        break;
    fi;
end do;
fi;
RETURN(outexpr - oldterm - newterm);
end proc:

```

```

_ibp_specifiedfn := proc(functions,newexpr,term,dparam,power,tryhard)
    local function, j, localexpr,exitparam, tmp, thecoeff, derivterm;
    exitparam := false;
    localexpr:=newexpr;
    for function in functions do
        if (has(term,diff(function,dparam $ power)) and
            not(has(term,diff(function,dparam $ power+1))) ) then
            if is(op(0,term)='*') then
                for j from 1 to nops(term) do
                    tmp := op(j,term);
                    if (has(tmp,diff(function,dparam $ power)) and
                        not(has(tmp,diff(function,dparam $ power+1))) )
                        then
                            if is(op(0,tmp) = '^') then
                                thecoeff := coeff(term,diff(function,dparam $ power)^op(2,tmp))*diff(↵
                                    ↵ function,dparam $ power)^(op(2,tmp)-1);
                                if is(tryhard=false) then
                                    exitparam := true;
                                fi;
                                break;
                            elif is(op(0,tmp) = 'diff') then
                                thecoeff := coeff(term,diff(function,dparam $ power));
                                break;
                            else
                                print("Error - could not determine power of term.");
                                RETURN(localexpr);
                            fi;
                        fi;
                    fi;
                fi;
            fi;
        fi;
    fi;
end proc:

```

```

        fi:
    end do:
    if is(exitparam = true) then
        break;
    else
        derivterm :=term/thecoeff;
        localexpr := _ibp_solveeqn(localexpr,term,thecoeff,derivterm,dparam);
        break;
    fi:
else
#Do nothing - this is a lone term!
#Unless it is a power of derivatives!
#In this case we can get a higher power derivative, (if we tryhard)
    if(op(0,term)='^') then
        tmp := op(1,term);
        if is(op(0,tmp) = 'diff') then
            if ((tryhard)) then
                thecoeff := tmp^(op(2,term)-1);
                derivterm :=term/thecoeff;
                localexpr := _ibp_solveeqn(localexpr,term,thecoeff,derivterm,dparam);
            else
                RETURN(localexpr);
            fi:
        else
            print("Error - could not parse the term",term,".");
            RETURN(localexpr);
        fi:
    fi:
fi:
fi:
end do:
RETURN(localexpr);
end proc:

```

```

ibp := proc(expr,power,dparam,functions:=[],tryhard:=false)
    local expr2,newexpr,exprlength,termlength,term,thecoeff,i,j,tmp,counter,derivterm;
    description "This utility integrates an expression by parts, picking out the terms of ↵
        ↵ power \'power\' and differentiating with respect to the other terms. Boundary ↵

```

↳ terms are always neglected. Arguments are: the expression, the power of derivative
 ↳ you wish to lower, the variable with respect to which you differentiate, a list
 ↳ of the functions which possess the higher derivatives which you wish to integrate
 ↳ (optional), and a boolean determining whether we integrate expressions inside of
 ↳ powers or not (optional - default no). If you do not specify the final option, I
 ↳ will assume you want to integrate all function that have a derivative of order
 ↳ power\'. Written by W. Brenna, Aug 14 2012. Version 0.5 - modified January 27,
 ↳ 2013.";

```
expr2 := expand(expr);
exprlength := nops(expr2);
```

```
newexpr := expr2;
```

```
#Make sure we have a reasonable power.
```

```
if not(power > 0 and is(power,integer)) then
  print("Error! Currently fractional or negative powers are unsupported.");
  RETURN(expr2);
fi:
```

```
if not(is(functions=[])) then
  if is(op(0,expr2)='+') then
    for i from 1 to exprlength do
      term := op(i,expr2);
      newexpr := _ibp_specifiedfn(functions,newexpr,term,dparam,power,tryhard):
    end do:
  else
    term := expr2;
    newexpr := _ibp_specifiedfn(functions,newexpr,term,dparam,power,tryhard):
  fi:
else
```

```
#populate the list of functions to be "all functions", if none were specified
```

```
if is(op(0,expr2) = '+') then
  for i from 1 to exprlength do
    term := op(i,expr2);
    termlength := nops(term);
    for j from 1 to termlength do
      if is(op(0,op(j,term)) = diff) then
        if is(op(2,op(j,term)) = dparam) then
```

```

tmp := op(j,term);
for counter from 1 to power+1 while is(op(0,tmp) = diff) do
  tmp := op(1,tmp);
  if is(counter = power) then
    if is(op(0,tmp) = diff) then
      print("Warning: you have a derivative higher than the power you ↵
        ↵ specified. It was ignored.");
    else
#bonus code to perform infinite integration by parts!
      thecoeff := coeff(term, op(j,term));
      derivterm := term/thecoeff;
      newexpr :=
        _ibp_solveeqn(newexpr,term,thecoeff,derivterm,dparam);
    fi:
    fi:
  end do:
  fi:
  end do:
end do:
elif is(op(0,expr2) = '^') then
#This is a lone term.
  print("This is a lone term. You need to specify tryhard=true and explicitly give ↵
    ↵ functions in order to solve this.");
else
  term := expr2;
  termlength := nops(term);
  for j from 1 to termlength do
    if is(op(0,op(j,term)) = diff) then
      if is(op(2,op(j,term)) = dparam) then
        tmp := op(j,term);
        for counter from 1 to power+1 while is(op(0,tmp) = diff) do
          tmp := op(1,tmp);
          if is(counter = power) then
            if is(op(0,tmp) = diff) then
              print("Warning: you have a derivative higher than the power you ↵
                ↵ specified. It was ignored.");
            else
              thecoeff := coeff(term, op(j,term));

```

```

        derivterm := term/thecoeff;
        newexpr :=
            _ibp_solveeqn(newexpr,term,thecoeff,derivterm,dparam);
    fi :
    fi :
end do:
fi :
fi :
end do:
fi :
fi :
RETURN(simplify(newexpr,size));
end:

```

C.2 Lifshitz Quasitopological Thermodynamics

This program, given a set of first order differential equations (the spherically symmetric field equations) and near-horizon expansions, will perform a shooting method to numerically yield the metric functions of the black hole. This is repeated for a range of horizon radii, and for each horizon radius the temperature and entropy of the black hole is computed.

The series expansion of the metric functions must be provided in a save file `seriesexpansion-5d.m`, where the variables defined in this file are `fs3`, `gs3`, `hs3` corresponding to the third order series expansions of $f(r)$, $g(r)$, $h(r)$ near the horizon r_0 .

The set of first order ODEs must be given in `firstorderodes-5d.m` using the variable names `DFR`, `DGR`, `DHR`, which respectively correspond to the right hand side of the ODEs $df(r)/dr = \dots$, $dg(r)/dr = \dots$, $dh(r)/dr = \dots$.

The remaining input is specified within the routine itself, allowing customization of values of z , r_h , l , higher curvature parameters, horizon topologies, and so on. This can be easily wrapped into more complicated routines, allowing one to probe a wide range of parameters space.

Output is saved as a text file in the `data/` subdirectory, with one file for each range of horizon radii considered. The files can be straightforwardly concatenated over a range of lengthscales to allow for a substantial dataset, which I use to render visualizations of the black hole thermodynamics.

```

restart;

Digits:=350:
kernelopts(printbytes=false):

#First we can load in the series solutions and the differential equations
read 'seriesexpansion-5d.m';
read 'firstorderodes-5d.m';
#These give us fs3,hs3,gs3 and DFR,DGR,DJR, respectively

#Enter the number of dimensions here, for computing the area and entropy:
#If you change this value, you must also change cosmConst's expression and ensure the ↵
    ↵ series expansion and odes are also fixed!
nDims:=5;
cosmConst:=- (1/16)*(-48*MU*ZZ - 32*LL^2*LAMBDA*ZZ + 8*LL^4*ZZ^2 - 48*LL^2*LAMBDA - 24*MU*ZZ ↵
    ↵ ^2 - 16*LAMBDA*ZZ^2*LL^2 + 16*LL^4*ZZ - 24*MU + 72*LL^4)/LL^6;

# We need the working series solution to perform this type of solution (and it has to be ↵
    ↵ first order).
with(plots):
ZZ:=2:MU:=-.0003:LAMBDA:=.04:QQ:=0.0:LL:=2.00:
large_R0:=1e35:K_init:=1:K_final:=1:
g_fact:=1.0:f_fact:=1.0:h_fact:=1.0:
large_radius:=0.45:res:=0.001:
small_radius:=0.020101:initial_point_scale:=1.000015:
mffun:=100000:

#####
#Code follows:
#####
set_lambda:=LAMBDA:set_ZZ:=ZZ:muparamresscale:=MU:KK:=0:
small_radius_save := small_radius:

init_time:=time():
print(init_time);

for set_KK from K_init to K_final do

    printcounter:=1:oldprintcounter:=50:

```

```

small_radius := small_radius_save:

whileFlag := true;
for obj_radius from small_radius by res while whileFlag do
  h_seed:=1/(obj_radius)/.38/4:f_seed:=h_seed*4/3:
  dd:=initial_point_scale:R0:=obj_radius:H1:=h_seed:F1:=f_seed:KK:=set_KK:ZZ:=set_ZZ:MU:=↵
    ↵ muparamresscale:LAMBDA:=set_lambda:
  icp := {g(R0*dd)=g_fact*subs(L=LL,Q=QQ,r0=R0,h1=H1,f1=F1,k=KK,mu=MU,lambda=LAMBDA,r=R0*↵
    ↵ dd,z=ZZ,gs3),
    f(R0*dd)=f_fact*subs(L=LL,Q=QQ,r0=R0,h1=H1,f1=F1,k=KK,mu=MU,lambda=LAMBDA,r=R0*dd,z=↵
    ↵ ZZ,fs3),
    h(R0*dd)=h_fact*subs(L=LL,Q=QQ,r0=R0,h1=H1,f1=F1,k=KK,mu=MU,lambda=LAMBDA,r=R0*dd,z=↵
    ↵ ZZ,hs3),
    j(R0*dd)=subs(L=LL,r0=R0,Q=QQ,h1=H1,f1=F1,k=KK,mu=MU,lambda=LAMBDA,r=R0*dd,z=ZZ,diff↵
    ↵ (hs3,r))}:
  diffequations := {diff(g(r),r)=subs(L=LL,Q=QQ,k=KK,mu=MU,lambda=LAMBDA,z=ZZ,DGR),
    diff(f(r),r)=subs(L=LL,Q=QQ,k=KK,mu=MU,lambda=LAMBDA,z=ZZ,DFR),
    diff(j(r),r)=subs(L=LL,Q=QQ,k=KK,mu=MU,lambda=LAMBDA,z=ZZ,DJR),
    diff(h(r),r)=j(r)}:
  diffsoln := dsolve(diffequations union icp,numeric,output=listprocedure,maxfun=mffun):
  dph:=subs(diffsoln,h(r)):dpf:=subs(diffsoln,f(r)):dpg:=subs(diffsoln,g(r)):dpj:=subs(↵
    ↵ diffsoln,j(r)):
  try:
    tmp1:=dpf(large_R0*R0);tmp2:=dph(large_R0*R0);
  catch:
    small_radius := obj_radius + res;
    large_radius := large_radius + res;
    print("Increasing small_radius...");
    print(small_radius);
    next;
  end try;

  dd:=initial_point_scale:R0:=obj_radius:H1:=h_seed:F1:=f_seed/tmp1:KK:=set_KK:ZZ:=set_ZZ↵
    ↵ :MU:=muparamresscale:
  icp := {g(R0*dd)=g_fact*subs(L=LL,Q=QQ,r0=R0,h1=H1,f1=F1,k=KK,mu=MU,lambda=LAMBDA,r=R0*↵
    ↵ dd,z=ZZ,gs3),
    f(R0*dd)=f_fact*subs(L=LL,Q=QQ,r0=R0,h1=H1,f1=F1,k=KK,mu=MU,lambda=LAMBDA,r=R0*dd,z=↵
    ↵ ZZ,fs3),
    h(R0*dd)=h_fact*subs(L=LL,Q=QQ,r0=R0,h1=H1,f1=F1,k=KK,mu=MU,lambda=LAMBDA,r=R0*dd,z=↵
    ↵ ZZ,hs3),

```

```

j(R0*dd)=subs(L=1,r0=R0,Q=QQ,h1=H1,f1=F1,k=KK,mu=MU,lambda=LAMBDA,r=R0*dd,z=ZZ,diff(↵
↵ hs3,r)):
diffequations := {diff(g(r),r)=subs(L=LL,Q=QQ,k=KK,mu=MU,lambda=LAMBDA,z=ZZ,DGR),
diff(f(r),r)=subs(L=LL,Q=QQ,k=KK,mu=MU,lambda=LAMBDA,z=ZZ,DFR),
diff(j(r),r)=subs(L=LL,Q=QQ,k=KK,mu=MU,lambda=LAMBDA,z=ZZ,DJR),
diff(h(r),r)=j(r)}:
diffsoln := dsolve(diffequations union icp,numeric,output=listprocedure,maxfun=mfun):
dph:=subs(diffsoln,h(r)):dpf:=subs(diffsoln,f(r)):dpg:=subs(diffsoln,g(r)):dpj:=subs(↵
↵ diffsoln,j(r)):
try:
tmp22:=dph(large_R0*R0);tmp11:=dpf(large_R0*R0);
catch:
small_radius := obj_radius + res;
large_radius := large_radius + res;
print("Increasing small_radius...");
print(small_radius);
next;
end try;

dd:=initial_point_scale:R0:=obj_radius:H1:=h_seed/tmp22:F1:=f_seed/tmp1:KK:=set_KK:ZZ:=↵
↵ set_ZZ:MU:=muparamresscale:
icp := {g(R0*dd)=g_fact*subs(L=LL,Q=QQ,r0=R0,h1=H1,f1=F1,k=KK,mu=MU,lambda=LAMBDA,r=R0*↵
↵ dd,z=ZZ,gs3),
f(R0*dd)=f_fact*subs(L=LL,Q=QQ,r0=R0,h1=H1,f1=F1,k=KK,mu=MU,lambda=LAMBDA,r=R0*↵
↵ dd,z=↵
↵ ZZ,fs3),
h(R0*dd)=h_fact*subs(L=LL,Q=QQ,r0=R0,h1=H1,f1=F1,k=KK,mu=MU,lambda=LAMBDA,r=R0*↵
↵ dd,z=↵
↵ ZZ,hs3),
j(R0*dd)=subs(L=LL,r0=R0,Q=QQ,h1=H1,f1=F1,k=KK,mu=MU,lambda=LAMBDA,r=R0*↵
↵ dd,z=ZZ,diff(↵
↵ (hs3,r))}:
diffequations := {diff(g(r),r)=subs(L=LL,Q=QQ,k=KK,mu=MU,lambda=LAMBDA,z=ZZ,DGR),
diff(f(r),r)=subs(L=LL,Q=QQ,k=KK,mu=MU,lambda=LAMBDA,z=ZZ,DFR),
diff(j(r),r)=subs(L=LL,Q=QQ,k=KK,mu=MU,lambda=LAMBDA,z=ZZ,DJR),
diff(h(r),r)=j(r)}:
diffsoln := dsolve(diffequations union icp,numeric,output=listprocedure,maxfun=mfun):
dph:=subs(diffsoln,h(r)):dpf:=subs(diffsoln,f(r)):dpg:=subs(diffsoln,g(r)):dpj:=subs(↵
↵ diffsoln,j(r)):
try:
tmp23:=dph(large_R0*R0);tmp13:=dpf(large_R0*R0);
catch:
small_radius := obj_radius + res;

```



```

    large_radius := large_radius + res;
    print("Increasing small_radius...");
    print(small_radius);
    next;
end try;

dd:=initial_point_scale:R0:=obj_radius:H1:=h_seed/tmp22:F1:=f_seed/tmp1/tmp13:KK:=↵
    ↵ set_KK:MU:=muparamresscale:
icp := {g(R0*dd)=g_fact*subs(L=LL,Q=QQ,r0=R0,h1=H1,f1=F1,k=KK,mu=MU,lambda=LAMBDA,r=R0*↵
    ↵ dd,z=ZZ,gs3),
    f(R0*dd)=f_fact*subs(L=LL,Q=QQ,r0=R0,h1=H1,f1=F1,k=KK,mu=MU,lambda=LAMBDA,r=R0*dd,z=↵
    ↵ ZZ,fs3),
    h(R0*dd)=h_fact*subs(L=LL,Q=QQ,r0=R0,h1=H1,f1=F1,k=KK,mu=MU,lambda=LAMBDA,r=R0*dd,z=↵
    ↵ ZZ,hs3),
    j(R0*dd)=subs(L=LL,r0=R0,Q=QQ,h1=H1,f1=F1,k=KK,mu=MU,lambda=LAMBDA,r=R0*dd,z=ZZ,diff↵
    ↵ (hs3,r))}:
diffequations := {diff(g(r),r)=subs(L=LL,Q=QQ,k=KK,mu=MU,lambda=LAMBDA,z=ZZ,DGR),
    diff(f(r),r)=subs(L=LL,Q=QQ,k=KK,mu=MU,lambda=LAMBDA,z=ZZ,DFR),
    diff(j(r),r)=subs(L=LL,Q=QQ,k=KK,mu=MU,lambda=LAMBDA,z=ZZ,DJR),
    diff(h(r),r)=j(r)}:
diffsoln := dsolve(diffequations union icp,numeric,output=listprocedure,maxfun=mffun):
entropy := r^(nDims-2)/4/1*(1 + 6*lambda*k*L^2/r^2 + 9*mu*k^2*L^4/r^4):
diffEntropy := diff(entropy,r);
tempera := r^(z+1)/4/Pi/L^(z+1)*sqrt(F1*subs(Q=QQ,h1=H1,g11)):
#Change this when we no longer use a built-in cosmological constant:
pressure := -1/8/Pi*cosmConst:

datapointproc := proc(i) local pointval; global set_KK,ZZ,MU,LAMBDA,areaCoeff;
    pointval:=i*1.0001;
    RETURN([
#Horizon radius:
        (evalf(pointval,90)),
#Entropy:
        #We'll assume the areacoeff is unity here.
        (evalf((subs(r=pointval,lambda=LAMBDA,mu=MU,k=set_KK,L=LL,z=ZZ,entropy)),90)),
#Temperature at horizon:
        (evalf((((subs(r=pointval,r0=pointval,k=set_KK,z=ZZ,mu=MU,lambda=LAMBDA,L=LL,↵
            ↵ tempera))))),90)),
#F1 and G1
        (evalf((((subs(r=pointval,r0=pointval,k=set_KK,z=ZZ,mu=MU,lambda=LAMBDA,L=LL,F1)↵

```

```

        ↪ ))) ,90)),
    (evalf((((subs(r=pointval,r0=pointval,k=set_KK,z=ZZ,mu=MU,lambda=LAMBDA,h1=H1,L=↪
        ↪ LL,Q=QQ,g11))))),90)),
#Pressure:
    (evalf((((subs(r=pointval,r0=pointval,k=set_KK,z=ZZ,mu=MU,lambda=LAMBDA,L=LL,↪
        ↪ pressure))))),90)),
#dEntropy
    (evalf((subs(r=pointval,lambda=LAMBDA,mu=MU,k=set_KK,L=LL,z=ZZ,diffEntropy)),90)↪
        ↪ )
    ]);
end:

mydatapoint[floor((obj_radius-small_radius)/res+.0001)]:=datapointproc(obj_radius):
dataptlist[floor((obj_radius-small_radius)/res+.0001)]:=obj_radius:
if(floor(ln(printcounter)) <> floor(ln(oldprintcounter)))
then
    print(printcounter,time()-init_time,obj_radius,evalf(H1,10),evalf(F1,10),evalf(↪
        ↪ datapointproc(obj_radius)));
    print("Final values of f(r) and h(r):");
    print(dpf(large_R0*R0));print(dph(large_R0*R0));
    oldprintcounter:=printcounter:
fi:

printcounter:=printcounter+1:
#We reach the end of the loop here:
if(obj_radius > large_radius)
then
    whileFlag := false;
fi:

end do:

dataset_list[set_KK+2] := [seq(mydatapoint[i],i=0..((large_radius-small_radius)/res))]:
filename2:=cat("data/stapplotdata-Q",convert(QQ,string),"-Z",convert(ZZ,string),"-l",↪
    ↪ convert(evalf(LL,3),string),"-L",convert(evalf(LAMBDA,3),string),"-M",convert(↪
    ↪ evalf(muparamessscale,3),string),"-r0",convert(evalf(small_radius,3),string),"-rf"↪
    ↪ ,convert(evalf(large_radius,3),string),"-k",convert(set_KK,string),".txt"):
writedata(filename2,dataset_list[set_KK+2],float);
end do:

```

C.3 Thermodynamic Mass and Volume

This program is written in Maxima; given an input of the metric function, the entropy, and the number of dimensions of the black hole spacetime, it will return the thermodynamically determined mass and volume of the black hole.

The prompts should be suitable to guide you through using this software.

```
/* Maxima file to solve for the mass given a metric function,
   dimension, and z.

   W. Brenna
   June 15, 2014
*/

nDims:read("Enter the number of dimensions:");
nZ:read("Enter the Lifshitz parameter z.");
nFr:read("Enter the metric function f(r) from ds^2 = -(r/l)^(2z) * f(r) * dt^2 + ...");
nEntropy:read("Enter the entropy of the solution as a function of r and l. Use %pi for Pi."↵
↵ );
nCosmo:read("Enter the cosmological constant as a function of l.");
nParam:read("Enter the name of a mass parameter for the metric function.");

P: -nCosmo/8/%pi;
dP: -diff(nCosmo,l)/8/%pi;
dSr: diff(nEntropy,r);

/* This gives the parameter in terms of horizon radius. */
nParamSolve: solve(nFr=0,nParam);

temperature: subst(nParamSolve,(r/l)^(nZ+1)/4/%pi * diff(nFr,r));

/* Express temperature as a sum of terms in length parameters: */

if sequal(string(reveal(reveal(expand(temperature),1),1)), "Sum") then tLength: length(↵
↵ expand(temperature)) else tLength : 1;

if sequal(string(reveal(reveal(expand(nEntropy),1),1)), "Sum") then tLength2: length(expand↵
↵ (nEntropy)) else tLength2 : 1;

tLengthTot: tLength*tLength2;
```

```

array(alphaArr,tLengthTot);
array(betaArr,tLengthTot);
array(tempArrEntropy,tLengthTot);
array(tempArrdEntropy,tLengthTot);

/* Expand the temperature in a series and store powers in arrays */

tmpVariableForLogExpand: logexpand;
logexpand: super;
/* Modded */
if (tLength > 1 and tLength2 > 1) then for i:1 thru tLength step 1 do ( for j:1 thru
↳ tLength2 step 1 do (tempArrEntropy[(i-1)*tLength2+j]: part(expand(temperature),i)*
↳ part(expand(nEntropy),j), tempArrdEntropy[(i-1)*tLength2+j]: part(expand(temperature
↳ ),i)*diff(part(expand(nEntropy),j),r), betaArr[(i-1)*tLength2+j]: coeff(expand(log(
↳ part(expand(temperature),i)*part(expand(nEntropy), j))),log(r)), alphaArr[(i-1)*
↳ tLength2+j]: coeff(expand(log(part(expand(temperature),i)*part(expand(nEntropy), j)
↳ ),log(l)))) else if (tLength = 1 and tLength2 > 1) then for j:1 thru tLength2 step 1
↳ do (tempArrEntropy[j]: (expand(temperature))*part(expand(nEntropy),j),
↳ tempArrdEntropy[j]: (expand(temperature))*diff(part(expand(nEntropy),j),r), betaArr[
↳ j]: coeff(expand(log((expand(temperature)*part(expand(nEntropy), j))))),log(r)),
↳ alphaArr[j]: coeff(expand(log((expand(temperature)*part(expand(nEntropy), j))))),log(
↳ l))) else if (tLength2 = 1 and tLength > 1) then for i:1 thru tLength step 1 do (
↳ tempArrEntropy[i]: part(expand(temperature),i)*(expand(nEntropy)), tempArrdEntropy[i
↳ ]: part(expand(temperature),i)*diff((expand(nEntropy)),r), betaArr[i]: coeff(expand(
↳ log((part(expand(temperature),i)*(expand(nEntropy))))),log(r)), alphaArr[i]: coeff(
↳ expand(log((part(expand(temperature),i)*(expand(nEntropy))))),log(l))) else (
↳ tempArrEntropy[1]: expand(temperature*nEntropy), tempArrdEntropy[1]: expand(
↳ temperature*dSr), betaArr[1]: coeff(expand(log(expand(temperature*nEntropy))),log(r)
↳ ), alphaArr[1]: coeff(expand(log((expand(temperature*nEntropy))),log(l)));
logexpand: tmpVariableForLogExpand;

print("Temperature (array):", expand(temperature));
print("Total number of items in T*S: ", tLengthTot);
print("Temperature * Entropy (array):", listarray(tempArrEntropy));
print("Temperature * dEntropy (array):", listarray(tempArrdEntropy));
tmp: listarray(alphaArr);
print("Alpha Array: ", tmp);
tmp: listarray(betaArr);
print("Beta Array: ", tmp);

```

```

/* Use the computation derived for mass and volume (unique) */
mass: 0;
volume: 0;
for i:1 thru tLengthTot step 1 do (if(betaArr[i]=0) then print("Warning, betaArr is zero ↵
↳ for some terms.") else mass: mass + tempArrdEntropy[i] * r / betaArr[i]);
for i:1 thru tLengthTot step 1 do (if(betaArr[i]=0) then garbage: 3 else volume: volume + (↵
↳ tempArrEntropy[i] * (nDims-2) * r^(betaArr[i]-1) * betaArr[i] - tempArrdEntropy[i] * ↵
↳ (nDims-3) * r^(betaArr[i]) ) / betaArr[i] / 2 / P / r^(betaArr[i]-1));

print("Mass:", mass);
print("Volume:", volume);

/* Check the reverse isoperimetric inequality for these bodies */
area: (nDims-1)*%pi^( (nDims-1)/2)/gamma( (nDims-1)/2 + 1)*r^(nDims-2);
isOmega: 2*%pi^( (nDims-1)/2)/gamma( (nDims-1)/2);
isoper: ((nDims-1)*volume/isOmega)^(1/(nDims-1))*(isOmega/area)^(1/(nDims-2));
print("Isoperimetric Parameter R:",isoper);

test:read("Do additional computations? (y/n)");
if sequal(string(test), "n") then quit();
rhorizon:read("Enter the horizon radius in terms of l.");
mparamSol: solve(subst(r=rhorizon,nFr),nParam);
mass2: subst(r=rhorizon,mass);
volume2: subst(r=rhorizon,volume);
print("Mass:", mass2);
print("Volume:", volume2);
print("Isoperimetric parameter:", subst(r=rhorizon,isoper));

/* Now to find the charge-potential term Phi*Q */
test:read("Continue to find charge? (y/n)");
if sequal(string(test), "n") then quit();
newFr:read("Enter the part of f(r) depending on charge q, where q scales as L^(D-3).");
newParamSolve: solve(nFr+newFr=0,nParam);
newTemp: subst(newParamSolve,(r/l)^(nZ+1)/4/%pi * diff(nFr + newFr,r)) - subst(q=0,subst(↵
↳ newParamSolve,(r/l)^(nZ+1)/4/%pi * diff(nFr + newFr,r)));
STQ:nEntropy*newTemp;
if sequal(string(reveal(reveal(expand(STQ),1),1)), "Sum") then tLength: length(expand(STQ))↵
↳ else tLength : 1;
array(stqArray,tLength);

```

```

array(stqArraycoeff,tLength);
array(stqArrayellcoeff,tLength);
if sequal(string(reveal(reveal(expand(STQ),1),1)), "Sum") then for i:1 thru tLength step 1 ↵
    ↵ do (stqArray[i]: part(expand(STQ),i), stqArraycoeff[i]: hipow(part(expand(STQ), i),q)↵
    ↵ ), stqArrayellcoeff[i]: hipow(part(expand(STQ), i),l)) else for i:1 thru tLength ↵
    ↵ step 1 do (stqArray[i]: expand(STQ), stqArraycoeff[i]: hipow(expand(STQ),q), ↵
    ↵ stqArrayellcoeff[i]: hipow(expand(STQ),l));

print("You entered the q temperature terms as: ", collectterms(ratsimp(newTemp),q));
print("You entered the q temperature*entropy terms as (array): ", listarray(stqArray));
print("The coefficients of ell in these terms are: ", listarray(stqArrayellcoeff));
print("The coefficients of q in these terms are: ", listarray(stqArraycoeff));

phiQ: 0;
tmpMass: 0;
tmpVol: 0;
tmpExpr: 0;
for i:1 thru tLength step 1 do (tmpExpr: (nDims-2) * stqArray[i] / ( (nDims - 3) * (1 - ↵
    ↵ stqArraycoeff[i]) - stqArrayellcoeff[i]),tmpMass: tmpMass + tmpExpr,phiQ: phiQ + ↵
    ↵ stqArraycoeff[i]*tmpExpr,tmpVol: tmpVol - stqArrayellcoeff[i]*tmpExpr/2/P);
mass: mass + ratsimp(tmpMass);
mass2: mass2 + ratsimp(tmpMass);
volume: volume + ratsimp(tmpVol);
print("The mass is now:",mass,"and the Phi*Q term is",phiQ, "while the volume is:",volume);
/* If mass is fixed we can solve for q in terms of rh */
qsqSoln: solve(subst(q=sqrt(qsq),subst(mparamSol,nFr+newFr)),qsq);
print("Equivalently, the mass might now be:",subst(qsqSoln,subst(q=sqrt(qsq),mass)), "and ↵
    ↵ the Phi*Q term",subst(qsqSoln,subst(q=sqrt(qsq),phiQ)));

/* Finally, the isoperimetric parameter. */
isoper2: subst(qsqSoln,subst(q=sqrt(qsq),isoper));
print("The isoperimetric parameter has become: ",isoper2);

```
